

Development of an Acceptance Test for Chip Seal Projects

FINAL REPORT SPR-1649

Project Research No. OR15 - 508

The Michigan Department of Transportation
Research Administration
8885 Ricks Road
P.O. Box 33049
Lansing, Michigan 48909

Authors:

M. Emin Kutay, Ph.D., P.E.
(Associate Professor)
Principal Investigator (PI)

Ugurcan Ozdemir
(Research Assistant)

Derek Hibner
(Research Assistant)

Yogesh Kumbarger
(Research Assistant)

Michele Lanotte, Ph.D.
(Research Associate)

Michigan State University
Department of Civil & Environmental Engineering
428 S. Shaw Lane, Room no. 3546,
Engineering Building
East Lansing, MI 48824

January 30, 2017

TECHNICAL REPORT DOCUMENTATION PAGE

1. Report No. SPR-1649		2. Government Accession No. N/A		3. Recipient's Catalog No. N/A	
4. Title and Subtitle Development of an Acceptance Test for Chip Seal Projects				5. Report Date November 21, 2016	
				6. Performing Organization Code OR15 – 508	
7. Author(s) M. Emin Kutay, Ugurcan Ozdemir, Derek Hibner, Yogesh Kumbarger and Michele Lanotte				8. Performing Organization Report No. N/A	
9. Performing Organization Name and Address Michigan State University, 428 S. Shaw Lane, Room no. 3546, Engineering Building East Lansing, MI 48824				10. Work Unit No. N/A	
				11. Contract or Grant No. Contract 2013-0066 Z3	
12. Sponsoring Agency Name and Address Michigan Department of Transportation (MDOT) Research Administration 8885 Ricks Road P.O. Box 33049 Lansing, Michigan 48909				13. Type of Report and Period Covered Final Report, 11/1/2014 to 1/31/2017	
				14. Sponsoring Agency Code N/A	
15. Supplementary Notes Conducted in cooperation with the U.S. Department of Transportation, Federal Highway Administration. MDOT research reports are available at www.michigan.gov/mdotresearch .					
16. Abstract Chip seals are among the most popular preventive maintenance techniques implemented by many DOTs, county road departments and cities. The deteriorated pavement surface is sprayed with an asphalt emulsion or binder, and then a layer of uniformly-graded aggregates is spread and compacted. Curing is required before opening the road to traffic to enhance bonding between aggregate particles and asphalt bitumen. Percent embedment of aggregate particles into the thin bituminous layer is one of the most significant parameters affecting the performance of asphalt chip seals. Bleeding or aggregate loss may be encountered in chip seal applications depending on the aggregate percent embedment. The main objective of this research project was to develop a standard test procedure to directly calculate the aggregate percent embedment into the asphalt binder in a chip seal project via digital image analysis. Three image analysis algorithms were developed and used to analyze chip seal samples. Forty-eight (48) chip seal cores were collected from eight different locations in Michigan and analyzed. Moreover, forty (40) laboratory samples were fabricated to investigate the impact of the binder and aggregate application rates on the percent embedment. The analyses were performed using the sand patch test, laser texture scanning and the image-based algorithms developed as part of this project. Performance of chip seal samples were also evaluated using sweep tests performed on the laboratory and field samples. Software, named CIPS, has been developed and it represents one of the primary outputs of this project. This software and the procedure developed herein can be used by road agencies and contractors as an acceptance test for chip seal projects.					
17. Key Words Chip seal, Embedment depth, image processing, sand patch test			18. Distribution Statement No restrictions. This document is also available to the public through the Michigan Department of Transportation.		
19. Security Classif. (of this report) Unclassified		20. Security Classif. (of this page) Unclassified		21. No. of Pages 95	22. Price N/A

ACKNOWLEDGEMENTS

The authors would like to acknowledge the U.S. Department of Transportation (USDOT) for funding the University Transportation Center for Highway Pavement Preservation (UTCHPP). This project was MDOT's match to the UTCHPP funding. The authors also thank Dr. Karim Chatti (the PI of the UTCHPP), Dr. Syed Haider and Larry Galehouse from the National Center for Pavement Preservation (NCPP).

RESEARCH REPORT DISCLAIMER

“This publication is disseminated in the interest of information exchange. The Michigan Department of Transportation (hereinafter referred to as MDOT) expressly disclaims any liability, of any kind, or for any reason, that might otherwise arise out of any use of this publication or the information or data provided in the publication. MDOT further disclaims any responsibility for typographical errors or accuracy of the information provided or contained within this information. MDOT makes no warranties or representations whatsoever regarding the quality, content, completeness, suitability, adequacy, sequence, accuracy or timeliness of the information and data provided, or that the contents represent standards, specifications, or regulations.”

TABLE OF CONTENTS

TECHNICAL REPORT DOCUMENTATION PAGE.....	i
ACKNOWLEDGEMENTS	ii
RESEARCH REPORT DISCLAIMER.....	iii
LIST OF FIGURES	viii
EXECUTIVE SUMMARY	1
1. INTRODUCTION.....	2
<i>1.1 Background.....</i>	<i>2</i>
<i>1.2 Objectives.....</i>	<i>3</i>
<i>1.3 Scope of Research.....</i>	<i>3</i>
1.3.1 Task 1: Sample Preparation and Image Acquisition.....	3
1.3.2 Task 2: Development of Image Processing Algorithms	3
1.3.3 Task 3: Laboratory Testing & Validation of Algorithms & Data Analysis.....	4
1.3.4 Task 4: Development of a user-friendly software package for analysis of chip seal samples (named CIPS).....	4
<i>1.4 Statement of Hypotheses</i>	<i>4</i>
2. LITERATURE REVIEW	6
<i>2.1 Chip Seal Design Procedures</i>	<i>6</i>
2.1.1 Hanson Method.....	6
2.1.2 Kearby Method	7
2.1.3 McLeod Design Method	7
2.1.4 Modified Kearby Method	8
2.1.5 Road Note 39 (Sixth Edition)	8
2.1.6 Austroads Design Method.....	9
2.1.7 South African Method, TRH3.....	9
<i>2.2 NCHRP 680 Procedure for Determining Percent Embedment</i>	<i>10</i>
<i>2.3 Performance Tests for Chip Seals.....</i>	<i>12</i>
2.3.1 ASTM D7000 Sweep Test.....	12
2.3.2 Vialit Adhesion Test	13
2.3.3 Frosted Marble Test	13
2.3.4 Australian Aggregate Pull-out Test	13
2.3.5 Pennsylvania Aggregate Retention Test	13
2.3.6 British Pendulum Test.....	14
2.3.7 Third Scale Model Mobile Loading Simulator	14
2.3.8 Pneumatic Adhesion Tension Test.....	14

2.4	<i>Image Processing Techniques for Performance Evaluation of Chip Seals</i>	14
2.5	<i>Numerical Studies on Asphalt Chip Seals</i>	15
2.6	<i>Summary of the Literature Review</i>	16
3.	METHODOLOGY	17
3.1	<i>Experimental design</i>	17
3.2	<i>Equipment and procedures</i>	17
3.2.1	Field Chip Seal Samples	17
3.2.2	Laboratory Chip Seal Samples.....	20
3.3	<i>Image Processing and Analysis Methods</i>	25
3.3.1	Sample Preparation and Image Acquisition.....	25
3.3.2	Image Adjustments	28
3.3.3	Finding the Pavement Substrate in the Image.....	29
3.3.4	Computing Percent Embedment using Peak & Valley Method.....	29
3.3.5	Computing Percent Embedment of Each Aggregate	31
3.3.6	Computing Aggregate Surface Coverage by the Binder.....	34
3.3.7	Development of a standalone software package (CIPS).....	34
3.4	<i>Validation of the Image Processing Algorithms</i>	35
3.5	<i>Traditional Methods for Estimating Percent Embedment</i>	36
3.5.1	Sand Patch Test.....	36
3.5.2	Laser Texture Scanning	38
3.6	<i>ASTM D7000 Sweep Test</i>	39
4.	FINDINGS	41
4.1	<i>Analyses of the Field Cores</i>	41
4.2	<i>Analyses of Laboratory-prepared Samples</i>	48
4.2.1	Investigation of the effect of binder and aggregate application rate on percent embedment.....	48
4.2.2	Sensitivity of the percent embedment to binder application rate and the effect of sweep test.....	49
4.3	<i>Application of Percent Within Limits (PWL) Concept to Percent Embedment</i>	52
5.	CONCLUSIONS	54
5.1	<i>Conclusions from the study</i>	54
5.2	<i>Recommendations for further research and implementation</i>	54
	BIBLIOGRAPHY	56
	APPENDIX A: Embedment Depth and Surface Coverage Area Results for Field Samples of M-57 near Pompeii	61
	APPENDIX B: Embedment Depth and Surface Coverage Area Results for Field Samples of M-20 near New Era	63

APPENDIX C: Embedment Depth and Surface Coverage Area Results for Field Samples of M-33 from Alger to Rose City..... 66

APPENDIX D: Embedment Depth and Surface Coverage Area Results for Field Samples of M-86 east of Plainwell..... 69

APPENDIX E: Embedment Depth and Surface Coverage Area Results for Field Samples of M-43 in Woodland 72

APPENDIX F: Embedment Depth and Surface Coverage Area Results for Field Samples of US-31 in Bear Lake..... 73

APPENDIX G: Embedment Depth and Surface Coverage Area Results for Laboratory Samples – Group 1 & 2..... 75

APPENDIX H: Percent Within Limits (PWL) results for embedment depths of field samples analyzed using image processing algorithms..... 80

LIST OF TABLES

Table 1 Parameters used in different chip seal design methods	10
Table 2 Various test methods used to evaluate asphalt chip seals	12
Table 3 Summary of field chip seal cores (single chip seals unless noted)	18
Table 4 Summary of group 1 laboratory samples	21
Table 5 Summary of group 2 lab samples	21
Table 6 Composition/ information on ingredients	22
Table 7 Average and standard deviation of the embedment depths computed using various methods	44
Table 8 The Coefficient of Variation (COV) values for each parameter	51
Table 9 PWL results for the field samples	53

LIST OF FIGURES

Figure 1 Conceptual illustration of Chip Seal.....	2
Figure 2 States of chip seal embedment (source: New Zealand Road Division 1968).....	7
Figure 3 Illustration of an idealized chip seal cross section used in NCHRP 680 methods.....	11
Figure 4 Illustration of the potential errors caused by the NCHRP 680 procedures	12
Figure 5 Experimental design flowchart.....	17
Figure 6 Procedure for taking cores from the field.....	19
Figure 7 Gradation of the aggregates used in the field M-33 from Alger to Rose City	20
Figure 8 (a) Original image obtained from a document camera (b) Aggregate determination	20
Figure 9 Gradation of the aggregates used in the laboratory	22
Figure 10 Binder application process: (a) pouring emulsion on the sample, and (b) spreading the binder by gravity & rotation	23
Figure 11 Sketch of the components of the aggregate spreader	24
Figure 12 Procedure for using aggregate spreader	24
Figure 13 Sweep test compactor and compaction using the MTS: (a) Sweep test compactor and (b) compaction with MTS.....	25
Figure 14 Sample cutting procedure	26
Figure 15 Illustration of sample preparation and image acquisition.....	26
Figure 16 Desired cross section image	27
Figure 17 Image-based problems from cross sections	27
Figure 18 The effect of painting on cross section image	28
Figure 19 Illustration of an (a) original image, (b) rotated image, (b) cropped image.	28
Figure 20 Illustration of the steps of determining the existing pavement surface	30
Figure 21 Steps of peak & valley method.....	31
Figure 22 Illustration of steps of identifying individual aggregates.	32

Figure 23 Illustration of computation of percent embedment of each aggregate	33
Figure 24 Aggregate surface coverage by the binder	34
Figure 25 Screenshot of CIPS software	35
Figure 26 Illustration of idealized chip seal images with exactly 50% embedment.....	36
Figure 27 Illustration of an idealized chip seal cross section used in sand patch test	37
Figure 28 (a) Illustration of the chip seal where binder exists below the chips and how this affects the percent embedment and (b) an example image where there is binder below the chips	38
Figure 29 Laser texture scanning procedure for laboratory and field chip seal samples.....	39
Figure 30 ASTM D7000 sweep test setup used in the current study.....	40
Figure 31 Cross sectional image of a double chip seal sampled in this study	41
Figure 32 Comparison of mean profile depth and mean texture depth measured on the chip seal sections utilized in this project.....	43
Figure 33 Examples of fully embedded aggregates	44
Figure 34 Comparison of different methods for (a) for M-57 Highway near Pompeii and (b) M-20 near New Era.....	45
Figure 35 Comparison of different methods for (a) M-33 and (b) M-86 Chip Seal Section.....	46
Figure 36 Comparison of different methods for (a) M-43 and (b) US-31 Chip Seal Section	47
Figure 37 Effect of binder application rate on the percent embedment.....	48
Figure 38 Effect of aggregate application rate on the percent embedment	49
Figure 39 Sensitivity of the (a) percent embedment and (b) aggregate surface coverage to binder application rate.....	50
Figure 40 An example histogram an the illustration of the limits used in computation of the PWL.	52

EXECUTIVE SUMMARY

Chip seals are among the most popular preventive maintenance techniques implemented by many Departments of Transportation (DOTs), county road departments and other road agencies. The chip seal is a method where the deteriorated pavement surface is sprayed with an asphalt emulsion (or hot binder), and then a layer of uniformly-graded aggregates is spread and compacted. Percent embedment of aggregate particles into the thin bituminous layer (created after setting of the emulsion) is one of the most significant parameters affecting the performance of asphalt chip seals. Bleeding or aggregate loss may be encountered in chip seal applications if adequate aggregate embedment depth level is not achieved. Historically, adequacy of percent embedment has been either visually evaluated or quantified using indirect test procedures (e.g., the sand patch test and the laser texture meter devices). These indirect methods typically assume perfectly smooth pavement surface, ignore the penetration of aggregate chips into the substrate and do not consider the size distribution of the aggregates (instead use an average size). Therefore, their accuracies in estimating the percent embedment are questionable. The primary objective of this research was to develop an image-based and practical test method to directly measure the embedment depth of chip seal applications. The procedure includes cutting/slicing samples, taking digital images of the vertical faces and computing the percent embedment using image analysis methods. In this research, three different image analysis algorithms, namely (i) peak valley method, (ii) surface coverage area method and (iii) embedment of each aggregate method were developed. These algorithms were implemented into a standalone software package (herein called CIPS) and validated using idealized images with known percent embedment.

The scope of the project involved the analysis of both laboratory-produced chip seal samples and cores collected from the field. In both cases, samples were sliced using a tile saw, then digital images of the vertical cross sections were captured and analyzed using the CIPS software. Forty-eight (48) chip seal cores were collected from 8 different road sections around the State of Michigan, and forty (40) laboratory samples were fabricated. Among the image analysis algorithms, the peak & valley method was found to show similar results to those obtained from the sand patch tests, which was expected. On the other hand, the surface-coverage area and the percent embedment of each aggregate methods are recommended to be the most accurate method to analyze chip seals. The analysis of the laboratory-produced and field chip seal samples revealed that aggregate and binder application rate limits within the MDOT specification leads to percent embedment values ranging from 50 to 70%, depending on the type of the aggregate used.

1. INTRODUCTION

1.1 Background

Since the 1920's, chip seals have been used as a method for re-surfacing pavements. Early projects involved the use of chip seal in the construction of new low-volume roads. In the last few decades, this methodology has turned into a maintenance and preservation treatment of deteriorated pavements. In general terms, chip seal applications consist of spraying hot asphalt cutback or emulsion over the surface of an existing pavement, and then before it hardens, aggregates (chips) are spread over the surface and compacted. The hot asphalt fills and seals existing cracks and establishes a waterproof layer. The primary role of the asphalt binder in the chip seal application is to provide a waterproof membrane that protects the pavement surface from sun, oxidation and moisture infiltration (Wood et al., 2006). Aggregates act as a 'bridge' and provide sufficient skid resistance.

Asphalt chip seals are preferably constructed on lower traffic volume roads since the structural capacity of asphalt chip seals is very low compared to typical pavements (HMA or concrete pavements). Therefore, while the existing pavement underlying the asphalt chip seal provides structural capacity, the chip seal seals fine cracks and deteriorations, prevents moisture infiltration and enhances skid resistance. Therefore, asphalt chip seals are not a good maintenance option for heavily distressed roads.

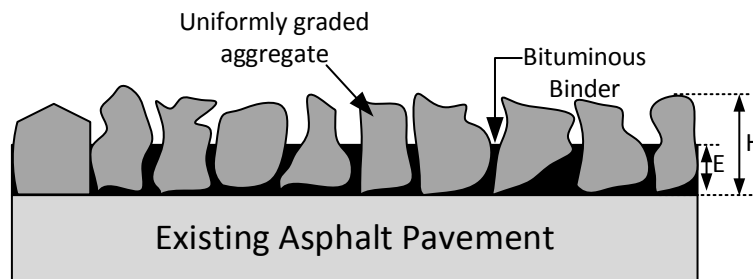


Figure 1 Conceptual illustration of Chip Seal

Embedment depth is one of the most important parameters related to the quality of chip seals. Embedment depth is defined as the average height of the binder divided by the average height of the aggregate as shown in Figure 1. Asphalt chip seal applications can achieve their service lives if proper embedment and aggregate orientation are provided. There are several opinions about selecting desired embedment depth right after the construction; however, all design methods have agreed that design criteria of embedment depth should be between 50% and 70% after construction (Gransberg and James 2005).

McLeod et al. (1969) pointed out the relationship between embedment depth and chip seal aggregate loss and bleeding. Asphalt chip seals having the embedment depth less than 50% are more susceptible to aggregate loss due to insufficient bonding between binder and aggregate; whereas, asphalt chip seals having the aggregate embedment higher than 70% may cause bleeding problems on the surface of the pavement. Therefore, it is very important to achieve desired aggregate embedment into the binder.

Determination of the embedment depth is typically achieved by pulling the aggregates out from the chip seal binder and visually examining the aggregate embedment depth into the binder. This method is difficult to implement and subjective, especially when angular and flat/elongated aggregates are used. Another method suggested by NCHRP Report 680 (2011) is spreading a certain volume of glass beads over the chip seal surface, followed by measurement of its diameter. The aggregate size and texture height calculated from volume of glass beads are used to estimate embedment depth. Another concept that has a direct relationship with embedment depth is texture depth (macro texture) of the chip seal. Texture depth (macro texture) of the chip seal is also an indicator of performance (Abdul-Malak et al. 1993 and Roque et al. 1991), primarily because this parameter is related to the embedment depth.

Current ways for obtaining embedment depth are subjective and contains inaccurate assumptions. For example, they assume perfectly smooth pavement surface, ignore the penetration of aggregate chips into the substrate and do not consider the size distribution of the aggregates (instead use an average size). Therefore, there is a need for a more accurate and objective method to directly calculate aggregate embedment depth into the binder. Obtaining embedment depth via image processing techniques can be reliable and objective method, as compared to current methods.

1.2 Objectives

The main objective of the research study was to develop a standard test procedure to directly evaluate the aggregate embedment into the asphalt binder in a chip seal project via digital image analysis. This method can be used as part of an acceptance specification, for forensic investigation purposes and to validate/refine chip seal design procedures in the future.

1.3 Scope of Research

1.3.1 Task 1: Sample Preparation and Image Acquisition

One of the significant tasks of this study was to develop a practical procedure to prepare chip seal samples for image acquisition and to investigate the most appropriate imaging approach before image analysis. For this purpose, the following tasks have been undertaken:

- Chip seal core samples were taken from the field with the help from Michigan DOT crew.
- Chip seal core samples were fabricated with a new methodology in the laboratory based on the recommendation of NCHRP 680 (2011) report.
- Desired chip seal cross sections were obtained for image acquisition.
- Different image acquisition and lighting conditions were investigated and the best method was determined for taking digital images of the chip seal cross sections.

1.3.2 Task 2: Development of Image Processing Algorithms

The scope of this task included development of image-based algorithms to directly measure percent embedment depth (ED) of chip seal samples. In addition to percent embedment depth, other concepts such as percent of aggregate surface coverage (ASC) by the binder, were studied

and image-based algorithms were developed. This task consisted of the following major components:

- Three different image processing algorithms were developed to calculate percent embedment depth (ED).
- One algorithm was developed to obtain percent of aggregate surface coverage (ASC) by the binder.
- Verification of the algorithms was performed by using idealized images which have particular embedment depth (ED) and aggregate surface coverage (ASC) by the binder.

1.3.3 Task 3: Laboratory Testing & Validation of Algorithms & Data Analysis

As part of this task, the algorithms were validated through laboratory tests, Also, the effect of binder application rate on the chip seal performance was investigated through both laboratory testing and image-based algorithms. This task included the following components:

- Both sand patch test and laser texture scans were conducted on field cores.
- Sand patch test was performed on laboratory-fabricated samples.
- Image analyses were completed on laboratory-fabricated samples and field cores.
- Statistical analysis of embedment depths obtained from image-based algorithms, sand patch test, laser texture scan, and the effect of binder application rate on the chip seal performance were performed.

1.3.4 Task 4: Development of a user-friendly software package for analysis of chip seal samples (named CIPS)

As part of this task, the algorithms that were validated in previous tasks were included in a holistic and user friendly software package loaded with various additional features. This software has been named CIPS. It is the primary tangible output of this research project. This software program can be distributed, installed and used easily by various road agencies or research institutions, to evaluate chip seal projects. This task included the following broad components:

- Development of a MATLAB-based software program (i.e., CIPS).
- The program was beta-tested several times and evaluated with respect to its user-friendliness and ability to deliver repeatable and robust results.

1.4 Statement of Hypotheses

Bleeding or aggregate loss may be encountered in chip seal applications if appropriate aggregate embedment is not achieved. Historically, appropriateness of embedment depth has been either visually evaluated or quantified using indirect test procedures (e.g., the sand patch test and the laser texture meter devices). These indirect methods typically assume perfectly smooth pavement surface, ignore the penetration of aggregate chips into the substrate and do not consider the size distribution of the aggregates (instead use an average size). Therefore, their accuracies in

estimating the aggregate embedment (or the bonding between the aggregate and binder) are questionable. It has been hypothesized that the image analysis techniques can be employed to measure the embedment depth more accurately and objectively. Furthermore, image analysis procedures can also be used to compute more accurate parameters (e.g., aggregate/binder surface coverage area) that can be used to better quantify the adequacy of the bond between the aggregates and the binders in chip seal applications.

2. LITERATURE REVIEW

Asphalt chip seals were first constructed as a main pavement for low volume roads in 1920s. With time, chip seal became a preservation technique for deteriorated hot mix asphalt pavements, primarily because of low initial costs (Gransberg and James 2005). The primary purposes of asphalt chip seal surface treatments can be summarized as follows: (1) to prevent existing surface from water and air infiltration by sealing small surface cracks on the surface, (2) to improve surface texture and skid resistance, (3) to reduce oxidation of existing pavement due to temperature and air, and (4) to provide anti-glare surface when the pavement is wet.

NCHRP synthesis 342 (Gransberg and James 2005) defined seven different types of chip seal applications: (i) single chip seal, (ii) double chip seal, (iii) racked-in seal, (iv) cape seal, (v) inverted seal, (vi) sandwich seal, and (vii) geotextile-reinforced seal. However, the focus of this research project is only the single chip seal, which consists of a single layer binder application followed by one stone thick aggregate application to provide protective surface wearing. Depth of aggregate embedment into the binder plays an important role to determine whether asphalt chip seal is properly constructed or not. There are two main distresses that occur in chip seal applications: (i) aggregate chip loss and (ii) bleeding. Aggregate chip loss is simply de-bonding of aggregates from the binder due to the effect of sweeping or traffic. Bleeding on the other hand refers to the condition where almost entire aggregates submerge into the binder. Embedment depth is a parameter that is related to both of these distresses.

In addition to binder and aggregate application rate, embedment depth depends on several parameters including aggregate size and shape, emulsion type, hardness of existing pavement, rolling patterns (and numbers) and traffic. (Schuler et al. 2011).

2.1 Chip Seal Design Procedures

Chip seal designs have been historically based on either past experience or certain engineering concepts. Due to the continuous change of material characteristics, construction equipment, climate and most importantly the changes of the existing surface condition in different regions, contractors have generally designed chip seals based on experiences in the field (Gransberg and James 2005). However, there are also engineering concepts used to design chip seals, which are described in the following subsections.

2.1.1 Hanson Method

First attempt to develop a design procedure for asphalt chip seals was made by F.M Hanson (1935). He stated that voids between the aggregates after spreading over the pavement, rolling and traffic condition becomes nearly 50%, 30% and 20%, respectively (see Figure 2). He also stated that after opening to traffic, due to aggregate shapes, aggregates tend to be lying on their flattest side and therefore, average least dimension (ALD) is nearly equal to the average thickness of the aggregates after the construction.

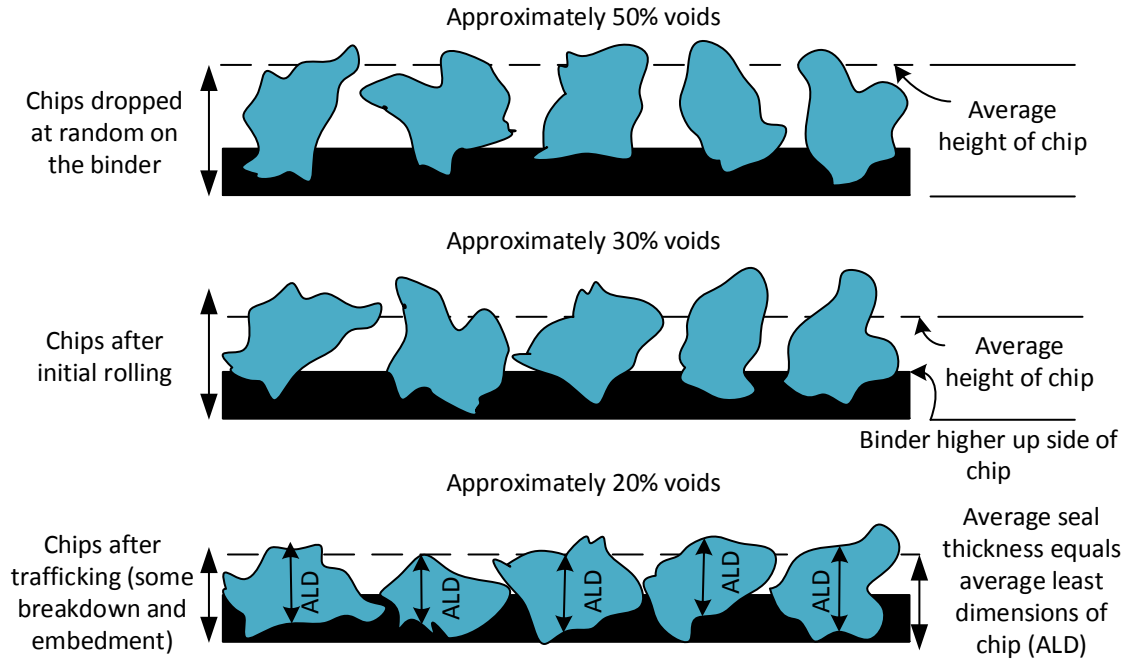


Figure 2 States of chip seal embedment (source: New Zealand Road Division 1968)

Hanson (1935) focused on the void percentage in his design method. He did not include embedment depth criterion; however, he pointed out that void area between aggregates should be filled with 60% to 75% residual binder which correspond to 60% to 75% embedment depth.

2.1.2 Kearby Method

Kearby (1953) was the first engineer to develop asphalt chip seal design method with respect to determining material application rates. He developed a monograph, which uses average size of aggregates, percent embedment depth and voids percentage between aggregates as inputs to obtain asphalt cement rate (in gallons per square yard). One of the drawbacks of Kearby design method is that void percentage and percentage embedment depth range is limited; and also aggregate size range varies between 1/8" and 1". Another drawback according to Kearby (1953) is that traffic effect and aggregate toughness are not included in the monograph.

2.1.3 McLeod Design Method

After Hanson's work (1935) on asphalt chip seal, N. McLeod created a new design procedure for chip seal based on Hanson's study. McLeod's goal was to find aggregate and binder application rates which should be applied at the construction (McLeod, 1969).

Aggregate size (gradation), shape and specific gravity play a significant role in calculation of aggregate application rate. However, for binder application rate, there are different types of parameters needed to be considered, including aggregate gradation and shape, traffic condition, residual percent of asphalt binder, binder leakage through existing pavement surface condition and binder absorption by aggregates.

McLeod used Hanson's theory and accepted that inter-particle voids in loose condition is about 50%, then after rolling and trafficking, it becomes nearly 30% and 20%, respectively. Voids between aggregates after a certain volume of traffic is 20%, which means that cover aggregates fill 80% of seal application.

Embedment depth is not a direct input for both the binder and aggregate application rate calculation. However, it is indirectly included in the traffic correction during binder application rate calculation. In other words, the traffic factor, which depends upon the anticipated traffic volume, is adjusted so that percent embedment depth after trafficking gives 70%.

2.1.4 Modified Kearby Method

First attempt for modification of Kearby Method was Epps et al. study (1974). They tried to change Kearby design monograph so that synthetic aggregates having high porosity can be used in the design. Then, in a different research activity, Epps et al. (1981) tried to adjust Kearby design method so that the design was consistent with field performances. Holmgreen et al. (1985) studied the performance of chip seal sections designed according to Kearby method by using data collected from the previous two studies and they found that calculated asphalt application rate was not sufficient to hold aggregates.

The aggregate application rate for modified Kearby method is calculated by using the measurement of a new laboratory test method "Board Test" which is used for finding aggregate quantity in one-thick stone position over one square yard. This test finds aggregate quantity in lb/yd² by dividing the weight of aggregate to the aggregate application area (half square yard is generally used). The asphalt rate was modified by adding traffic and existing pavement surface condition. The other modification was shifting the curve in relationship between average mat depth and percentage of embedment (Epps and Gallaway 1974).

Percent embedment depth can be obtained by using average mat thickness; in other words, average aggregate height. At the same time, percent embedment depth can be chosen manually without suggestion of the method according to average mat depth. In the design, it was suggested that 30±10% and 70±10% embedment depth should be achieved just after the construction and after two years of service, respectively.

2.1.5 Road Note 39 (Sixth Edition)

The design procedure Road Note 39 was developed by The United Kingdom's Transport Research Laboratory in the United Kingdom (Roberts and Nicholls 2008). This design procedure was developed by designing different kinds of systems based on different parameters simulating different conditions and traffics on the pavement (Colwill et al. 1995). The design steps included selection of dressing type (such as single chip seal, double chip seal etc.), selection of binder and aggregate type, determination of binder and aggregate rate. Traffic level, existing pavement hardness and size of aggregates are primary inputs for determining binder application rate. Aggregate type and shape, existing surface condition, climate, geometry of pavement and speed of traffic are secondary inputs used for determining binder application rate. On the other hand, aggregate application rate, determined by BS EN 12272-1, takes aggregate shape, size and relative density into account.

In Road Note 39 (Sixth Edition), although embedment depth is mentioned while stating the effect of certain parameters such as the road stiffness and climate on the embedment depth, there is no direct specification on the embedment depth.

2.1.6 Austrroads Design Method

The Austrroads method (Sprayed Seal Design Project Group 2001) considers many factors during calculation of binder and aggregate application rate. This design procedure is also selected by the NCHRP 680 report as a recommended design method for chip seal applications in the U.S.

Austrroads method is based on certain assumptions on aggregate, traffic and embedment consideration (Schuler et al. 2011). Aggregates are assumed to be one stone layer thick with a flakiness index between 15% and 25%. This design procedure is valid for less than 10% heavy traffic and about 2 years after construction, percent embedment depth is assumed to range from 50% to 60%.

In this design method, the basic binder application rate is calculated by percentage of void between aggregates filled with asphalt (VFA), void content between aggregates (VMA), traffic volume and type. In addition to basic binder application rate, design binder application rate is calculated by adding other modifications depending on texture of existing surface, aggregate embedment into existing surface (substrate), binder absorption into substrate and aggregate. The aggregate application rate is determined by considering traffic level, aggregate size and shape and loose unit weight. In Austrroads design method, aggregate rate is only calculated in unit of square meter per cubic meter (m^2/m^3). The authors of NCHRP 680 report converted this to aggregate application rate in units of pound per square yard (lb/yd^2).

2.1.7 South African Method, TRH3

The South African design method was developed for designing different kind of sealing types such as single and double chip seal (with either conventional or modified binder), cape seal, slurry seal and sand seal. South African designs for different seal types are mostly based on Hanson's design concept, where asphalt binder fills the voids between aggregates and average least dimension determines these voids (The South African National Roads Agency 2007). One of the assumptions this design method made is that, in order to prevent aggregate loss, approximately 42% of voids between aggregates (which is equivalent about 30% of height) should be filled by the binder.

There are two different binder rates described in South African design method; cold and hot binder application rates. Hot binder application rate is the net binder application rate used in construction; whereas, the cold binder application rate is the application rate before subtracting extra part such as water in the emulsions before evaporation. Residual binder application rate is referred to as the net cold binder rate. Aggregate size in terms of average least dimension, traffic level, road stiffness measured by ball penetration test and desired texture at the end are necessary input parameters in order to calculate cold binder application rate. Climate, existing surface condition determined by sand patch test, road geometry in terms of slope are secondary inputs for adjusting cold binder application rate. At the end, the hot binder application rate used in construction is calculated by multiplication of the net cold binder rate and the conversion factor

depending on binder type. The aggregate spread rate is obtained by design chart in which average least dimension, flakiness index and type of chip seal information are taken as input. Summary of the Chip Seal Design Methods

The factors affecting both aggregate and binder application rate for each chip seal design method is summarized in Table 1. Although embedment depth criterion is not a direct input in design equations at these chip seal design methods, all design methods mention that embedment depth is one of the most significant criteria that should be achieved at a certain level. Also, all design methods propose certain percent embedment depths just after construction and then after some years of service.

Table 1 Parameters used in different chip seal design methods

DESIGN METHODS: FACTORS	Hanson	Kearby	McLeod	Modified Kearby	Road Note 39	Austrroads	South African, TRH3
Voids between aggregates	✓	✓	✓			✓	
Aggregate Size and Shape		✓	✓	✓	✓	✓	✓
Aggregate Dry Unit Weight			✓	✓	✓	✓	✓
Percent Embedment Depth		✓	✓	✓			
Traffic Level			✓	✓	✓	✓	✓
Residual Binder Content			✓			✓	✓
Existing Pavement Condition			✓	✓	✓	✓	✓
Absorption of Aggregate			✓			✓	
Existing Pavement Hardness					✓	✓	✓
Climate					✓		✓
Geometry of Road					✓	✓	✓

2.2 NCHRP 680 Procedure for Determining Percent Embedment

NCHRP Report 680 (2011) recommends two procedures that are very similar to the sand patch method. These two approaches estimate percent embedment via (i) spreading and (ii) submerging procedures. For both, the goal is to find texture height, and then the aggregate embedment is calculated by subtracting available texture height from average aggregate height. In spreading procedure, a known volume of glass beads is poured on chip seal surface in a way that

all voids are filled by glass beads. It is assumed that the cross section is similar to the idealized cross section shown in Figure 3.

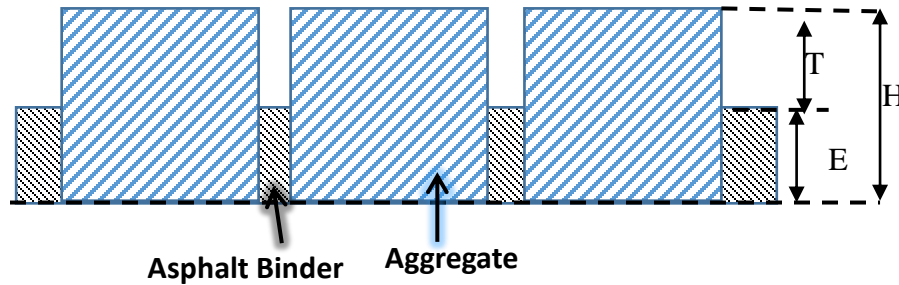


Figure 3 Illustration of an idealized chip seal cross section used in NCHRP 680 methods

Average height of the aggregate particles (H) is equal to texture height of glass beads (T) plus the height of binder (E) (Schuler et al. 2011). Texture height (T) is calculated by dividing volume of beads and aggregate above the asphalt surface by plan area of beads and aggregate. Since the average height of the aggregate (H) is known from the size of the aggregate chips, height of the binder (E) is obtained subtracting texture height (T) from the average particle height. Percent embedment depth is calculated by using the following formulas:

$$E = H - T \quad [2.1]$$

$$PE (\%) = \frac{E}{H} \times 100 \quad [2.2]$$

where PE = percent embedment, E = embedment depth, H = height of aggregate particles and T = texture height of glass beads, PE = percent embedment depth.

In the submerging procedure, the chip seal sample surface is completely covered with a variable volume of glass beads at a fixed height above particles. In this procedure, it is important to subtract the excess volume of glass beads on the chip seal surface from the total glass bead volume for calculating texture height (T). The volume of glass bead filled voids (B) is estimated by subtracting volume of excess glass beads on the chip seal surface from total volume of glass beads (C). Texture height is then calculated by dividing the volume of glass bead filled voids (B) by the plan area of the beads using Equation 2.3. After the calculation of texture height, the percent embedment depth is estimated by using formulas 2.1 and 2.2.

$$B = C - [(M - S - H) \times A] \text{ and } T = B/A \quad [2.3]$$

where B = volume of glass beads in the voids, C = total volume of glass beads, M = total height including excess volume of glass beads on the surface, S = base thickness, H = average particle height and A = plan area of the chip seal, T = texture height

Estimation of percent embedment by using these methods (recommended by NCHRP Report 680) is straightforward. However, size distribution of aggregates and aggregate penetration into the substrate is ignored (see Figure 4). Also, the substrate is considered to be perfectly straight and no binder leakage into the existing pavement is assumed.

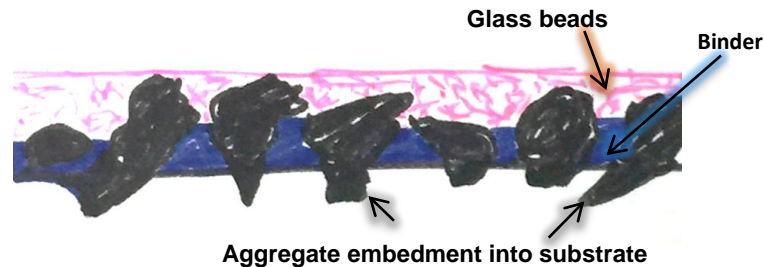


Figure 4 Illustration of the potential errors caused by the NCHRP 680 procedures

2.3 Performance Tests for Chip Seals

A summary of various tests to evaluate chip seal characteristics is shown in Table 2.

Table 2 Various test methods used to evaluate asphalt chip seals

Test Methods	Applicability		Property measured
	Lab	Field	
ASTM D7000 Sweep Test	x		% mass loss
Vialit Adhesion Test	x		% mass loss
Frosted Marble Test	x		% mass loss
Australian Aggregate Pull-out Test		x	Necessary pull-out force
Pennsylvania Aggregate Retention Test	x		% mass loss
British Pendulum Test	x	x	British Pendulum Number (BPN)
Locked Wheel Skid Test		x	Skid Number (SN)
Third Scale Model Mobile Loading Simulator (MMLS3)	x		% mass loss
Pneumatic Adhesion Tension Test	x		Pull-off adhesion strength achieved at failure

2.3.1 ASTM D7000 Sweep Test

The sweep test (ASTM D7000) is one of the laboratory test methods suggested by the NCHRP Report 680 (2011) for evaluation of the performance of asphalt chip seals in terms of aggregate loss. The test procedure includes fabrication of asphalt chip seal samples, and testing by applying shear force to the surface of aggregates by using a nylon strip brush affixed to the mixer. Before and after testing, the sample is weighed and the percentage of mass loss is calculated (ASTM D7000). The goal of sweep test is to measure adhesive properties of the emulsion just after the construction, not to simulate traffic effect. In other words, this test method is designed to assess the curing characteristics of chip seals. However, researchers have used this method to evaluate the performance of the chip seals (Wasiuddin et al. 2013 and Johannes et al. 2011).

2.3.2 Vialit Adhesion Test

The Vialit Adhesion Test (European Standard EN 12272-3) was first introduced in France to measure the effect of binder and aggregate type on performance. It consists of three components: metal base with the vertical rod, steel ball and metal test plates. Jordan III et al. (2011) studied applicability of the Vialit test on surface seal treatments with respect to performance. The authors concluded that results from the Vialit test are always questionable and it is not sufficient to make conclusions regarding performance of seal treatments. Another study from Epps et al. (2001) also suggested that results from the Vialit test are so inconsistent that they cannot differentiate between good and poor performance of the seal treatments.

2.3.3 Frosted Marble Test

The frosted marble test (FMT) was first introduced by Benedict (1990). The FMT intended to measure binder adhesion by applying torque to marbles fixed to a base tray with the binder. The test setup consists of a torque wrench, a hooked foot for applying shear and a tray on which binder is spread and marbles are placed, respectively. Howard et al. (2009) made a modification to the FMT setup by including temperature control using an environmental chamber. They also modified the curing procedure. Howard et al. (2009) stated that, even though the results from the FMT seem to be valuable for evaluating performance of binder adhesion and curing, it is not enough by itself and other test methods should be used to make comprehensive evaluation. Also, they concluded that the testing variability is another issue of the FMT, primarily because of the hooked foot position and marble positions on the tray of the test.

2.3.4 Australian Aggregate Pull-out Test

This test method (Road and Traffic Authority of New South Wales RTA T-238) was developed for finding the necessary pull-out force to separate aggregates from the asphalt bitumen material in surface seal treatments. After the surface seal treatment is prepared, the embedded aggregates are fixed by a crocodile clip and 20 g/sec pull-out rate is applied to the stone until it is detached. During this procedure, load measurements are taken continuously (Queensland Department of Transport and Main Roads 2012). One of the uses of this test method is to determine the duration of traffic control after construction. In addition, coated average area of the binder on the aggregate can be observed visually to correlate with the peak tensile stress needed to pull out the aggregate (Senadheera et al. 2006).

2.3.5 Pennsylvania Aggregate Retention Test

The Pennsylvania aggregate retention test (PART) was first developed by National Center for Asphalt Technology Auburn University (Kandhal and Motter 1991). The test simulates the effect of traffic on surface seal treatments by using a 'Humboldt "Mary Ann" Laboratory Sieve Shaker'. The surface seal treatment sample is prepared within the pan and after compression and curing process, initial aggregate loss is obtained by turning the pan upside down. Then, the pan is placed in the sieve shaker upside down at an inclination of 45°. After 5 minutes of shaking, aggregate loss is measured and calculated as a percentage.

2.3.6 British Pendulum Test

The British Pendulum Test (BPT) is one of the tools used for measuring surface frictional properties. The measurement values obtained from the British Pendulum Test are scaled as BPN (British Pendulum Number), which represents frictional properties by measuring the energy loss when rubber slider slips over the sample (ASTM E303-93, 2013). The primary advantage of BPT is its applicability to both field and laboratory testing. However, Lu et al. (2006) stated that since BPT is capable of applying low speed to the surface (6 mph), the test only can measure the skid resistance due to microtexture of the surface. Higher speed is required to obtain the effect of macrotexture. In addition, the ASTM standard (ASTM E 303-93) does not have any temperature correction. The British standard (BS 7976-2) includes temperature factors only up to 35°C. Therefore, temperature factor for BPT is an issue for the places having warmer climates.

2.3.7 Third Scale Model Mobile Loading Simulator

The third scale model mobile loading simulator (MMLS3) is one of accelerated pavement testing devices for determining performance of different kinds of pavements by simulating traffic effect in a determined scale. Lee (2003) first introduced the MMLS3 to measure the hot mix asphalt (HMA) performance with respect to fatigue cracking and rutting. This test machine consists of 4 bogies, 1 axle per bogie and 1 wheel/tire per axle (Bhattacharjee et al., 2004). Each wheel has a diameter of 80 mm and is capable of applying max 800 kPa pressure, and between 1.9 kN and 2.7 kN load. Since the MMLS3 is inside an environmental chamber, the desired temperature can be sustained. In addition to applicability of MMLS3 to HMA pavements, this test is also applicable to surface seal treatments. Lee (2007) came up with design modification for Hanson design method for asphalt seal surface treatments by stating reference voids content after MMLS3 tests for lightweight and granite aggregate types.

2.3.8 Pneumatic Adhesion Tension Test

The pneumatic adhesion tension testing instrument (PATTI) (ASTM D4541) is used for evaluating bond strength of an asphalt binder by applying direct tension. Unlike the direct tensile bond tests such as the ASTM C1583 or D7234, in PATTI, the same pulling rate can be applied to each test sample (Zhou et al. 2014).

2.4 Image Processing Techniques for Performance Evaluation of Chip Seals

Kim et al. (2008) used image analysis techniques to quantify the texture differences in chip seals compacted using different rolling patterns. Chip seal cores were taken before and after the different rolling procedures, then the cores were sliced and images were obtained by using a scanner. Macrotexture profiles were obtained by using MATLAB-based algorithms and the root mean square roughness of the chip seal profiles were estimated (ASME 2002). Then rolling effectiveness was investigated by looking roughness values derived from the chip seal profiles. One drawback of this method comes from the imaging technique. Kim et al. (2008) also stated that some of the aggregates seemed to be flying on the image since they attached to surface at different place. Therefore, the algorithm was not always able to compute the profile accurately.

An extensive study was conducted by Kodippily (2013) to investigate the flushing mechanism of chip seals. In this study, the effect of volumetrics and the distribution of air voids in chip seal samples was studied via analysis of X-ray Computed Tomography (X-ray CT) images and flushing models were developed. This study showed that X-ray CT imaging is a viable option for determining internal structure of chip seal surfaces non-destructively. However, X-ray CT is not a practical method of obtaining images because of its cost and the expertise necessary to obtain images.

Wielinski et al. (2011) selected three different sections on a road and pictures were taken at these sections over time. With the help of image processing techniques, they differentiated aggregates and binder from the chip seal texture pictures at different time periods, and then calculated aggregate retention of the specific sections. The main drawback of this technique is that dust on the binder in the field caused some problems during differentiation of binder and aggregate during image processing.

In general, image processing techniques used in the current literature on asphalt chip seal focused on obtaining the surface texture, or air voids within the chip seal samples. None of the methods were able to provide percent embedment directly.

2.5 Numerical Studies on Asphalt Chip Seals

A first attempt at developing a numerical model in order to evaluate the performance of an asphalt chip seal was made by Huurman et al. (2004). This study showed the applicability of finite element methods on surface seal treatments. Due to some deficiencies, an improved model was established. In the prototype model, asphalt bitumen was placed between aggregates; whereas, a mastic like (bitumen-rich) layer was defined below the aggregates due to embedment of aggregate into the existing pavement. Spherical aggregates were first randomly generated on a surface and gaps between the aggregates were filled with the bitumen. In order to simulate the surface angularity of the aggregates, the coordinates of the finite element nodes on the surface of the aggregates were adjusted (by another randomly selected multiplier) to create ‘angular/rough’ surfaces. A simulated tire load was applied to each stone individually and the vertical, lateral and longitudinal stress values were calculated by considering axle load and pressure, tire speed and distinguished shape functions proposed by Groenendijk (1998). Aggregate was assumed to be linear elastic, whereas the bitumen was assumed to follow the generalized Burger’s viscoelastic model.

Huurman’s FEM study (Huurman 2010) included the evaluation of the performance of the chip seals by examining punching and aggregate rotation, fatigue cracking, low-temperature cracking, moisture damage and adhesion failure.

Henderson (2006) used images of actual two-dimensional chip seal slices to develop a finite element model (FEM) to study the performance of chip seals. Due to limitations in computational time, aggregates were taken as rigid (instead of linearly elastic). Bitumen material behavior was modeled by using Prony series. Quadrilateral and triangular elements were used for aggregates and binder, respectively. Applied load was determined by the study of de Beer (1994), which free rolling truck tire was simulated in the way that tire surface contacted all surface and rolled in or out of the page. The results with respect to stress and strain were determined.

Although these studies give an insight into performance of chip seal surfaces under different conditions like using different sizes of cover aggregates and different types of binder, it is still so far away from giving actual results due to modeling chip seal in a perfect pattern. In other words, chip seal models in FEM analysis in current studies have been modeled in a perfect arrangement in terms of aggregate and binder position in the model. In that way, Henderson's study (2006) is much better to simulate actual chip seal performance by using slice images of the cores taken by the field. However, only 2D analysis of performance of chip seal was done.

2.6 Summary of the Literature Review

It can be concluded from the review of the relevant literature that aggregate embedment into the binder plays a significant role for prevention of distresses (e.g., aggregate loss and bleeding) in chip seals. Most of the design methods mentioned in this chapter recommended a desired percent embedment right after the construction and after certain traffic. However, all these recommendations were based on the observations and field experiences. There is no study that directly developed relationship between embedment depth and performance of the chip seals.

Methods such as the sand patch test (recommended by NCHRP Report 680) and texture scanning make certain assumptions while calculating the embedment depth. First, the existing pavement is assumed to be perfectly flat; therefore, pavement deteriorations on the surface are ignored. Aggregate embedment into the existing substrate is also neglected; however, aggregates do embed into the existing substrate in chip seal construction when the existing pavement is relatively soft (especially during hot summer days). In addition, binder seepage into existing substrate due to existing cracks on the surface is also ignored. These assumptions may have significant effects on the percent embedment. Therefore, this study focused on developing a method of estimating percent embedment without such assumptions.

The other test methods to measure the performance of chip seal applications are not related to the embedment depth. The target of these test methods is generally about adhesion properties of emulsion binder under different conditions. They do not include embedment depth concept as a performance criteria or one of the factors affecting the performance.

The work regarding image analysis techniques on chip seals done so far is not related to obtaining the percent embedment. Texture properties of the chip seals and air voids existing in the chip seal were investigated through image processing techniques. Therefore, there is a need for developing image-based algorithms to directly estimate embedment depth of chip seals.

The numerical study of chip seals is a relatively new topic. Modeling of chip seal in the most appropriate and field performance suitable way is still being investigated. Therefore, the effect of the embedment depth on performance is not studied in numerical studies on chip seals. This is the primary research gap, which has been attempted to be filled by this research project. In this project, image analysis based algorithms have been developed to compute the embedment depths of chip seal pavement sample, thus opening a new door to objective investigation of chip seal samples, without making any assumptions (as discussed before).

3. METHODOLOGY

3.1 Experimental design

In this research project, laboratory and field samples were analyzed for percent embedment with the image analysis tool and methods (that were designed in the course of project) and final conclusions were made. Forty-eight (48) chip seal cores were collected from 8 different road sections in total and forty (40) laboratory samples were fabricated. The broad outline has been given in Figure 5.

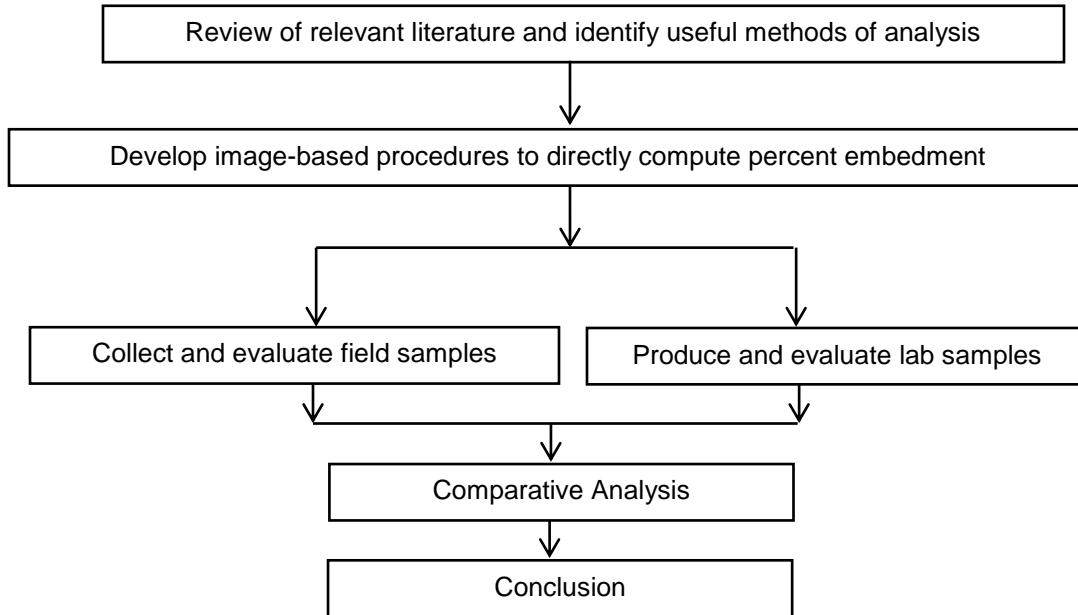


Figure 5 Experimental design flowchart

3.2 Equipment and procedures

During the course of the project, a gamut of equipment and procedures were used to acquire field samples, fabricate lab samples, and to prepare and analyze samples. The following section contains a stepwise explanation.

3.2.1 Field Chip Seal Samples

Chip seal samples initially were obtained by taking cores from the field. Forty-eight (48) chip seal cores were collected from 8 different sections in Michigan. The surface types of these chip seals were different. Chip seal cores collected from the field are summarized in Table 3. Among these 48 samples, thirty-nine (39) single chip seal samples could be analyzed. Image analysis was not possible for the remaining 9 field chip seal cores, including all five that were taken on a double chip seal project (more details are given further in the report). Chip seal samples from the M-57 near Pompeii, M-20 near New Era, M-33 from Alger to Rose City, M-86 east of Plainwell, M-43 in Woodland and US-31 in Bear Lake were sliced and analyses were completed. The aggregate and binder properties were not available for most of the sections. However, it can

be assumed that contractors constructed the chip seal sections according to MDOT specifications for construction. Desired minimum aggregate physical requirements, emulsion chemical properties, as well as application rate ranges are given in MDOT specifications in division 5 under the chip seals section (2012). One of the most important parameters for aggregates affecting performance is the size distribution. According to MDOT specification (2012), 90 to 100% aggregates and 0 to 10% aggregates should pass through 3/8 inch sieve size and No.4 sieve size, respectively. The sizes of the aggregates were also verified using the image analysis procedure. Also, in MDOT's specification, the aggregate application range is from 20 to 24 lb/yd² (depending on the existing surface condition), and the binder application range is from 0.39 to 0.46 gal/yd².

Table 3 Summary of field chip seal cores (single chip seals unless noted)

Field section	Number of cores
M-57 near Pompeii	5
M-20 near New Era	8
M-33 from Alger to Rose City	8
M-86 east of Plainwell	8
M-43 in Woodland	4
US-31 in Bear Lake	6
M-57 near Clio (double chip seal)	5
M-57 near Carson City	4
Total number of cores	48

The field sections were selected by the MDOT crew. Before taking cores from the chip seal sections, the MDOT crew performed both a sand patch test and a laser texture scan to measure texture depth of corresponding section. Then, chip seal samples were taken with a coring machine. The procedure for collecting chip seal core samples from the field is illustrated in Figure 6.

Contractors are responsible to use a specified aggregate size for chip seal treatments based on MDOT chip seal specification (2012) in Michigan. Aggregates were collected from the section on M-33 from Alger to Rose City. Since construction was already complete the day of the site visit, no aggregate stockpiles or haul trucks were available for sampling. Therefore a sample was obtained from a location where there was a significant amount of loose aggregate swept off the newly applied chip seal onto the shoulder. The size distribution of aggregates is shown in the Figure 7, which is based on the laboratory sieve analysis as well as the image processing techniques. The size distribution for aggregates was determined using image-based algorithm developed by following the recommendations of Kumara et al. (2012). The 2-D images were used and areas of the particles were estimated with some assumptions. The gradation was obtained by using area of an ellipse, which is calculated by using the following formula:

$$A = \pi \times \left(\frac{a}{2}\right) \times \left(\frac{b}{2}\right) \quad [3.1]$$

where A = area of the aggregate, a = the length of long axis, and b = the length of the intermediate axis. From the 2-D images, a and b values were directly obtained from image-based algorithms. The percentage passing through a sieve was calculated by using the formula 3.2:



Figure 6 Procedure for taking cores from the field

$$\text{Percent Passing} = \frac{\sum_i^p (A_i \times b_i)}{\sum_i^n (A_i \times b_i)} \times 100\% \quad [3.2]$$

where A = area of the aggregate, b = intermediate axis length p = number of aggregate passing through the grain size, and n = total number of particles.

The procedure for computing gradation of aggregates by image-based algorithms is as follows:

- The aggregates are placed on the light table and pictures are taken by a document camera (see the Figure 3.3(a)).
- Aggregates are obtained separately (see the Figure 3.2(b)) and long and intermediate axis properties are taken from the algorithm. The resolution is calculated as mm/pixel.
- Area of each aggregate is calculated and percent passing through each grain size is obtained by using Equation 3.2.

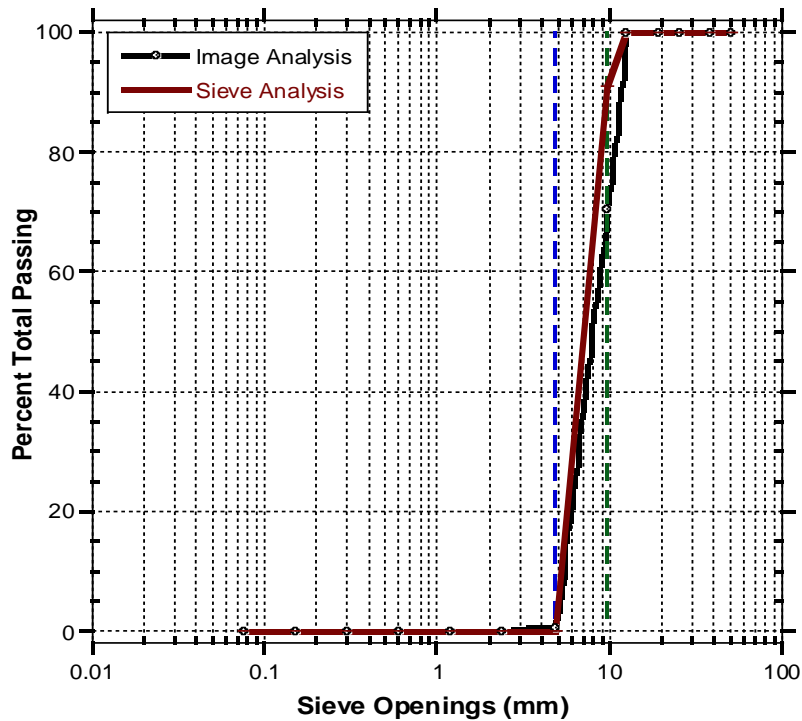


Figure 7 Gradation of the aggregates used in the field M-33 from Alger to Rose City

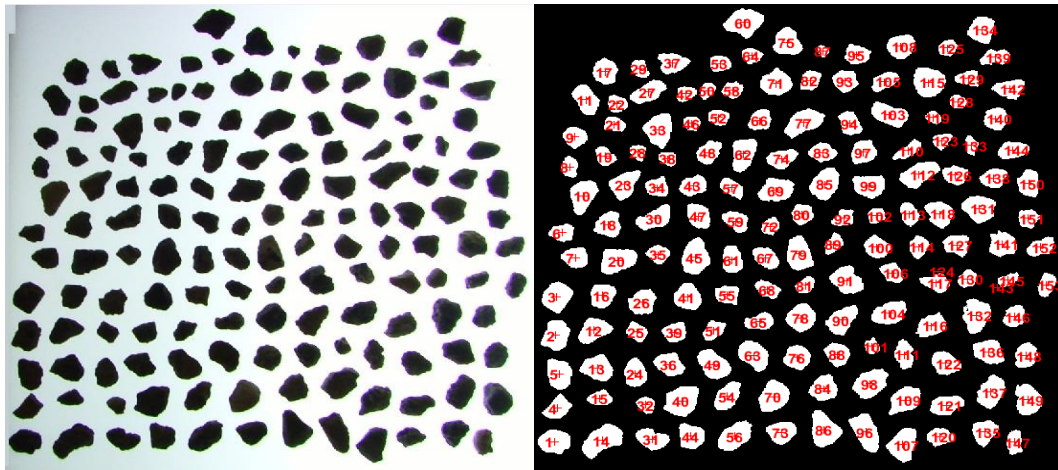


Figure 8 (a) Original image obtained from a document camera (b) Aggregate determination

3.2.2 Laboratory Chip Seal Samples

In this section, the physical properties of aggregates, the chemical properties of emulsion and the procedure for fabricating chip seal samples in the laboratory are discussed. A total of 40 laboratory samples were fabricated. These 40 samples can be divided into two groups:

- Group 1:** This group included 8 chip seal samples. The goal was to investigate the effect of binder and aggregate application rate on percent embedment depth. For that purpose, 8 chip seal samples were fabricated by using the lowest and highest binder and aggregate application rates specified in the MDOT Standard Specifications for Construction (2012). Each set consisted of 2 replicates, and 4 different sets (8 samples) (see Table 4)

Table 4 Summary of group 1 laboratory samples

Set No.	Binder App. Rate (gal/yd ²)	Aggregate App. Rate (lb/yd ²)
1	0.39	20
2	0.39	24
3	0.46	20
4	0.46	24

- Group 2:** This group consisted of thirty-two (32) chip seal samples (see Table 5). The aim was to investigate the effect of sweep test on percent embedment and surface coverage area. Sixteen (16) sets of chip seal samples were prepared, and two replicates were prepared for each set (32 total chip seal samples were tested). Eight (8) sets were analyzed without performing sweep test, and remaining eight (8) of them were analyzed after sweep test was performed on the samples.

Table 5 Summary of group 2 lab samples

Sample No.	Binder App. Rate (gal/yd ²)	Aggregate App. Rate (lb/yd ²)
1	0.39	20
2	0.40	20
3	0.41	20
4	0.42	20
5	0.43	20
6	0.44	20
7	0.45	20
8	0.46	20

3.2.2.1 Gradation of Aggregates and Sieve Analysis

The aggregates used for fabricating chip seal samples were selected according to MDOT Standard Specifications for Construction (2012). The size distributions of the aggregates obtained

using laboratory sieve analysis and image based algorithms are shown in the Figure 9. As shown, uniformly graded aggregates were used to fabricate the chip seal samples. The two-dashed lines represent 3/8 inch (9.75mm) and No.4 (4.75 mm) sieve size, from left to right respectively. It can clearly be seen that the aggregates satisfied the condition of 90 to 100% passing 3/8" sieve and 0 to 10% passing #4 sieve in accordance with the MDOT Standard Specifications for Construction (2012). In addition to the gradation, relatively round gravel aggregates were used during chip seal fabrication.

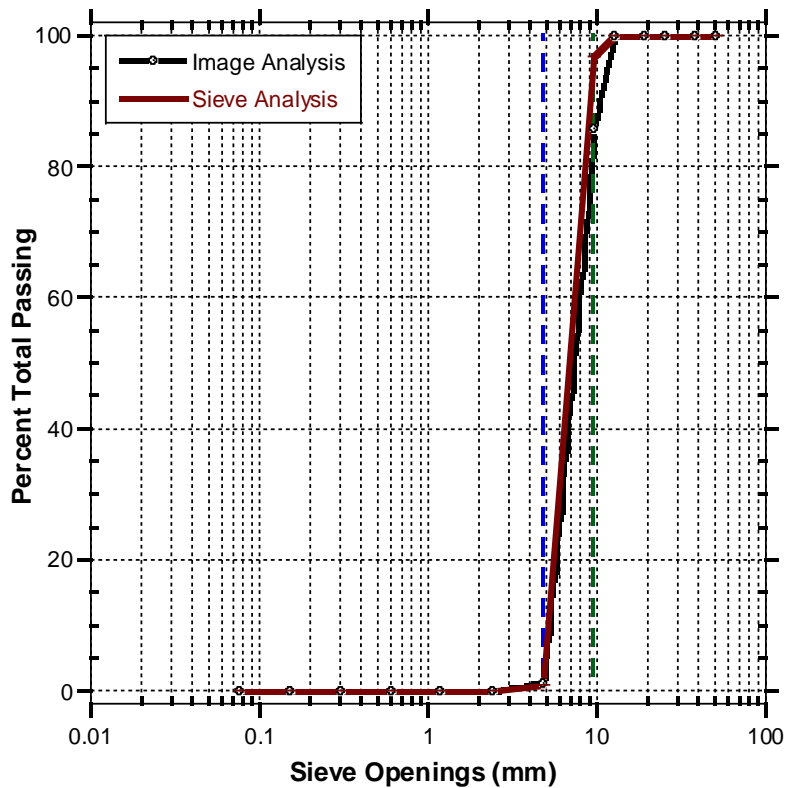


Figure 9 Gradation of the aggregates used in the laboratory

3.2.2.2 Emulsion Binder

The emulsion binder used for laboratory chip seal was obtained from Ergon Asphalt & Emulsions, Inc. The emulsion type was CRS-2, which is a cationic rapid-setting type emulsified asphalt. Rapid setting emulsions are frequently used for chip seal construction (NCHRP Report 680, 2011), but CRS-2 is not currently specified by MDOT for that use. Compositions on ingredients of emulsion are summarized in Table 6.

Table 6 Composition/ information on ingredients

Chemical Name	% in the Composition
Asphalt	50 - 70
Water	20 - 40
Hydrochloric Acid	< 1

3.2.2.3 Procedure for Chip Seal Sample Fabrication

The chip seal fabrication procedure can be divided into 3 steps: (i) binder application, (ii) aggregate application and (iii) compaction. Before preparing chip seal samples, hot mix asphalt samples with height of 40 mm were fabricated using a gyratory compactor to act as a pavement substrate for the chip seal.

- **Emulsion Binder Application:** The emulsion binder was applied as follows: (1) The required mass of emulsion binder was calculated by using the specific gravity for the emulsion and the surface area. (2) The emulsion binder was placed in the oven at 80°F for an hour. (3) Tape was used to make a barrier around the HMA sample edge to prevent the emulsion from spilling over the HMA sides (Figure 10a). (4) The desired emulsion binder mass was poured onto the HMA surface and spread to cover the sample's entire surface by rotating the sample (Figure 10b).



Figure 10 Binder application process: (a) pouring emulsion on the sample, and (b) spreading the binder by gravity & rotation

- **Aggregate Application:** Aggregate application on the HMA specimens was performed by using an aggregate spreader designed and manufactured in MSU's Advanced Asphalt Characterization Laboratory (AACL). The working principle of aggregate spreader is based on the study of Howard et al. (2013). A sketch of the components of the aggregate spreader is shown in Figure 11. Using the spreader, aggregate application on four HMA specimens can be performed at the same time and a uniform aggregate spread can be sustained. Steps of aggregate spreading are summarized as follows: (1) Four cylindrical HMA mixtures are placed in the box of the aggregate spreader, (2) The desired mass of aggregate (according to the target application rate) is placed on the spreader sheet, (3) The aggregate controller (which ensures a single aggregate layer is spread) is placed on the top of the aggregate spreader, (4) The spreader plate which holds the aggregates is pulled off to drop the aggregates on the HMA surface. This general procedure is illustrated in Figure 12.

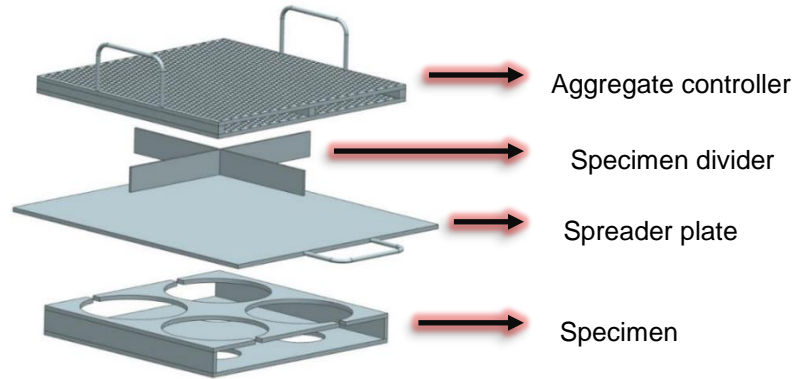


Figure 11 Sketch of the components of the aggregate spreader



(1&2)



(3)



(4)

Figure 12 Procedure for using aggregate spreader

- Compaction:** Compaction of the chip seal was conducted by using both the sweep test compactor and a cyclic load testing system. Also, a rubber sheet was placed on the top of the chip seal surface to simulate the effect of a rubber tire roller. In addition to the sweep test compactor, each chip seal sample was compacted by a cyclic load testing machine. About 600 ± 18 kPa pressure (2383 ± 70 pound-force for 6-inch diameter sample) was applied in stress-controlled cyclic haversine mode at a frequency of 0.1 Hz for 25 cycles. The pressure was the same as the one used in AASHTO T312 (2015), which is the

procedure for preparing hot mix asphalt samples by gyratory compactor. Compaction procedure is illustrated in Figure 13.

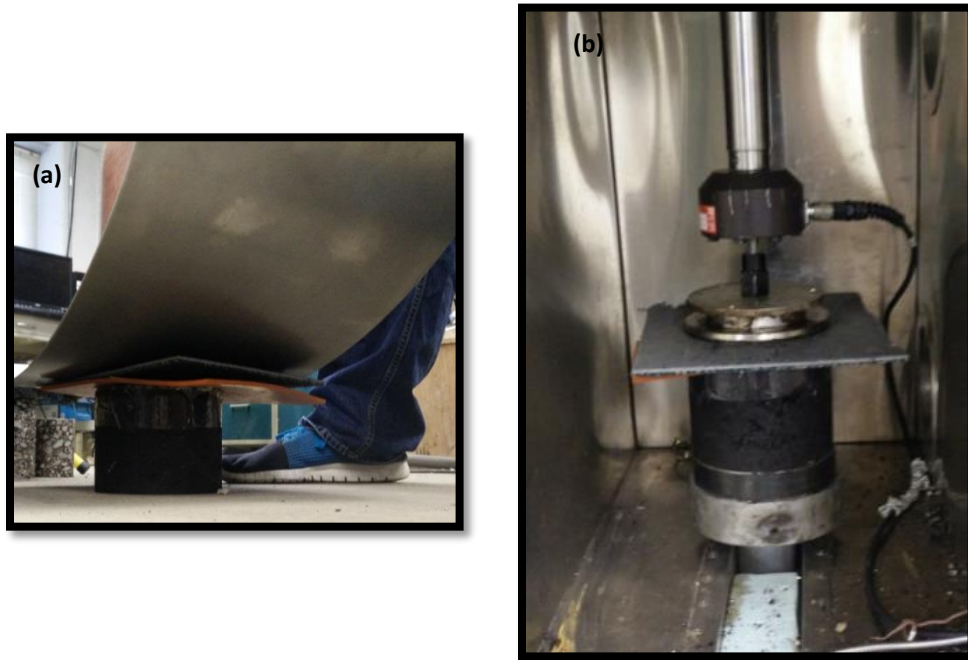


Figure 13 Sweep test compactor and compaction using the MTS: (a) Sweep test compactor and (b) compaction with MTS

3.3 Image Processing and Analysis Methods

3.3.1 Sample Preparation and Image Acquisition

As shown in Figure 14, the chip seal samples need to be sliced vertically to form a clean vertical face so that the different phases (aggregate and chip seal binder) are distinctly visible and clear. Then, the digital images are captured using a digital camera. There are two steps applied for cutting chip seal core samples in order to slice them properly (Figure 14). The first step was a horizontal cutting procedure to make the core sample height smaller. The height of shortened chip seal cores was about 1.5 inches. Primary reason for the ‘shortening’ was to be able to fit the cores into the sweep test setup. The second cutting operation was vertical slicing. Typically, four (4) slices can be obtained from a six (6) inch diameter core. Image of the two faces of each slice can be acquired and analyzed, providing total eight (8) images per core. For cutting the 6” diameter cores horizontally, a typical asphalt diamond saw was used (Covington brand, 20-inch diameter wet slab saw with maximum cutting speed of 1150 rpm). The sawing was done wet (using tap water). For cutting the samples vertically, a small tile saw was used (Ridgid brand, 7-inch diameter wet tile saw with maximum cutting speed of 3450 rpm). This tile saw was purchased from a local hardware store. After obtaining physical cross sections (slices) from the chip seal cores, cross section pictures were taken by using a document camera (see Figure 15). There are some important sample preparation criteria that are necessary for algorithms to work properly. These criteria are listed as follows:

- The top of the chip seal surface should be covered with a uniformly colored substance. Blue play dough was used in this project to cover the top of the chip seal during imaging.
- Good color contrast between the aggregate and binder is necessary.

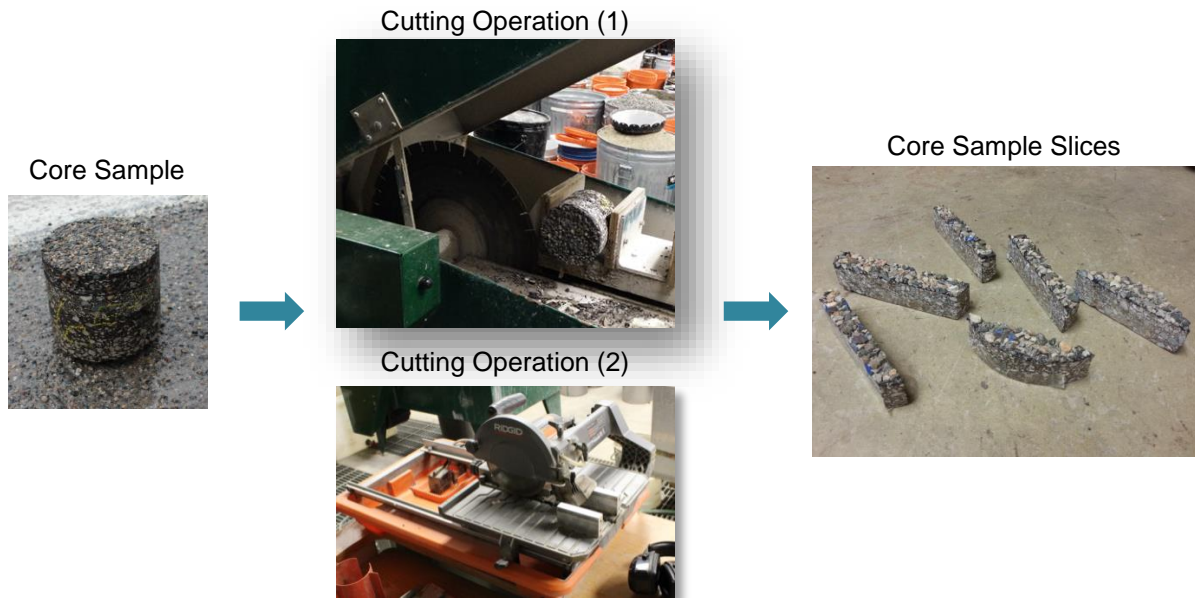


Figure 14 Sample cutting procedure

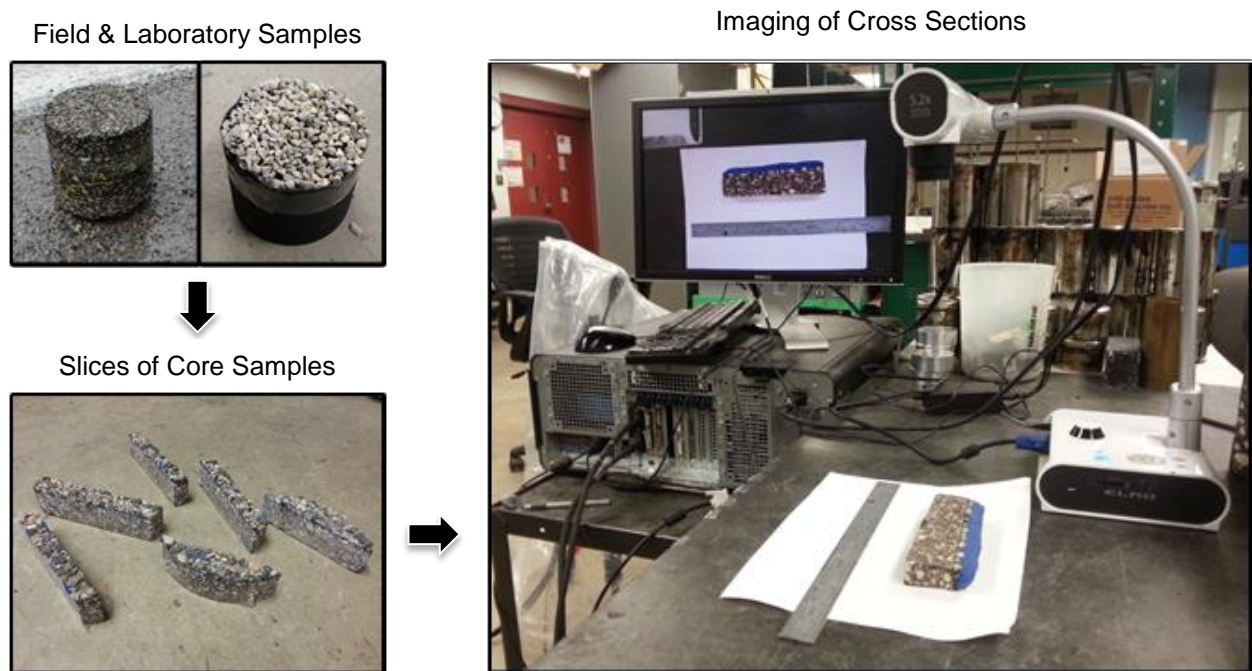


Figure 15 Illustration of sample preparation and image acquisition

- There should be no light reflection on the binder or the aggregates during imaging. Several imaging techniques had been tried before getting good imaging results. Practicing for taking pictures with professional camera at different light conditions was done. However, a document camera (Elmo Model TT02RX) with indoor white fluorescent light was found to be the best option for imaging. A desirable cross section image is illustrated in Figure 16.



Figure 16 Desired cross section image

- Another issue encountered in most of the cores from the field was the appearance of the aggregates because of their type. Blast furnace slag aggregates are commonly used in Michigan because of their availability, their low specific gravity (less windshield damage reported), their low cost and their porous nature helping in the friction. However, this kind of aggregate has a lot of holes, which prevents the image-based algorithms to work properly. Another difficulty with the blast furnace slag aggregates was their dark color. Since color contrast between aggregate and binder is poor; it is very difficult to analyze these images without improving the cross section surface for imaging. Figure 17 illustrates an example problematic cross section.

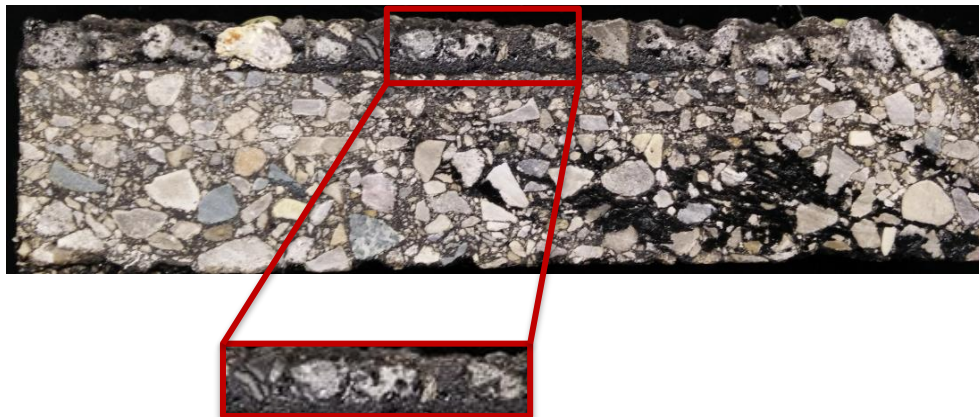
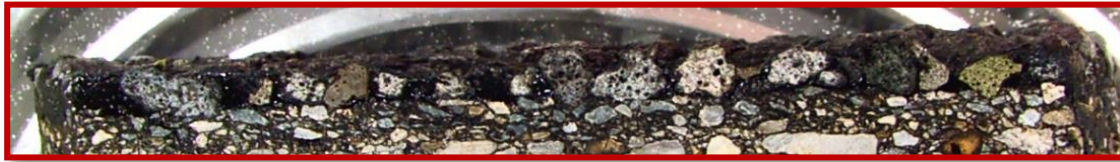


Figure 17 Image-based problems from cross sections

- After several trials for improving cross sections, painting aggregates using a fine tip white pen was found to be promising. The aggregates were painted by using fine tip board marker (DecoColor opaque paint marker with white color code 300 – S White) the holes on the aggregate surface were filled. This method appeared to be successful after cross section images were analyzed by using image-based algorithms. The Figure 3.14 illustrates the

field chip seal cross section before and after modification. This modification was performed on all the field cross sections having blast furnace slag aggregates.



(a) Cross section before the painting



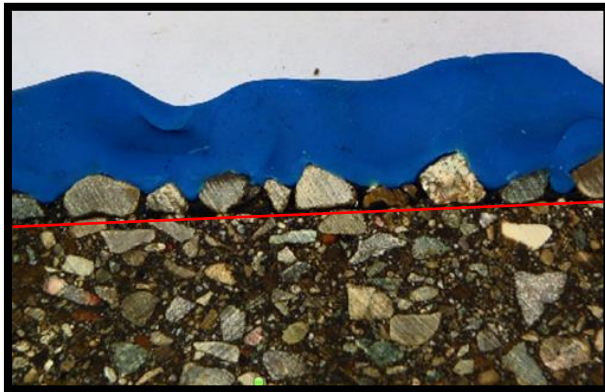
(b) Cross section after the painting

Figure 18 The effect of painting on cross section image

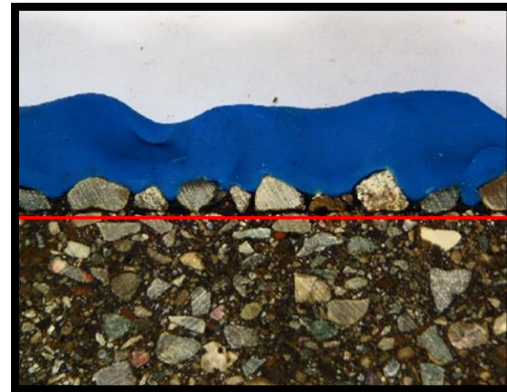
3.3.2 Image Adjustments

Before processing the chip seal cross-section images, some further adjustments were necessary. First, since some cross sections were not aligned horizontally in the images, they were rotated until the substrate surface is horizontal (see Figure 19). Then, the images were cropped such that only the desired portion of the image, in the vicinity of the chip seal, is visible. This also prevented the algorithms from being computationally expensive. All these adjustments were made through a MATLAB graphical user interface (GUI) algorithm, developed as part of this study.

(a) Original Image



(b) Rotated Image



(c) Cropped Image



Figure 19 Illustration of an (a) original image, (b) rotated image, (b) cropped image.

3.3.3 Finding the Pavement Substrate in the Image

One of the important steps was to find the existing pavement surface underlying the chip seal (i.e., the substrate). For that purpose, certain points were initially set on the existing pavement manually in the algorithm (as input). These points were placed just below the emulsion of the chip seal and care was taken to select sharp changes of color as shown in Figure 20a. The algorithm connects these points and forms a discrete curve (red line shown in Figure 20b) consisting of multiple straight lines. Another parallel line (blue line shown in Figure 20b) is automatically drawn 15 pixels above the red curve. Then, the color image was converted to a grayscale image by applying some of the filtering techniques, including a Gaussian filter and image sharpening. These filtering techniques were used to hide the noise in the grayscale image. Then, for each x-coordinate, the intensities of the pixels located between blue line to red line were plotted as a profile (see Figure 20c). The direction of the profile was from the blue line towards the red line. The pixel locations, which had normalized pixel value smaller than 0.2 (which is the intensity threshold for transitioning from (dark) binder to (bright) substrate), were determined. It should be noted that theoretically, since the binder is black, it should have a pixel intensity of 0 out of 255, where 255 correspond to pure white (any pixel intensity between 0 and 255 corresponds to different shades of gray). Therefore, the normalized pixel intensity of $0/255 = 0$ should correspond to asphalt binder. However, depending on brightness of the image, binder color intensity may be slightly greater than 0. After looking at many images, it was determined that the normalized pixel intensity of 0.2, which corresponds to $0.2 * 255 = 51$ is about the maximum value for a binder. Any intensity larger than 51 usually corresponds to other objects, e.g., dark aggregates, therefore not classified as binder. The algorithm starts from binder and moves towards the substrate (top to down in the image). When the last pixel value less than 0.2 was found, it is taken as the transition point between existing pavement and chip seal surface emulsion. For instance, in Figure 20c, pixel values are taken from top to bottom at a specific x-coordinate. The last pixel value less than 0.2 (see plot in Figure 20c) is the transition point. This process is repeated for all columns of pixels (from left to right) to obtain the profile shown in Figure 20d.

3.3.4 Computing Percent Embedment using Peak & Valley Method

In this method, first, the chip seal surface is determined by using color contrast between the blue play dough and aggregates (Figure 21). Then, local maxima and minima values are found on this line. Peak values are assumed to be the top of the aggregate and valley values are assumed to be the top of the binder. Since all local maxima and minima values are found on the profile, a user-defined threshold value (defined as delta in the algorithm) is used to limit number of peak and valley points. The steps of the algorithm for limiting the number of peak and valley points are as follows:

- All peak and valley values are found.
- The algorithm looks at the height difference between two adjacent points (peak and valley points)
- If the height difference between these points is smaller than the delta value defined by the user, points are ignored until the condition is satisfied.

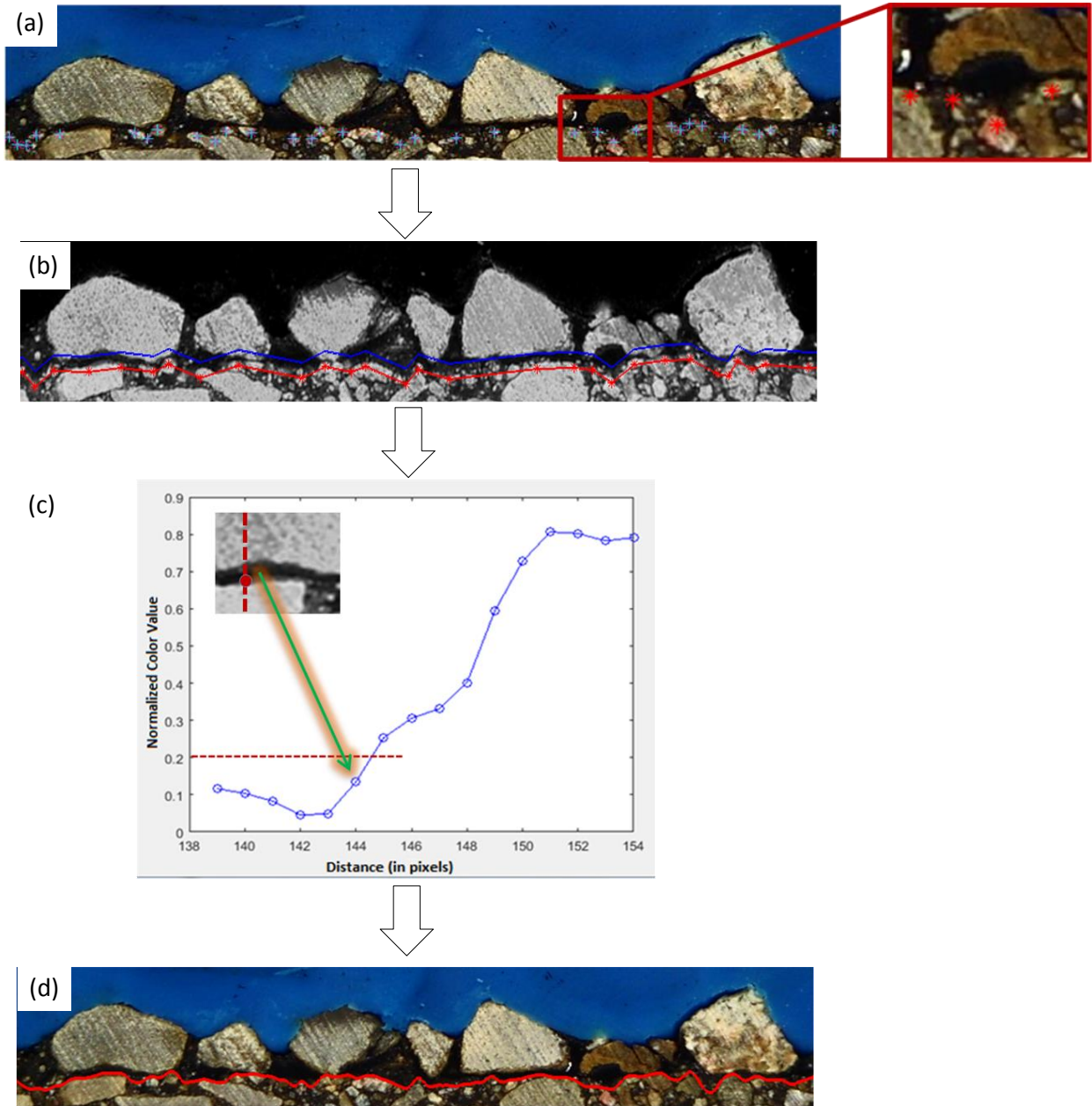


Figure 20 Illustration of the steps of determining the existing pavement surface

The average y-coordinate of existing pavement (found in a previous step) is taken and used as the existing pavement substrate line (Figure 3.18b). One of the aggregate heights is calculated by subtracting the existing pavement line height from the peak height corresponding to the top of an aggregate particle. The same procedure is applied for calculating the binder height by using

valley points (Figure 3.18c). Then, averages for the aggregate and binder heights are estimated and the ratio of binder height to aggregate height times 100 gives percent embedment depth.

$$PE_{pv}(\%) = \frac{h_b}{h_s} \times 100 \quad [3.3]$$

where PE_{pv} =percent embedment based on peak/valley method, h_b = average binder height, h_s = average aggregate height.

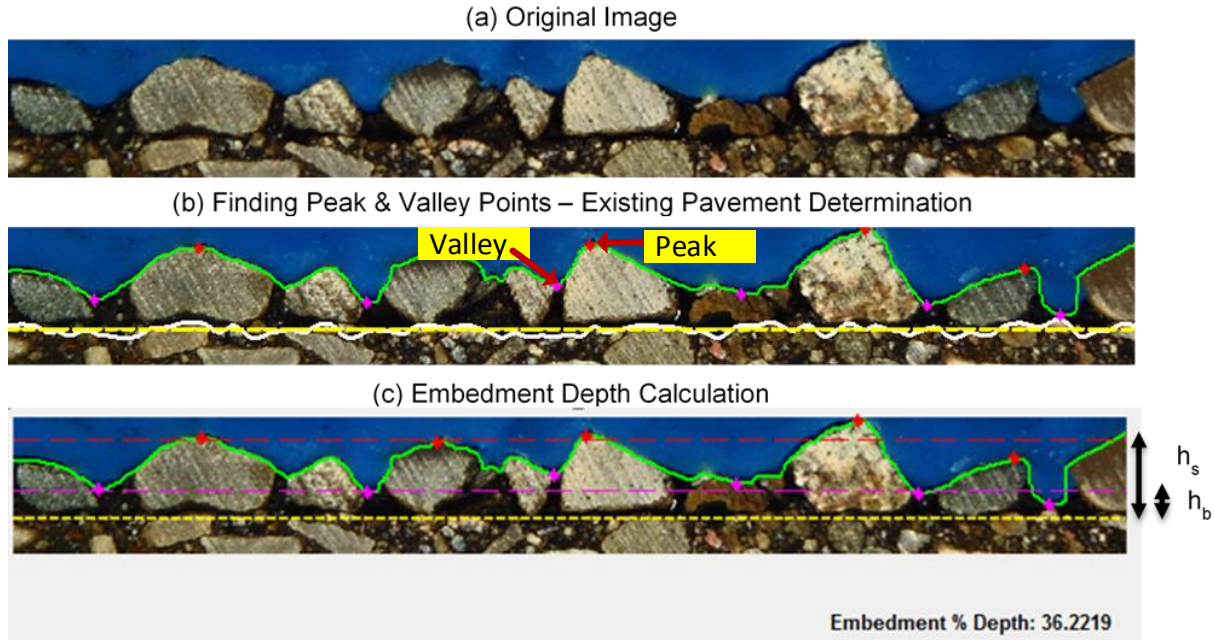


Figure 21 Steps of peak & valley method

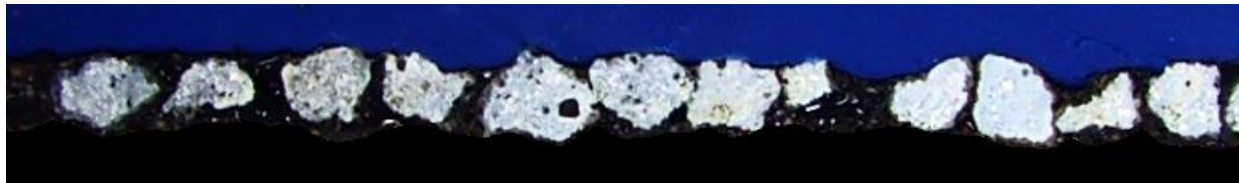
3.3.5 Computing Percent Embedment of Each Aggregate

This algorithm computes the percent embedment of each aggregate individually, followed by a statistical analysis to compute the distribution of percent embedment. The algorithm steps for this method are as follows:

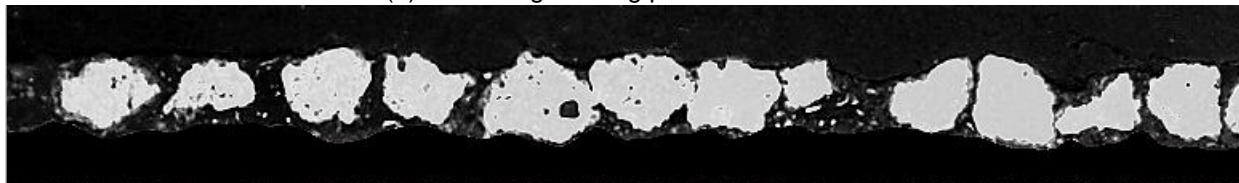
- All pixels under the existing surface are converted to black color in order to remove irregularities on the existing pavement (see Figure 22a).
- The true color (RGB) image is sharpened. This makes the features of the image such as edges to look sharper. After the sharpening of the image, the image is transformed to grayscale image by manipulating red, green and blue color indexes of the image so that aggregates become a lighter color and the remaining parts including the blue play dough turn dark (see Figure 22b).
- The grayscale image is then modified by applying 2-D median filtering (see Figure 22c). This modification removes the irregularities (noise) on the image and this filtered image is

converted into a black and white image. Then a series of dilation and contraction operations were performed to fill the holes on the aggregate surface (see Figure 22d and Figure 22e).

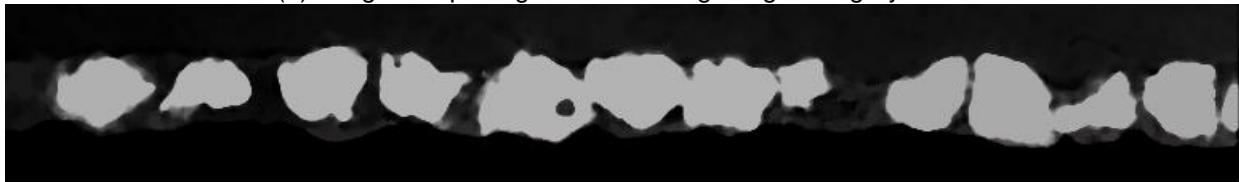
- Finally, watershed transformation is performed to separate the aggregates that appear to be sticking to each other (see Figure 22f)



(a) Removing existing pavement section



(b) Image sharpening and converting image into gray-scale



(c) Application of 2-D median filtering



(d) Converting gray-scale image into black and white image



(e) Filling the holes on the aggregate surface



(f) Watershed transform application to separate aggregates

Figure 22 Illustration of steps of identifying individual aggregates.

- Aggregate properties such as x and y coordinates of their perimeters can easily be computed once they appear to be ‘islands’ of white pixels in an image. This was accomplished using the ‘regionprops’ command in MATLAB.

- Once the perimeter pixels of individual aggregates are obtained, the intersection between the chip seal surface line and an aggregate perimeter is determined as shown in Figure 23.
- The left and right end points of intersecting lines for each aggregate are assumed to be peak binder heights.
- The binder height for each aggregate is the average of two binder peak points from the base (lowest y-coordinate) of the corresponding aggregate (see Figure 23b).
- Each aggregate height is calculated by subtracting the lowest y-coordinate from the highest y-coordinate for the corresponding aggregate (see Figure 23b).
- The embedment depth for each aggregate is calculated by dividing the binder height by the aggregate height.

$$P_{e(i)}(\%) = \frac{h_{b(i)}}{h_{s(i)}} \times 100 \quad [3.7]$$

where P_e = percent embedment of i^{th} aggregate, $h_{b(i)}$ = binder height for the corresponding to the i^{th} aggregate, $h_{s(i)}$ = i^{th} aggregate aggregate height.

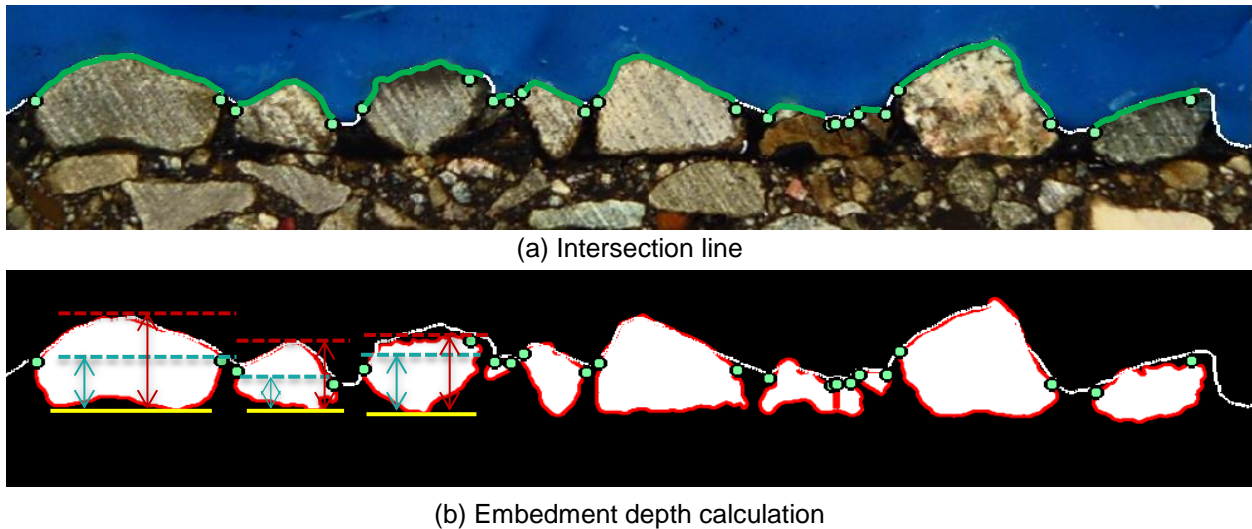


Figure 23 Illustration of computation of percent embedment of each aggregate

- Then the average embedment depth is computed as follows:

$$PE_{EA}(\%) = \frac{\sum_i P_{e(i)}}{N} \quad [3.8]$$

where PE_{EA} = Percent embedment based on each aggregate, $P_{e(i)}$ = percent embedment of i^{th} aggregate, N = number of aggregate for that particular cross section.

3.3.6 Computing Aggregate Surface Coverage by the Binder

Another concept that may be considered as one of the performance criteria is aggregate surface coverage (ASC) by the binder. Adhesion between binder and aggregate prevents aggregates from being pulled out. Therefore, it is hypothesized that as the percentage of aggregate surface covered by the binder increases, the probability of aggregate loss decreases.

The algorithm detects binder around each aggregate and estimates (two dimensionally) the percent surface coverage area for each aggregate. The average of these coverage areas gives a general aggregate surface coverage area.

$$PC_{EA} = \frac{\left(\sum_i \left(\frac{(A_{BS})_i}{(A_{PS})_i} \times 100\right)\right)}{N} \quad [3.9]$$

where PC_{EA} = average percent coverage of the binder (based on analysis of each aggregate), A_{BS} = binder coverage around the i^{th} aggregate, A_{PS} = perimeter the i^{th} aggregate, and N = total number of aggregates in a cross sectional image. The percent coverage of the binder around each aggregate is illustrated in Figure 24.

The steps of calculation of are as follows:

- Each aggregate's coordinates are computed, as well as the perimeter pixels.
- For each aggregate, the center coordinates (x and y coordinates) are calculated. For each perimeter coordinate, the direction from center to the perimeter is obtained (see Figure 24). Then, the pixel intensity at five (5) pixel outside a given perimeter coordinate is obtained. If the pixel intensity does not correspond to the 'blue color', it assumes that the perimeter coordinate is in contact with the binder (i.e., covered by the binder).

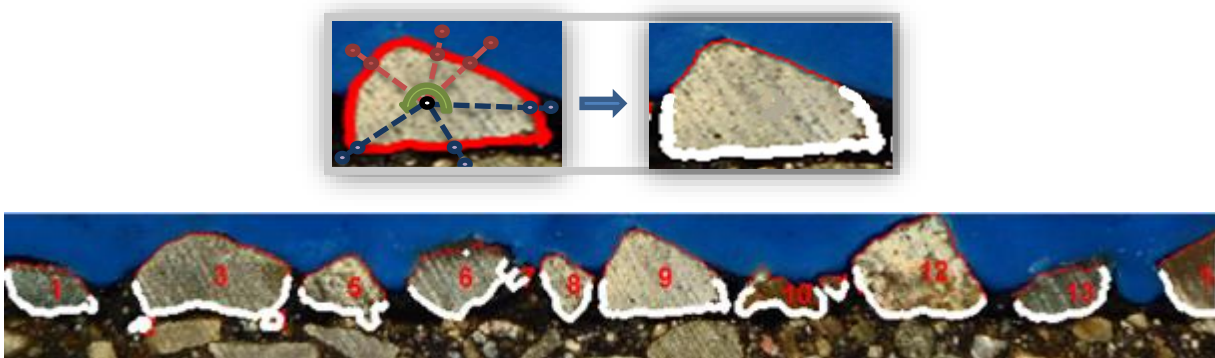


Figure 24 Aggregate surface coverage by the binder

3.3.7 Development of a standalone software package (CIPS)

The algorithms described above were implemented into a standalone software named CIPS. It is a MATLAB-based computer software package. Data is input in the form of an image

of a sliced chip seal sample. Furthermore, certain additional outputs such as binder and aggregate application rates have also been included in the software. A screenshot of CIPS is shown in Figure 25. Another additional feature of this software program is that the results can be stored in the form of Excel files for future analysis. The concept of Percent Within Limits (PWL) has also been implemented in the software. The explanation of PWL is provided later in this report.

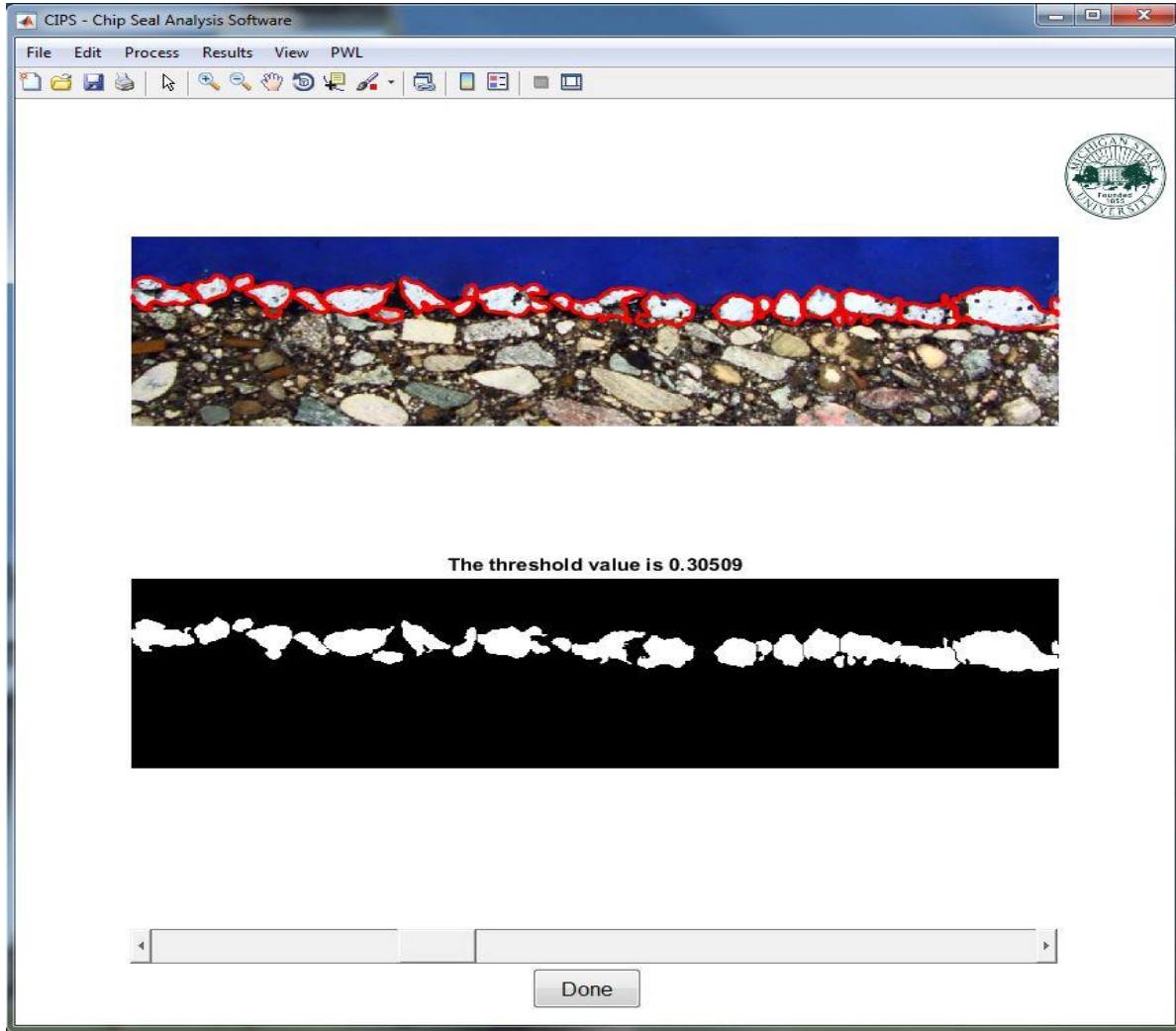


Figure 25 Screenshot of CIPS software

3.4 Validation of the Image Processing Algorithms

In order to validate the algorithms described above, a synthetic chip seal image was generated such that the percent embedment was exactly 50%. This image was used as input for the algorithms and the corresponding parameters were computed. Figure 26 shows the results of the analyses, where an excellent match is visible between the computed results and the actual percent embedment of 50%.

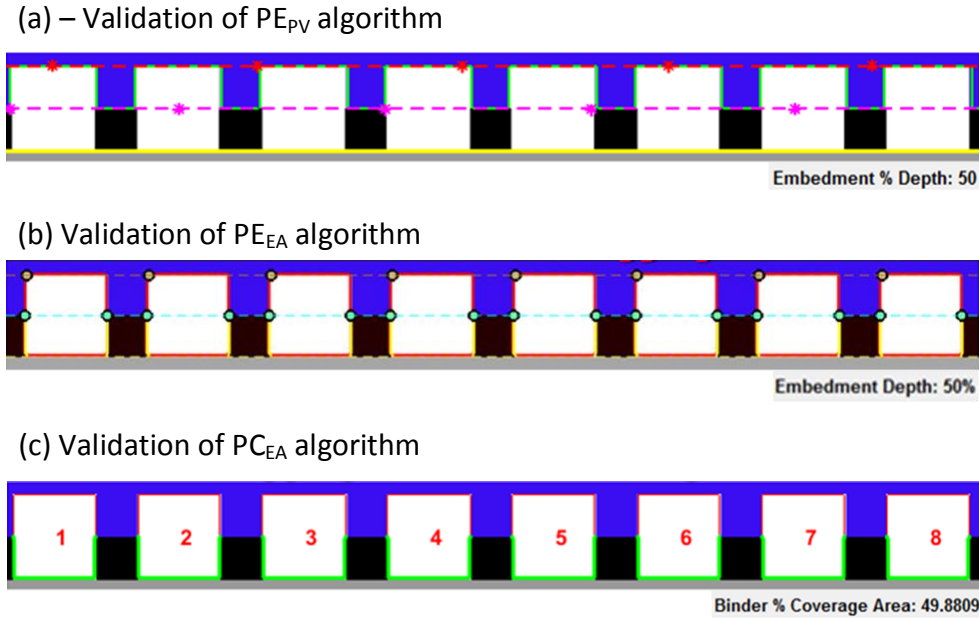


Figure 26 Illustration of idealized chip seal images with exactly 50% embedment

3.5 Traditional Methods for Estimating Percent Embedment

This section describes two traditional methods used in the laboratory for calculating embedment depth.

3.5.1 Sand Patch Test

One of the common methods used in the field to calculate the road surface texture is the sand patch test (ASTM E965). The result of a sand patch test is not sufficient to calculate the embedment depth. The mean texture depth obtained from sand patch test and average aggregate height are used together to calculate the embedment depth.

While performing the sand patch test in the laboratory, following steps were carried out:

- Ottawa sand was spread on the chip seal surface so that all voids between particles were filled and the mass of Ottawa sand was measured by using Equation 3.10. This step was repeated 3 times and mass values were noted.

$$M_O = M_{SO} - M_S \quad [3.10]$$

where M_O = mass of Ottawa sand, M_{SO} = mass of sample with Ottawa sand, M_S = mass of specimen itself.

- Since the density of the Ottawa sand was known, the volume of the Ottawa sand used for the sand patch test was computed by using the mass obtained from the previous step.
- With the information of the diameter of Ottawa sand patch covering the surface and the volume, the mean texture depth was calculated by using the following formula:

$$MTD = \frac{4 \times V_{GS}}{\pi \times (D)^2} \quad [3.11]$$

where MTD = mean texture depth, V_{GS} = volume of Ottawa sand, and D = diameter of the surface

- Mean texture depths obtained from 3 repeated measurements were averaged. Aggregates typically tend to lie on their flattest side after compaction or exposure to traffic (McLeod et al. 1969). Therefore, the average least dimension of the aggregates was estimated by using the following formula (Wood et al. 2006):

$$H = \frac{M}{1.139285 + (0.011506) \times (FI)} \quad [3.12]$$

where H = average least dimension (inches), M = median particle size (inches), and FI = percent flakiness index (in percent). Percent embedment depth is calculated by using the following formula:

$$PE_{SP} = \frac{H - MTD}{MTD} \times 100 \quad [3.13]$$

where PE_{SP} = percent embedment from sand patch method, H = average least dimension (inches), MTD = mean texture depth (inches) (shown in Figure 27).

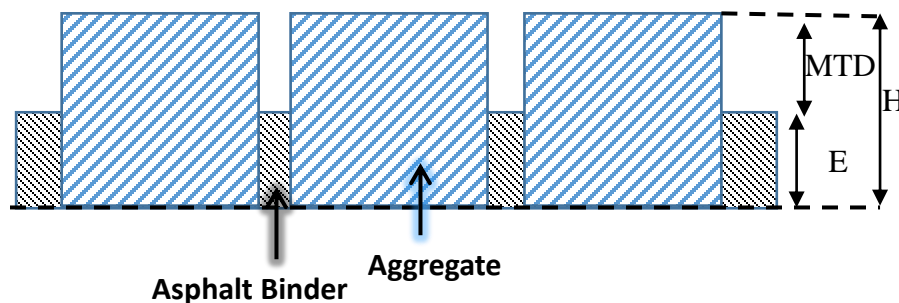


Figure 27 Illustration of an idealized chip seal cross section used in sand patch test

It should be noted that the Sand Patch method ignores the possibility of having binder underneath the aggregate chips as illustrated in Figure 28a. This was observed in some of the field cores obtained in this project (see Figure 28b). The percent embedment (PE_1) calculated when aggregates sitting perfectly on the ground is less than the percent embedment depth (PE_2) while considering the binder under the aggregates (see Figure 3.23). Furthermore, if aggregates bridge over each other, the accuracy of the Sand Patch method will also be questionable. Both of these issues are also applicable to the Laser Texture scanning described in the next section.

(a)

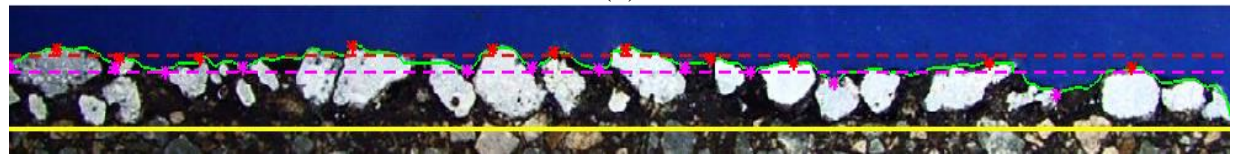
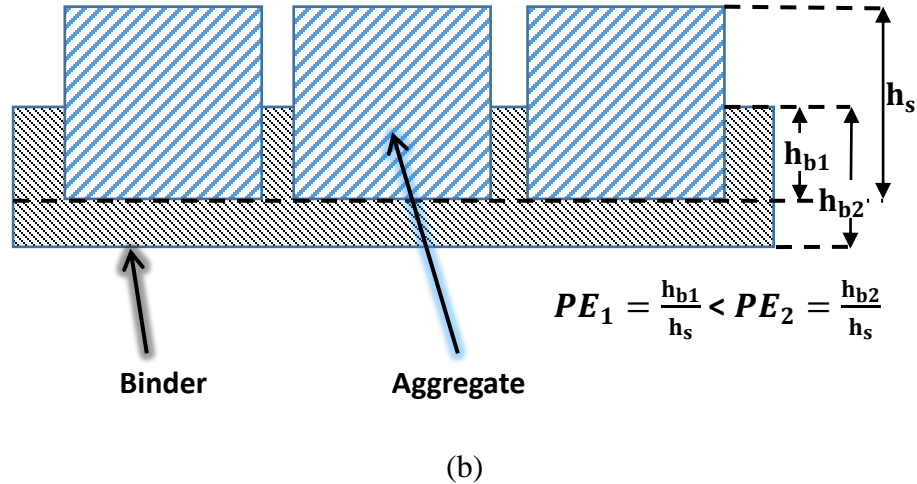


Figure 28 (a) Illustration of the chip seal where binder exists below the chips and how this affects the percent embedment and (b) an example image where there is binder below the chips

3.5.2 Laser Texture Scanning

Another way to estimate the chip seal surface texture is the use of a laser texture scanner. In this project, an Ames model 9300 laser texture device was used to measure the macro texture of the chip seal surfaces. The Ames laser texture device can scan an area with a length of 107.95 mm and width of 72.01 mm. After scanning, the scanner estimates and displays mean profile depth (MPD) and estimated texture depth (ETD). The parameter called Mean Texture Depth (MTD), which is obtained from the sand patch test, is not exactly equivalent to the Mean Profile Depth (MPD) measured using the laser texture device. Therefore, ASTM E1845 provides an empirical procedure to ‘estimate’ the texture depth which is equivalent to the MTD as follows:

$$ETD = 0.2 + 0.8 \times MPD \quad [3.14]$$

where ETD = estimated texture depth (in mm), MPD = mean texture depth (in mm). Similar to the sand patch test formulation, the percent embedment is computed as follows:

$$PE_{LT} = \frac{H - ETD}{ETD} \times 100 \quad [3.15]$$

where PE_{LT} = percent embedment from laser texture meter, H = average least dimension, ETD = estimated texture depth.

In order to calculate mean profile depth (MPD), the laser texture meter divides the profile into 100 mm length baselines. Then two peak levels are determined for the first and second half

of the baseline. The difference between peak levels and average height level is estimated and then averaged. This procedure is repeated for all baselines along the profile and the average is taken as mean profile depth (MPD), or mean segment depth. Estimated texture depth (ETD) is prediction of mean texture depth (MTD) by using MPD. Based on the Freitas et al. (2008) study, the MTD results acquired from the sand patch test are consistent with the ETD results estimated from MPD.

Estimated texture depth was assumed to be equivalent to the mean texture depth (MTD) in the results and analysis section of this report. The estimated texture depth is obtained line-by-line depending on the selected resolution. The average of these estimated texture depths gives the mean texture depth of the chip seal surface.

In this project, samples taken from the field and fabricated in the laboratory were scanned by using Ames laser texture device, which is shown in Figure 29.

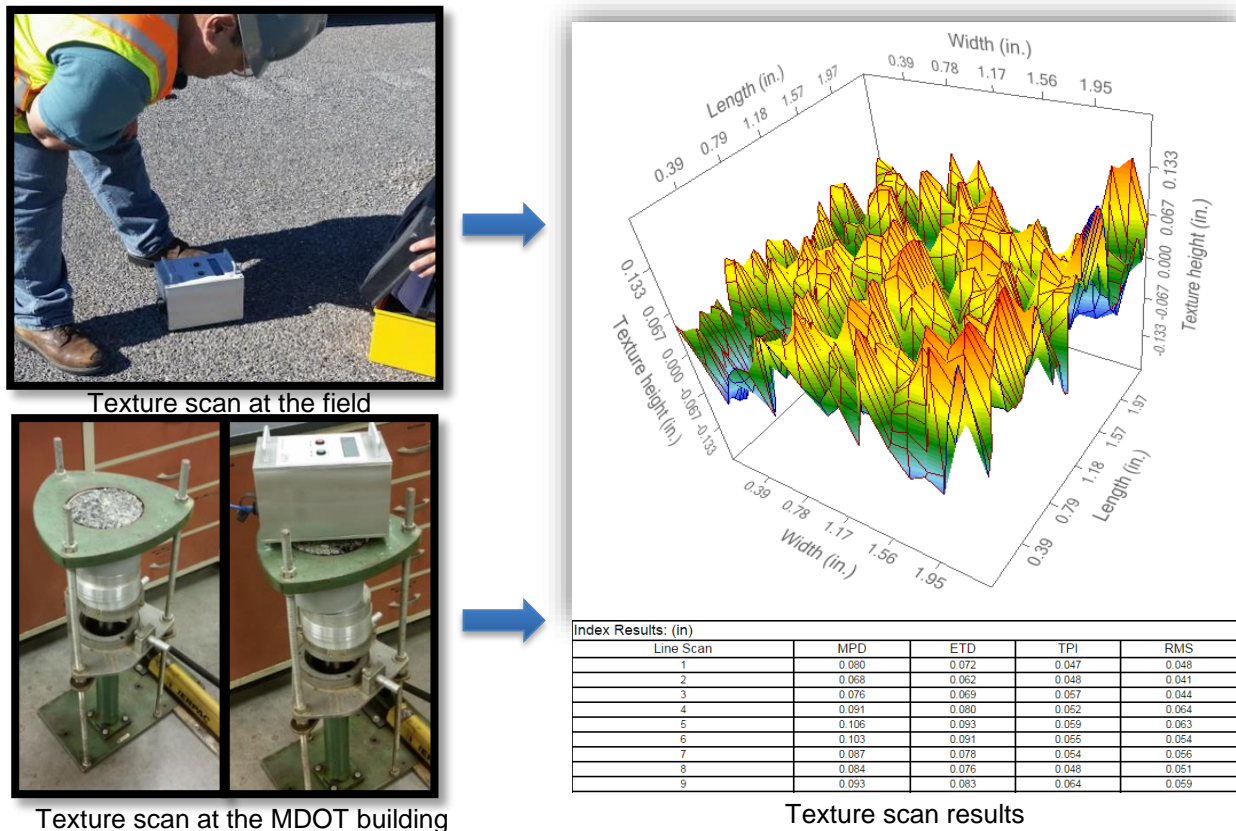


Figure 29 Laser texture scanning procedure for laboratory and field chip seal samples

3.6 ASTM D7000 Sweep Test

In this study, the ASTM D7000 sweep test was performed on chip seal samples fabricated in the laboratory. The sweep test apparatus was the same specified in ASTM D7000 except for the mixer type (see Figure 30). The specification suggests a Hobart A120 mixer; however, a Hobart N50 mixer, which is equivalent to the A120 model, was used for the sweep test due to the fact that A120 model is no longer available. The sweep test procedure was performed according to the

ASTM D7000 “Standard Test Method for Sweep Test of Bituminous Emulsion Surface Treatment Samples” and the steps followed applied during test can be summarized as follows:

- The chip seal samples were conditioned at 35°C in 30% of relative humidity for an hour.
- The chip seal sample weight was measured before the sweep test (A).
- The sweep test was performed at mixer setting #1 (0.83 gyrations per second) for 1 minute.
- The chip seal sample weight was measured after the test (B).
- Note that the hot mix asphalt (HMA) weight of the sample below the chip seal was measured before chip seal fabrication (C). The percent mass loss was calculated by using the equation 3.16.

$$\% \text{ Mass Loss} = \frac{A - B}{A - C} \times 100 \quad [3.16]$$

where A = chip seal sample weight before the test, B = chip seal sample weight after the test, and C = HMA sample weight below the chip seal surface.



Figure 30 ASTM D7000 sweep test setup used in the current study

4. FINDINGS

4.1 Analyses of the Field Cores

Forty-eight (48) chip seal samples were collected by MDOT from different locations in Michigan (see Table 3). Thirty-nine (39) samples taken from (i) M-57 highway near the Pompeii, (ii) M-20 near New Era, (iii) M-33 from Alger to Rose City, (iv) M-86 east of Plainwell, (v) M-43 in Woodland, and (vi) US-31 in Bear Lake from Michigan were analyzed. In addition, sand patch testing was conducted on all these field samples and also laser texture scanning, using the laser texture device. Cross sections obtained from the remaining 9 chip seal sample cores could not be analyzed. Five (5) of these 9 cores were taken from a double chip seal project (M-57 near Clio). On these cores, it was difficult to identify the existing pavement surface (Figure 31). Lastly, there was too much binder leakage into the substrate. The remaining 4 cores were obtained from M-57 near Carson City. These cores were damaged during coring, therefore, could not be analyzed.



Figure 31 Cross sectional image of a double chip seal sampled in this study

Table 7 shows the average and standard deviation of the embedment depths computed using various methods. Appendices A through F include all data obtained for each sample and each slice. Figure 34, Figure 35 and Figure 36 show the embedment depths for each core sample collected from different road sections. Based on Table 7 Figure 34 through 35 Figure 36, the following general conclusions may be made:

- Although embedment depth results from the sand patch test and the laser texture are different, their trends are quite similar. The reason why the error bars are higher for laser texture scan results is possibly the large differences between embedment depths based on the estimated texture depths obtained at various line scans on one sample. For the sand patch test, only one data point is obtained for a given area/sample tested.
- Laser texture scanning gives generally higher percent embedment as compared to the sand patch test. The reason can be the inaccuracy of the empirical relationship between mean profile depth (MPD) and the estimated texture depth (ETD), that is supposed to correspond to mean texture depth (MTD) obtained from sand patch test (see Figure 32). Figure 32 shows the comparison of mean profile depth and mean texture depth measured on the chip seal sections utilized in this project. As shown, the ETD equation ($ETD = 0.2 + 0.8MPD$) underestimates the MTD measured by the sand patch test when the texture depth is larger than 2 mm.
- Embedment depths of the each aggregate method (PEEA) generally produced higher embedment depths as compared to the other methods. This is primarily because of the fully-embedded aggregates (see Figure 33), which are better considered during embedment depth calculations in the each aggregate method.
- Embedment depth from the each aggregate (PE_{EA}) and aggregate surface coverage (PC_{EA}) methods seem to produce lower variability than the other methods. Also, these parameters are thought to be better than the rest of the parameters since they include analysis of each and every aggregate, rather than an overall average.
- For M-43, both sand patch and laser texture methods produced lower embedment depths because there was a significant amount of binder under the chips, which lead to an underestimation of embedment depth.

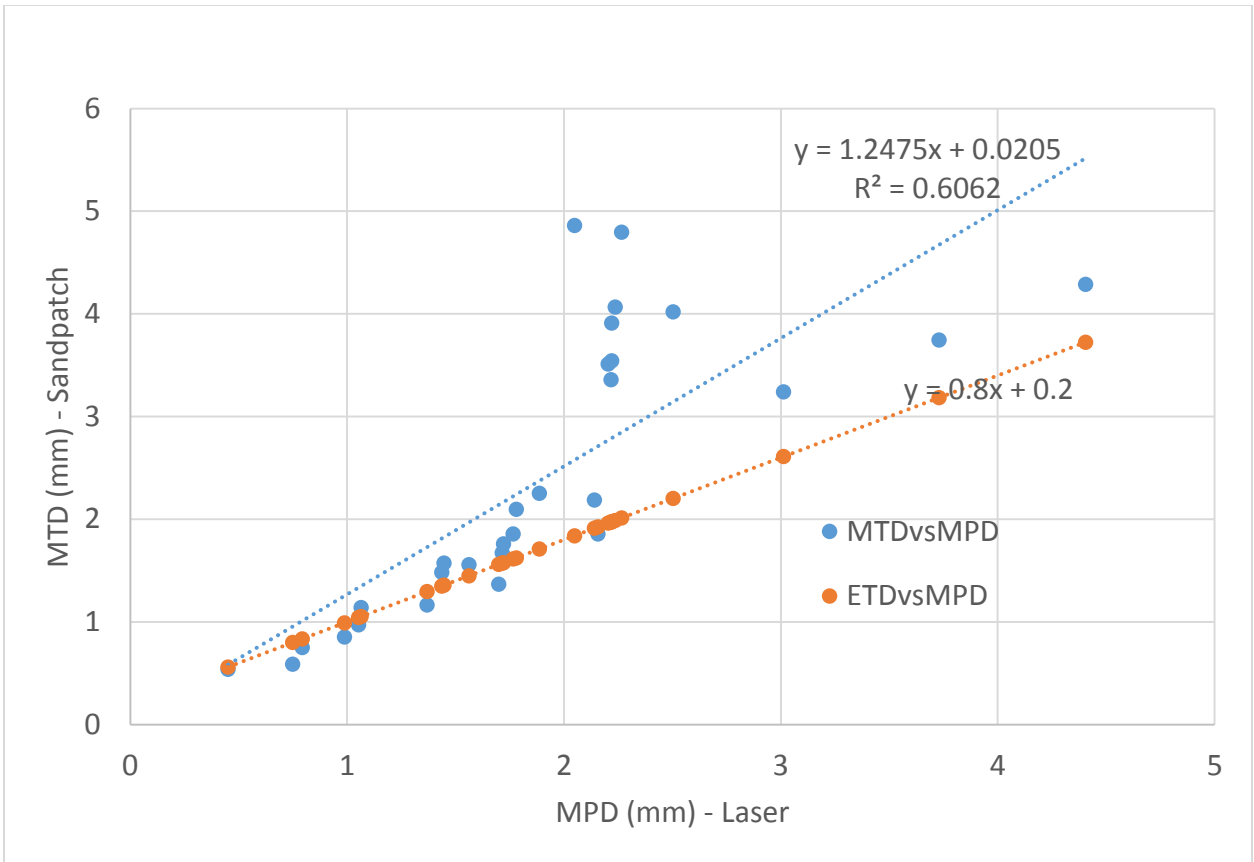


Figure 32 Comparison of mean profile depth and mean texture depth measured on the chip seal sections utilized in this project

Table 7 Average and standard deviation of the embedment depths computed using various methods

	Average				
	Embedment Depth - Peak/valley (PE _{PV})	Aggregate surface coverage (PCEA)	Embedment Depth - Each Aggregate (PEEA)	Sand Patch Test (PE _{SP})	Laser Texture Scan (PE _{LT})
M-57	53.2	51.0	81.9	56.7	69.5
M-20	63.1	60.3	78.2	56.8	72.3
M-33	70.5	61.3	79.8	65.9	72.5
M-86	67.2	64.7	81.5	76.4	77.1
M-43	79.0	84.3	91.1	43.5	53.1
US-31	65.8	54.3	73.9	83.3	83.0
Coefficient of Variation (COV) – Sample to sample variability					
	Embedment Depth - Peak/valley (PE _{PV})	Aggregate surface coverage (PCEA)	Embedment Depth - Each Aggregate (PEEA)	Sand Patch Test (PE _{SP})	Laser Texture Scan (PE _{LT})
M-57	11.1%	3.6%	3.2%	8.4%	4.1%
M-20	8.9%	6.8%	3.5%	3.7%	3.9%
M-33	8.2%	5.1%	4.1%	16.4%	10.6%
M-86	12.8%	6.1%	5.3%	8.9%	6.4%
M-43	15.5%	15.1%	7.1%	33.3%	27.2%
US-31	14.4%	26.7%	9.3%	7.8%	6.1%

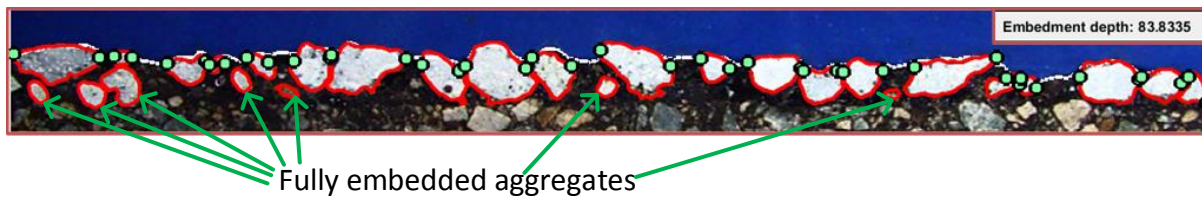


Figure 33 Examples of fully embedded aggregates

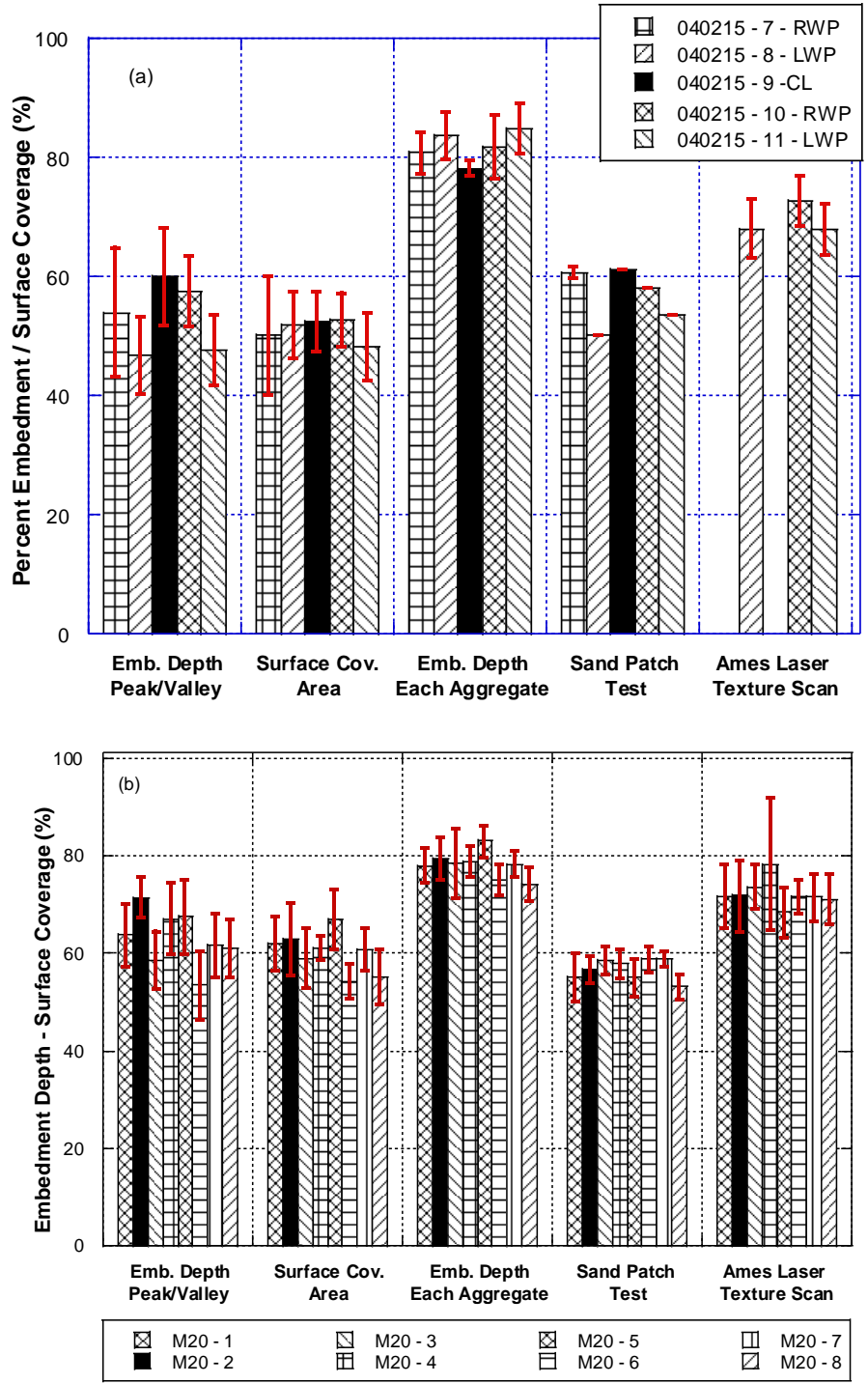


Figure 34 Comparison of different methods for (a) for M-57 Highway near Pompeii and (b) M-20 near New Era

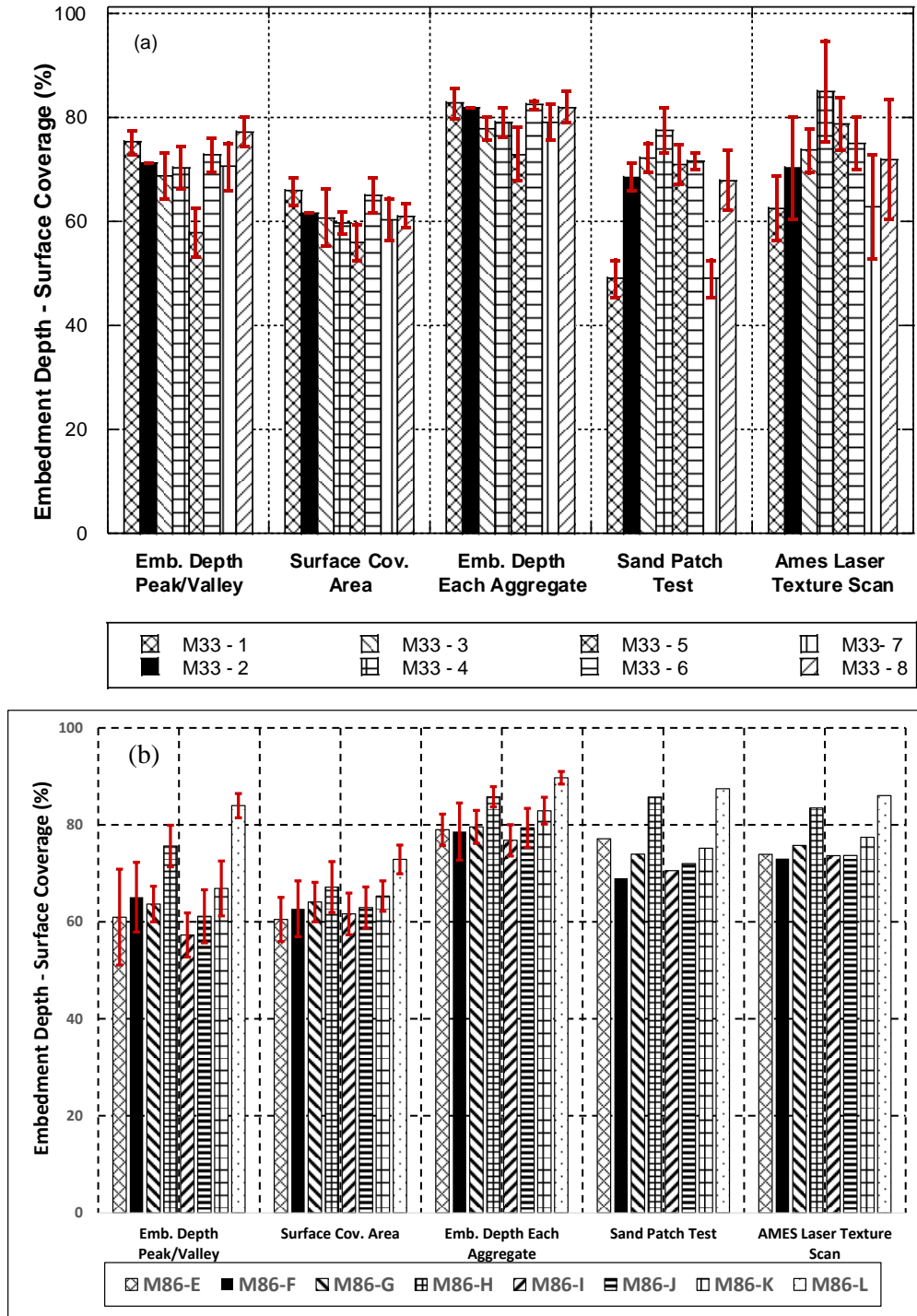


Figure 35 Comparison of different methods for (a) M-33 and (b) M-86 Chip Seal Section

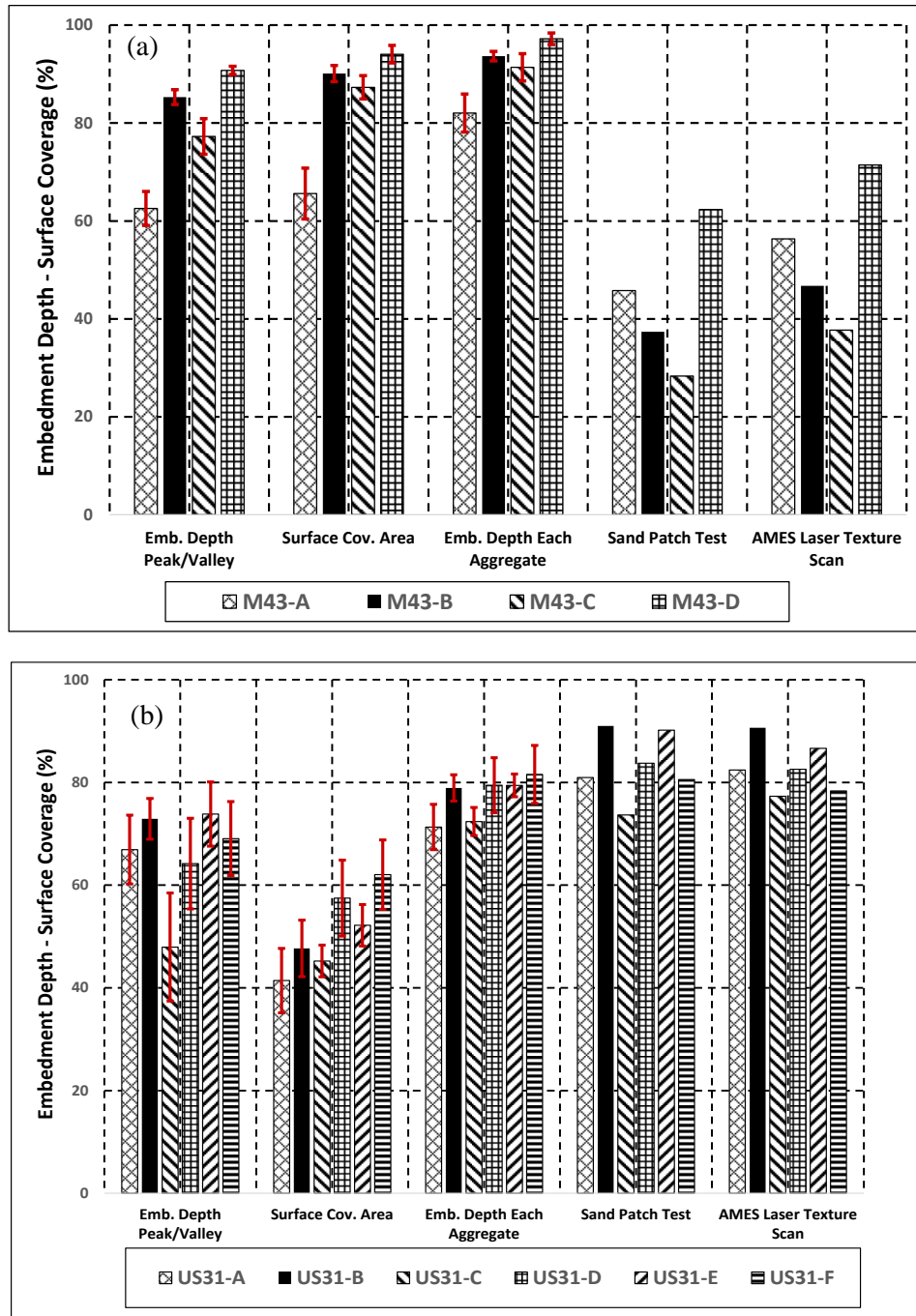


Figure 36 Comparison of different methods for (a) M-43 and (b) US-31 Chip Seal Section

4.2 Analyses of Laboratory-prepared Samples

4.2.1 Investigation of the effect of binder and aggregate application rate on percent embedment

Eight (8) chip seal samples were tested to investigate the effect of application rates (both aggregate and binder) on embedment depth and surface coverage area. Samples were prepared with upper and lower limits of both the binder and aggregate application rates. For each combination, two replicates were tested. Figures 36 and 37 show the effect of binder and aggregate application rate on the embedment depth, respectively. As shown, binder application rate has a greater influence on percent embedment as compared to the aggregate application rate. As the binder application rate increases (Figure 36), both the percent embedment depth and aggregate surface coverage increases. One of the reasons why aggregate application rate does not affect the results may be that there was already a sufficient number of aggregate chips on the surface even after application of 20 lb/yd² rate. In other words, the application rate of 20 lb/yd² is already high and leads to more than a single layer of aggregates on the surface. Since excess aggregates were taken off the surface by brushing before the cutting process, the remaining amount of aggregates on the surface were about the same whether the original aggregate application rate is 20 lb/yd² or 24 lb/yd². As a result, embedment depths obtained by image-based algorithms were close to each other.

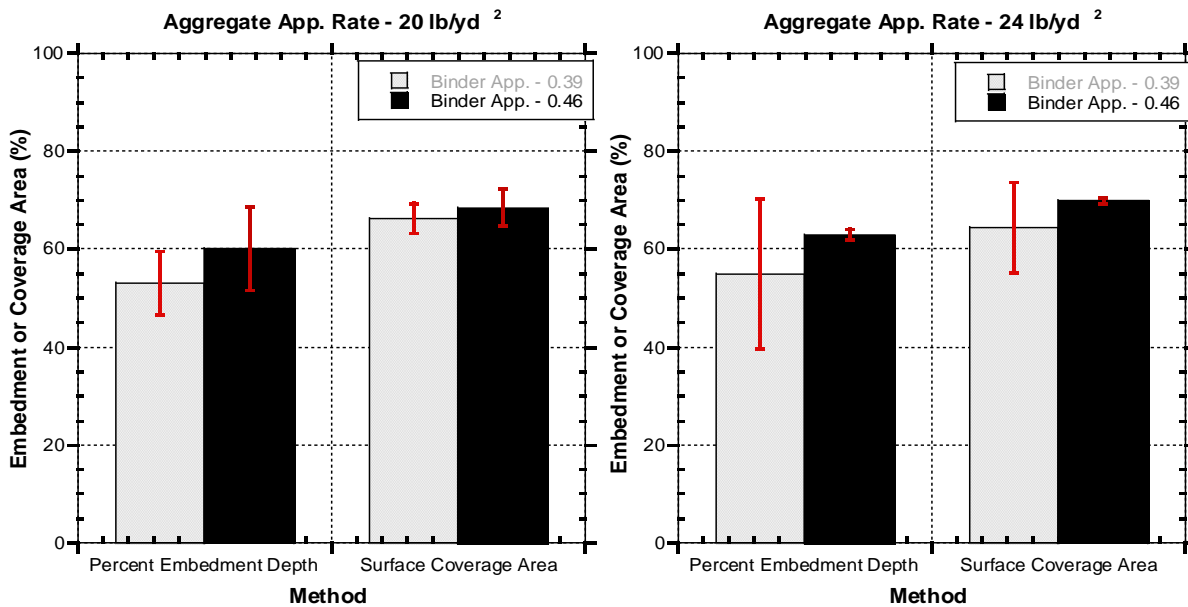


Figure 37 Effect of binder application rate on the percent embedment

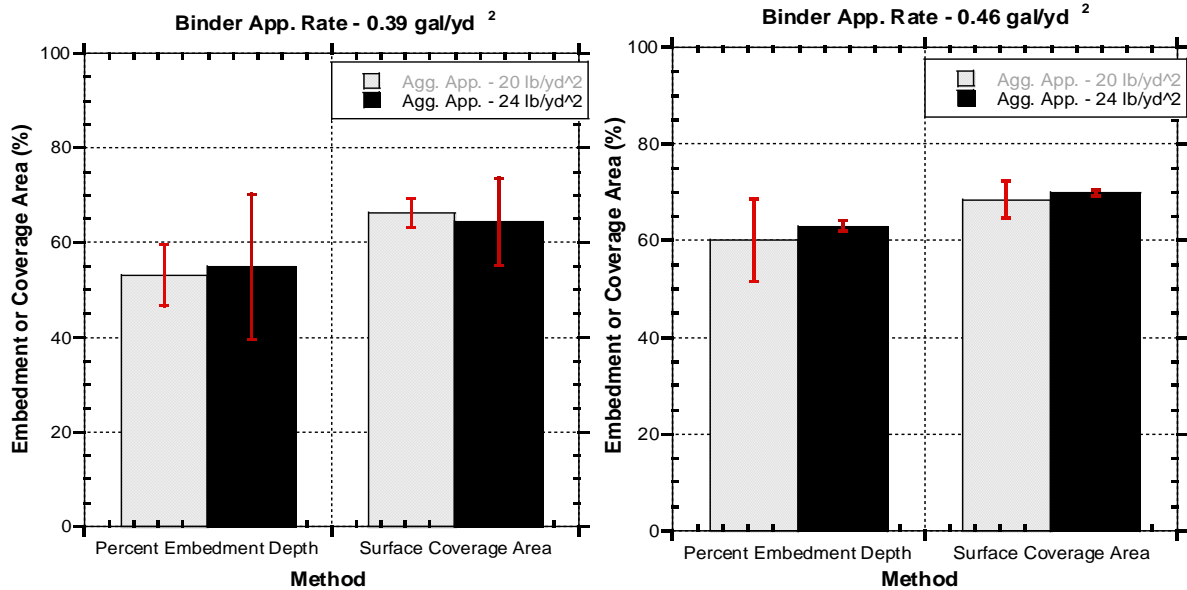


Figure 38 Effect of aggregate application rate on the percent embedment

4.2.2 Sensitivity of the percent embedment to binder application rate and the effect of sweep test

Thirty-two (32) chip seal samples were prepared and tested to further investigate the effect of the binder application rate on the percent embedment and the effect of the sweep test on the percent embedment. Since the aggregate application rate was found not to affect the embedment depth, it was kept constant at 20 lb/yd². The binder application was varied in a range between 0.39 gal/yd² and 0.46 gal/yd². A total of four replicates were prepared at each binder application rate. Two replicates were sliced and analyzed using the image analysis techniques and the other two were tested using the ASTM D7000 sweep test, then sliced and analyzed using the image processing algorithms.

Figure 39 shows the sensitivity of the percent embedment and aggregate surface coverage to the binder application rate. As expected, the percent embedment generally increases with the binder application rate. It is noted that the error bars illustrate the variability observed in the percent embedment parameters obtained from various slices of the two replicate laboratory samples (for a given application rate). The effect of the sweep test on the percent embedment is also shown in Figure 39, where a decrease in the percent embedment was consistently observed in all samples tested. This phenomenon may be due to the possibility that the brushing action of the test lifts up the aggregates that are laying on their flattest side.

Another conclusion that can be drawn from the results shown in Figure 39 is that the binder application range specified by MDOT does produce the desirable percent embedment, which is between 55 and 70 after construction.

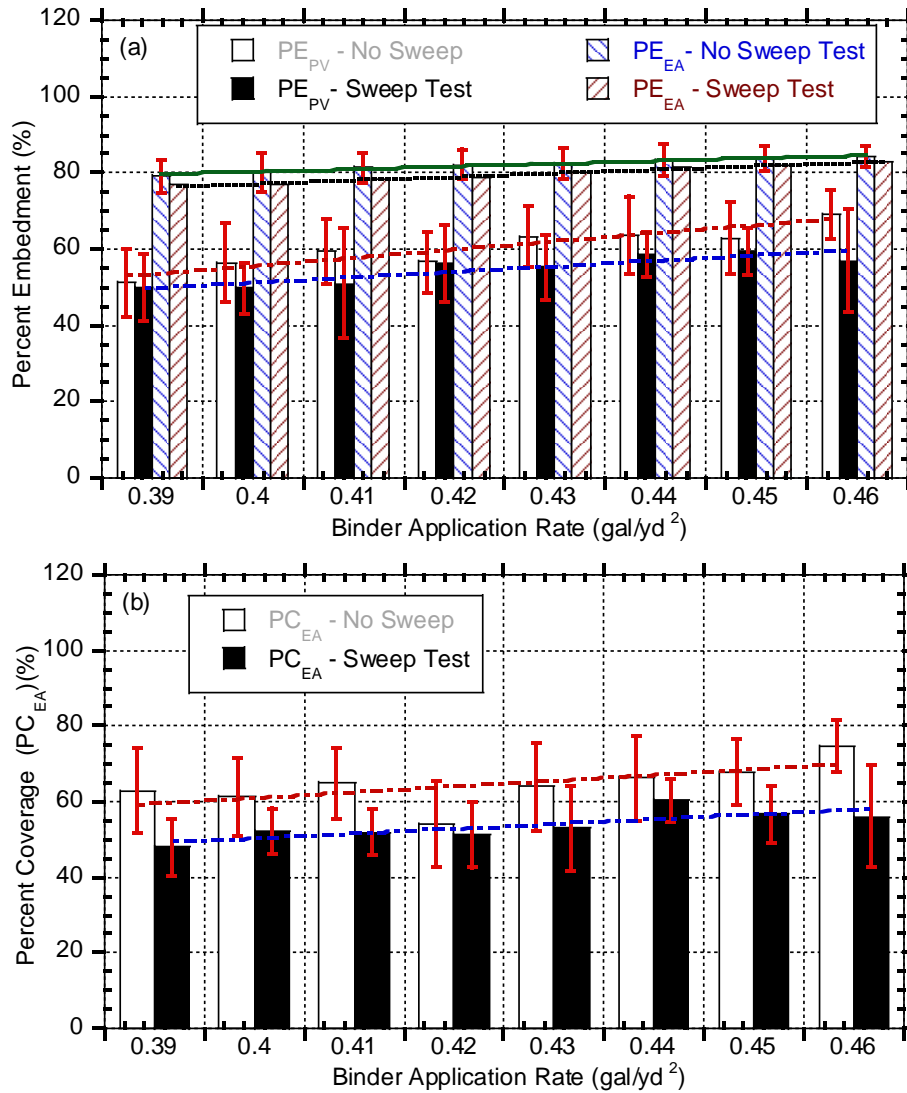


Figure 39 Sensitivity of the (a) percent embedment and (b) aggregate surface coverage to binder application rate.

In an effort to illustrate the variability of the computed parameters within each sample, Table 8 was generated. The Coefficient of Variability (COV) was computed using the parameters computed from 8 slices obtained from each sample. See Appendix G for the individual results of each slice from a given sample. As shown in Table 8, the PE_{EA} (Percent Embedment based on each aggregate) parameter shows the lowest and consistent variability with the median COV of 4%. The median COV's of the other parameters PE_{PV} and PC_{EA} were 9% and 6%, respectively.

Table 8 The Coefficient of Variation (COV) values for each parameter

Samples for	Sample	Application rates		COV = Standard Deviation / Mean		
		Binder app. rate (gal/yd ²)	Agg. app. rate (lb/yd ²)	PE _{PV} (peak valley)	PC _{EA} (surface coverage)	PE _{EA} (each aggregate)
Sweep	1	0.39	20	15%	16%	6%
	2	0.39	20	14%	4%	5%
	1	0.4	20	17%	16%	4%
	2	0.4	20	20%	8%	5%
	1	0.41	20	16%	17%	5%
	2	0.41	20	14%	9%	4%
	1	0.42	20	12%	15%	2%
	2	0.42	20	15%	21%	6%
	1	0.43	20	10%	21%	5%
	2	0.43	20	7%	8%	5%
	1	0.44	20	13%	17%	6%
	2	0.44	20	9%	9%	5%
	1	0.45	20	12%	11%	2%
	2	0.45	20	18%	12%	5%
	1	0.46	20	11%	9%	3%
	2	0.46	20	7%	9%	3%
No sweep	1	0.39	20	9%	13%	4%
	2	0.39	20	20%	20%	3%
	1	0.4	20	39%	13%	3%
	2	0.4	20	13%	8%	3%
	1	0.41	20	39%	17%	4%
	2	0.41	20	15%	5%	4%
	1	0.42	20	19%	23%	9%
	2	0.42	20	17%	9%	4%
	1	0.43	20	16%	19%	4%
	2	0.43	20	15%	18%	5%
	1	0.44	20	11%	8%	2%
	2	0.44	20	8%	11%	6%
	1	0.45	20	11%	11%	2%
	2	0.45	20	6%	6%	2%
	1	0.46	20	27%	28%	3%
	2	0.46	20	9%	17%	3%
			Median =	9%	6%	4%

4.3 Application of Percent Within Limits (PWL) Concept to Percent Embedment

The “Percent Within Limits (PWL)” is defined as the percentage of the lot falling above the lower specification limit (SLS), beneath the upper specification limit (USL), or between the LSL and the USL. The reason that many agencies use PWL specifications can be related to the following advantages:

- PWL, as a quality measure, is sensitive to variability. This sensitivity gives an advantage to contractors with lower variability in their production.
- When PWL is utilized, the sample size is accounted for in the estimate of quality, which is not the case when the average of the test data is used.
- Both a contractor and an agency can calculate their risks using PWL.
- The PWL is compatible with American Association of State Highway and Transportation Officials (AASHTO) specifications because it is presented as the “featured method” in R9 'Standard Recommended Practice for Acceptance Sampling Plans for Highway Construction'.
- FHWA technical advisory T6120.3 presents PWL as the recommended quality measure.

Because of its benefits, the research group decided to implement the PWL analysis for all the field chip sample projects monitored and include this parameter in the software. The screenshot of the graph depicting PWL in the software is shown in Figure 40.

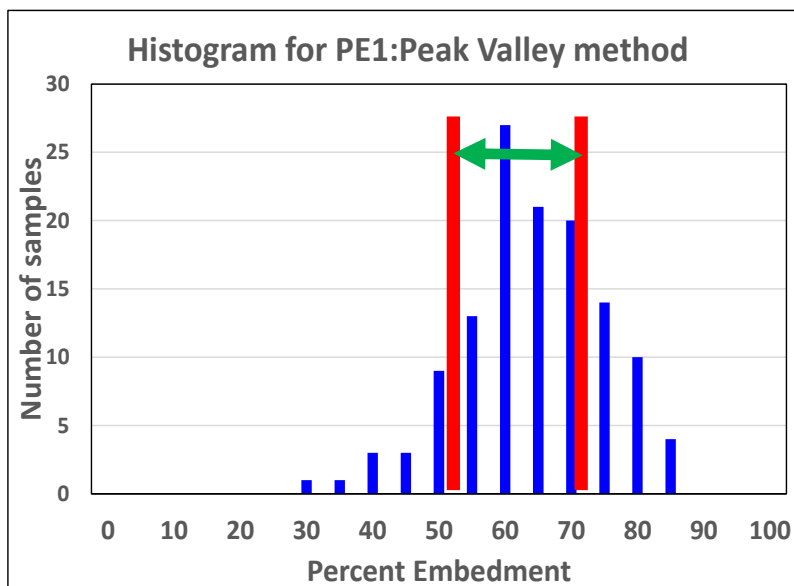


Figure 40 An example histogram an the illustration of the limits used in computation of the PWL.

CIPS was used to compute the PWL for 18 cores of three highway sections M-86 east of Plainwell, M 43 in Woodland and US 31 in Bear Lake. The lower and upper threshold limits given

as inputs in the analyses were 55% and 70% respectively. The PWL results are tabulated in Table 9. The histograms for these road sections have been presented in Appendix H.

Table 9 PWL results for the field samples

Algorithm/Parameter	M-57	M-20	M-33	M-86	M-43	US-31
Peak Valley (PE_{PV})	52.4	60.6	38.1	52.4	33.3	39.6
Surface Coverage Area (PC_{EA})	35.7	74.2	92.1	77.8	23.8	29.2
Each Aggregate (PE_{EA})	0.0	3.0	3.2	1.6	0.0	8.3

5. CONCLUSIONS

5.1 Conclusions from the study

This research produced a novel methodology to directly measure percent embedment depth of chip seals using an image analysis procedure. Digital images were captured from the vertical cut cross sections of both laboratory-produced samples and cores collected on the Michigan road network and analyzed using the image analysis algorithms developed as part of this study. Forty-eight (48) chip seal cores were collected from the field from 8 different road sections and forty (40) laboratory samples were fabricated. Furthermore, a user-friendly software package was developed to analyze the chip seal samples. Major conclusions of this study can be summarized as follows:

- The procedure for chip seal sample acquisition by both taking cores from the field and fabricating in the laboratory seemed to be suitable for image processing techniques. Only one extra step (slicing the cores and placing blue play dough on the slices) is needed to obtain images of the samples.
- The laboratory equipment (e.g. camera, saw, play dough) required for capturing the images can be easily afforded by any road agency or contractor.
- Three image analysis algorithms, namely (i) the peak valley method, (ii) the surface coverage area method and (iii) the each aggregate method were developed to analyze the chip seal samples. These algorithms were validated by testing standard idealized pictures with known embedment depths.
- The peak & valley method showed similar results as those obtained using the in-situ sand patch test.
- Variability of the embedment depth obtained from the each aggregate method is less than the embedment depth obtained from the other methods.
- Analyses for the laboratory chip seal samples revealed that aggregate application rate limits of the current MDOT chip seal specification did not affect the percent embedment; whereas, the binder application rates of 0.39 gal/yd² and 0.46 gal/yd² played a significant role on embedment depth.

5.2 Recommendations for further research and implementation

This research produced a novel methodology to directly measure the percent embedment of chip seals using an image analysis procedure. Although the results obtained by these image-based methods are precise and robust, there are certain unresolved issues in the evaluation of chip seal applications. For example;

- Appropriate limits of percent embedment parameters need to be identified. This can be done by collecting cores from good-performing chip seals and chip seals with known bleeding as well as chip loss problems and analyzing the core samples using the methodology presented herein.

- Chip seal pavements at different stages within the fix's lifecycle need to be analyzed (i.e. just after construction and after several years of traffic). This data should be used to understand the effect of traffic on embedment depths of chip seal pavements, which in turn can be correlated to performance. Furthermore, this would help road agencies to analyze the percentage embedment for newly constructed pavements and predict the future embedment depths in its course of lifetime, thus planning the next treatment in advance.
- If any performance related tests are developed or adopted, they should be correlated to percent embedment values obtained from image analysis and/or field tests.
- In addition to field sample acquisition, chip seal samples need to be fabricated with different types of aggregate in terms of size and shape in the laboratory so that the effect of aggregate properties can be observed on the embedment depth.
- The effect of different types of asphalt emulsion should be investigated to find relationship between the type of binder and the performance of chip seals and embedment depth.

BIBLIOGRAPHY

- AASHTO T 312-15 Preparing Hot-Mix Asphalt (HMA) Specimens by Means of the Superpave Gyratory Compactor, 2011, American Association of State Highway and Transportation Officials, Washington, D.C.
- Abdul-Malak, M.U., Fowler, D.W. and Meyer, A. H. (1993) “Major Factors Explaining Performance Variability of Seal Coat Pavement Rehabilitation Overlays”, *Transportation Research Record: Journal of the Transportation Research Board*, No. 1388, pp 140-149.
- Ames Engineering, 2014. Ames Engineering Laser Texture Scanner User Manual Model 9300
- American Society of Mechanical Engineers. (ASME) (2002) An American National Standard Surface Texture (Surface Roughness, Waviness, and Lay).
- ASTM E 1845-15. (2015). Standard Practice for Calculating Pavement Macrotexture Mean Profile Depth, ASTM International, West Conshohocken, PA.
- ASTM E 303-93. (2013). Standard Test Method for Measuring Surface Frictional Properties Using the British Pendulum Tester, ASTM International, West Conshohocken, PA.
- ASTM D 7000. (2011). Standard Test Method for Sweep Test of Bituminous Emulsion Surface Treatment Samples, ASTM International, West Conshohocken, PA.
- ASTM D 7234-12. (2012). Standard Test Method for Pull-off Adhesion Strength of Coatings on Concrete Using Portable Pull-off Adhesion Testers, ASTM International, West Conshohocken, PA.
- Bazlamit, S. M., and Reza F. (2005). “Changes in Asphalt Pavement Friction Components and Adjustment of Skid Number for Temperature”, *Journal of Transportation Engineering*, ASCE, Vol. 131, No.6, 470-476
- Benedict, C. R. (1990). Laboratory measurement of chip retention strength by the frosted marble modified ISSA cohesion tester. In Joint AEMA/ISSA Conference, Atlanta, GA.
- Beer, M. D. (1996). Measurement of Tyre/Pavement Interface Stresses Under Moving Wheel Loads. *International Journal of Heavy Vehicle Systems*, 3(1-4), 97-115.
- Bhattacharjee, S., Gould, J.S., Mallick, R.B. and Hugo, F. (2004). “Use of MMLS3 Scaled Accelerated Loading For Fatigue Characterization of Hot Mix Asphalt (HMA) In The Laboratory”, 2nd International Conference on Accelerated Pavement Testing, Minneapolis, Minnesota
- British Standard Institute BS 7976-2, 2002. Pendulum testers, London, UK.
- BS EN 12272-1. (2002). Surface dressing. Test methods. Rate of spread and accuracy of spread of binder and chippings

- Choubane, B., Holzschuher, C.R., and Gokhale, S. (2004). "Precision of Locked-Wheel Testers for Measurement of Roadway Surface Friction Characteristics", *Transportation Research Record: Journal of the Transportation Research Board*, No.1869, pp. 145-151
- Colwill, D.M., John, M. and J. Clifford, N. (1995). "U.K Design Procedure for Surface Dressing", *Transportation Research Record*, 1507. Washington DC: Transportation Research Board, pp. 13–22.
- Epps, J.A., Chaffin, C.W., and Hill, A.J. (1980) Research Report 214-25: "Field Evaluation of a Seal Coat Design Method", Research Report 83-2F, Texas Transportation Institute, Austin
- Epps, J.A., and Gallaway, B.M. (1974) Research Report 83-1: "Synthetic Aggregate Seal Coats- Current Texas Highway Department Practices", Texas Transportation Institute, Austin
- Epps, A. L., Glover, C. J., & Barcena, R. (2001). A performance-graded binder specification for surface treatments (No. FHWA/TX-02/1710-1,)
- Freitas, E. F., Pereira, P. A., Antunes, M. L., & Domingos, P. (2008). Analysis of test methods for texture depth evaluation applied in Portugal. *Seminário Avaliação das Características de Superfície dos pavimentos*.
- Gransberg, D. and James, D.M.B. (2005) *Chip Seal Best Practices*, NCHRP Synthesis 342, National Cooperative Highway Research Program, National Research Council, Washington, DC.
- Groenendijk, J. (1998) *Accelerated Testing and Surface Cracking of Asphaltic Concrete Pavements* (Doctoral Dissertation). Retrieved From Delft University of Technology Institutional Repository
- Hanson, F.M. (1934) *Bituminuos Surface Treatment of Rural Highways*, *Proceedings of the New Zealand Society of Civil Engineers*, pp. 189-220
- Henderson, R., Herrington, P. and Patrick, J. (2006). "Finite-element Modelling of a Chip Seal Road Surfacing: A Preliminary Study", *A Journal of Australian and New Zealand Research and Practice, Road & Transport Research*, Vol. 15, No.3, pp. 3-18
- Holmgreen, R. J., Epps, J.A., Hughes, C.H. and Gallaway, B.M. (1985) Research Report 297-1F: "Field Evaluation of The Texas Seal Coat Design Method", Texas Transportation Institute, Austin, 174p.
- Howard, I. L., Hemsley Jr, M., Baumgardner, G. L., & Jordan III, W. S. (2009). Chip and scrub seal binder evaluation by frosted marble aggregate retention test. In *Transportation Research Board 88th Annual Meeting* (No. 09-1662).
- Howard, I.L., Alvarado, A., and Floyd, W.C. (2013) *Performance Oriented Guidance for Mississippi Chip Seals-Volume II, Final Report FHWA/MS-DOT-RD-13-211-Volume II*, Mississippi Department of Transportation, Mississippi.

- Huurman, M., Milne, T. I., van de Ven, M.F.C and Scarpas, A. (2004) Development of a structural FEM for road surfacing seals, ICCES, Corfu, Greece
- Huurman, M. (2010). “Developments in 3D surfacing seals FE modelling”, International Journal of Pavement Engineering, Vol.11, No.1, pp. 1-12
- Johannes, P.T., Mahmoud, E. and Bahia, H. (2011). “Sensitivity of ASTM D7000 Sweep Test to Emulsion Application Rate and Aggregate Retention”, Transportation Research Record: Journal of the Transportation Research Board, No. 2235, pp. 95-102, Washington D.C.
- Jordan III, W.S. and Howard, I.L. (2011). “Applicability of Modified Vialit Adhesion Test for Seal Treatment Specifications”, Journal of Civil Engineering and Architecture, Vol. 5, No.3 (Serial No. 40)
- Kandhal, P.S. and Motter, J.B. (1991) Criteria For Accepting Precoated Aggregates for Seal Coats and Surface Treatments, Transportation Research Board, No. 1300, pp. 80-89, Washington D.C.
- Kearby, J.P. (1953) Tests and Theories on Penetration Surfaces, Highway Research Board Proceedings, Vol.32, pp. 232-237
- Kim, H. B., Lee, S. W., Hyun, T. J., & Lee, K. H. (2013). Measurement of Texture Depth of Pavement Using Potable Laser Profiler. Journal of the Eastern Asia Society for Transportation Studies, 10(0), 1576-1589.
- Kim, Y. R and Lee, J. (2008) Research Report FHWA/NC/2006-63: “Quantifying the Benefits of Improved Rolling of Chip Seals”, North Carolina Department of Transportation, Raleigh, NC
- Kodippily, S. (2013). Modelling the Flushing Mechanism of Thin Flexible Surface Pavements (Doctoral Dissertation). Retrieved From The University of Auckland Libraries and Learning Services
- Kumara, G. H. A. J. J., Hayano, K., & Ogiwara, K. (2012). Image analysis techniques on evaluation of particle size distribution of gravel. Int. J. Geomate, 3(1), 290-297.
- Lee, S. (2003) Long-Term Performance Assessment of Asphalt Concrete Pavements Using The Third Scale Model Mobile Loading Simulator And Fiber Reinforced Asphalt Concrete (Doctoral Dissertation). Retrieved From North Carolina State University Libraries
- Lee, J.S. and Kim, Y.R. (2008). “Understanding the Effects of Aggregate and Emulsion Application Rates on Performance of Asphalt Surface Treatments”, Transportation Research Record: Journal of the Transportation Research Board, No. 2044, pp. 71-78, Washington D.C.
- Lu, Q., and Steven, B. (2006). Technical Memorandum UCPRC-TM-2006-10: “Friction Testing of Pavement Preservation Treatments: Literature Review”, California Department of Transportation

- McLeod, N.W., Chaffin, C.W., Holberg, A.E., Parker, C.F., Obrcian, V., Edwards, J.M., Campen and Kari, W.J. (1969) "A General Method of Design for Seal Coats and Surface", Journal of the Association of Asphalt Paving Technologists, Vol. 38, pp.537-628
- Michigan Department of Transportation (2012). "2012 Standard Specifications for Construction"
- New Zealand Roading Division, (1968) Manual of Sealing and Paving Practice. National Roads Board, New Zealand.
- Queensland Department of Transport and Main Roads (2012). Materials Testing Manual, The State of Queensland, Department of Transport and Main Roads.
- Roberts, C. and Nicholls J.C. (2008) Design Guide for Road Surface Dressing, Road Note RN39 Sixth Edition, Transport Research Laboratory
- Roque, R., Anderson, D. and Thompson, M. (1991). "Effect of Material, Design, and Construction Variables on Seal Coat Performance", Transportation Research Record: Journal of the Transportation Research Board, No. 1300, pp. 108-115, Washington D.C.
- Senadheera, S., Tock, R.Wm., Hossain, S., Yazgan, B. and Das, S. (2006) Research Report FHWA/TX-06/0-4362-1: "A Testing and Evaluation Protocol to Assess Seal Coat Binder-Aggregate Compatibility", Texas Department of Transportation, Austin
- Schuler, S., Lord, A., Epps, A., and Hoyt, D. (2011) Manual for Emulsion-Based Chip Seals for Pavement Preservation, NCHRP Report 680, National Cooperative Highway Research Program, National Research Council, Washington DC.
- Sprayed Seal Design Project Group (2001) Austroads Provisional Sprayed Seal Design Method Revision 2000, Austroads Project No. N.T.&E.9902, Austroads Incorporated Level 9
- The South African National Roads Agency, (2007). Technical Recommendations for Highways. Technical Recommendations of Highways, Pretoria, South Africa.
- Wasiuddin, N.M., Marshall, A., Saltibus, N.E., Saber, A., Abadie, C. and Mohammad, L.N. (2013) "Use of Sweep Test for Emulsion and Hot Asphalt Chip Seals: Laboratory and Field Evaluation", Journal of Testing and Evaluation, Vol. 41, No. 2, pp. 1-10
- Wielinski, J.C., Brandenburg, J. and Wissel, H. (2011) The Monroe Michigan Chip Seal Case Study: An Evaluation of Multiple Chip Seals' Cold Weather Field Performance. Transportation Research Board 90th Annual Meeting, CD-ROM.
- Wood, J., Thomas, Janisch, D.W., and Gaillard, F.S. (2006) Final Report: "Minnesota Seal Coat Handbook 2006", Minnesota Department of Transportation, December 1998, Revised 2007
- Zhou, F., Li, H., Chen, P. and Scullion T. (2014) Research Report FHWA/TX-14/0-6674-1: "Laboratory Evaluation of Asphalt Binder Rutting, Fracture, and Adhesion tests", Texas Department of Transportation, Austin

APPENDIX A: Embedment Depth and Surface Coverage Area Results for Field Samples of M-57 near Pompeii

Table A. 1 Embedment depth and surface coverage area for cross sections of field samples of M-57 near Pompeii Chip Seal Section

Sample ID	- file name	Average % Embedment Depth (Peak and Valley)	Average % Coverage	Average % Embedment Depth (Each Aggregate)
040215-8	1A	38.1	44.6	80.9
	1B	52.0	47.4	77.9
	2A	42.8	49.9	86.0
	2B	40.0	56.8	82.7
	3A	49.7	52.6	83.5
	3B	55.6	61.2	78.8
	4A	49.1	50.7	75.7
	Avg.	46.8	51.9	80.8
	COV	14%	11%	4%
040215-10	1A	51.5	48.4	76.3
	1B	54.9	65.3	88.5
	2A	58.7	59.0	84.5
	2B	48.7	54.5	86.8
	3A	55.9	56.2	84.1
	3B	56.1	48.6	83.2
	4A	53.4	52.6	75.9
	4B	65.0	55.1	85.2
	5A	65.1	57.7	88.3
	5B	58.3	45.0	82.1
	Avg.	57.5	52.8	83.7
	COV	10%	9%	5%
040215-11	1A	44.8	55.8	71.6
	1B	44.3	43.9	72.5
	2A	56.2	52.7	84.4
	2B	50.0	50.9	78.7
	3A	51.2	55.8	78.4
	3B	42.5	48.0	77.4
	4A	46.0	40.8	77.0
	4B	38.5	42.4	80.6
	5A	48.5	53.9	78.1
	5B	56.5	46.2	76.9
	Avg.	47.6	48.3	78.2
	COV	12%	12%	2%

Table A.1 (contd')

Sample ID	- file name	Average % Embedment Depth (Peak and Valley)	Average % Coverage	Average % Embedment Depth (Each Aggregate)
040215-7	1A	53.4	55.4	86.0
	1B	24.4	51.9	82.1
	2A	40.6	48.0	80.6
	2B	38.6	38.3	70.7
	3A	55.8	56.4	86.6
	3B	57.5	45.4	82.1
	4A	63.8	60.2	84.3
	Avg.	53.9	50.1	81.8
	COV	20%	20%	7%
040215-9	1A	57.6	53.9	88.6
	1B	63.9	47.5	76.5
	2A	56.9	56.0	87.3
	2B	45.3	49.7	85.3
	3A	64.5	59.4	84.2
	3B	73.7	52.5	86.2
	4A	60.7	43.7	81.3
	4B	57.9	56.6	89.7
	Avg.	60.1	52.4	84.9
	COV	13%	10%	5%

APPENDIX B: Embedment Depth and Surface Coverage Area Results for Field Samples of M-20 near New Era

Table B. 1 Embedment depth and surface coverage area for cross sections of field samples of M-20 near New Era Chip Seal Section

Sample ID	Slice ID	Average % Embedment Depth (Peak and Valley)	Average % Coverage	Average % Embedment Depth (Each Aggregate)
M20 - CORE 1	1A	73.1	72.6	80.6
	1B	62.1	59.8	73.7
	2A	68.0	58.8	81.7
	2B	67.7	67.7	83.0
	3A	55.1	58.9	78.0
	3B	61.4	55.0	75.8
	4A	67.1	62.7	78.4
	4B	55.8	61.2	73.0
	Avg.	63.8	62.1	78.0
	COV	9.9%	9.0%	4.7%
M20 - CORE 2	1A	71.7	77.6	86.4
	1B	71.7	69.0	81.9
	2A	70.9	64.0	77.6
	2B	68.3	66.6	82.8
	3A	76.7	57.5	75.7
	3B	71.2	62.3	82.2
	4A	69.7	49.4	71.2
	4B	78.5	63.4	81.9
	5A	63.3	60.3	79.0
	5B	72.3	58.9	76.9
	Avg.	71.4	62.9	79.5
	COV	5.9%	11.9%	5.5%
M20 - CORE 3	1A	4.2	7.5	4.4
	1B	67.7	69.2	85.7
	2A	52.0	52.0	72.3
	2B	52.0	57.1	76.2
	3A	64.5	57.6	79.1
	3B	61.9	56.1	83.1
	4A	59.7	52.6	65.4
	4B	57.7	64.4	86.2
	Avg.	54.0	63.4	79.8
	COV	58.7	59.0	78.5

Table B.1 (contd')

Sample ID	Slice ID	Average % Embedment Depth (Peak and Valley)	Average % Coverage	Average % Embedment Depth (Each Aggregate)
M20 - CORE 4	1A	71.0	64.3	77.7
	1B	76.6	63.3	84.0
	2A	59.9	62.9	81.4
	2B	64.5	59.8	77.7
	3A	54.7	59.0	72.8
	3B	67.1	57.3	79.7
	4A	68.2	62.4	78.0
	4B	74.8	59.7	79.3
	Avg.	67.1	61.1	78.8
	COV	11.0%	4.0%	4.1%
M20 - CORE 5	1A	75.6	67.5	77.0
	1B	60.4	57.7	79.7
	2A	64.7	61.3	84.9
	2B	66.8	68.5	82.3
	3A	56.2	62.2	84.1
	3B	64.9	69.2	84.1
	4A	77.4	76.3	87.9
	4B	74.2	73.4	84.7
	Avg.	67.5	67.0	83.1
	COV	11%	9%	4%
M20 - CORE 6	1A	40.0	52.5	75.6
	1B	46.2	59.2	78.6
	2A	59.9	57.5	72.7
	2B	59.7	53.7	79.1
	3A	57.1	47.1	70.3
	3B	52.0	54.0	74.2
	4A	56.9	55.0	77.4
	4B	56.5	56.3	72.4
	Avg.	53.5	54.4	75.0
	COV	13%	7%	4%

Table B.1 (contd')

Sample ID	Slice ID	Average % Embedment Depth (Peak and Valley)	Average % Coverage	Average % Embedment Depth (Each Aggregate)
M20 - CORE 7	1A	70.6	62.1	79.9
	1B	61.3	66.4	79.9
	2A	50.7	57.8	79.4
	2B	68.3	59.7	81.0
	3A	57.3	56.3	80.9
	3B	64.5	57.0	76.7
	4A	63.1	58.5	73.2
	4B	57.1	67.8	76.1
	Avg.	61.6	60.7	78.4
	COV	11%	7%	4%
M20 - CORE 8	1A	60.4	47.4	71.5
	1B	65.3	51.3	71.3
	2A	70.1	57.0	80.3
	2B	64.3	55.3	69.7
	3A	62.7	53.3	76.8
	3B	59.6	64.3	73.7
	4A	53.6	50.9	74.9
	4B	52.9	61.6	74.8
	Avg.	61.1	55.1	74.1
	COV	10%	10%	5%

APPENDIX C: Embedment Depth and Surface Coverage Area Results for Field Samples of M-33 from Alger to Rose City

Table C. 1 Embedment depth and surface coverage area for cross sections of field samples of M-33 from Alger to Rose City

Sample ID	Slice ID	Average % Embedment Depth (Peak and Valley)	Average % Coverage	Average % Embedment Depth (Each Aggregate)
M33 - CORE 1	1A	66.5	60.0	78.2
	1B	69.8	56.4	78.9
	2A	74.6	60.9	75.1
	2B	63.8	67.6	80.8
	3A	74.7	68.8	80.1
	3B	70.2	59.4	75.2
	4A	63.1	61.2	78.4
	4B	67.4	52.0	76.6
	Avg.	68.8	60.8	77.9
	COV	6%	9%	3%
M33 - CORE 2	1A	71.5	59.7	71.6
	1B	68.8	69.1	86.7
	2A	74.2	60.8	85.0
	2B	69.2	63.1	83.3
	3A	76.3	59.4	82.9
	3B	66.2	59.9	79.7
	4A	71.1	55.9	83.2
	4B	73.1	64.6	82.6
	Avg.	71.3	61.6	81.9
	COV	5%	6%	6%
M33 - CORE 3	1A	65.8	57.7	74.1
	1B	75.4	63.9	82.8
	2A	75.3	67.3	85.0
	2B	70.0	55.4	77.6
	3A	62.8	56.3	76.5
	3B	70.9	62.4	80.0
	4A	69.8	58.8	79.1
	4B	74.0	60.4	78.8
	Avg.	70.5	60.3	79.2
	COV	6%	7%	4%

Table C.1 (contd')

Sample ID	Slice ID	Average % Embedment Depth (Peak and Valley)	Average % Coverage	Average % Embedment Depth (Each Aggregate)
M33 - CORE 4	1A	78.8	65.5	82.1
	1B	75.9	66.8	81.0
	2A	74.6	68.6	86.6
	2B	76.1	63.3	86.7
	3A	73.6	62.3	80.3
	3B	76.4	69.5	83.0
	4A	71.5	64.9	79.2
	Avg.	75.3	65.9	82.7
	COV	3%	4%	4%
M33 - CORE 5	1A	75.3	56.7	76.6
	1B	83.4	63.2	83.7
	2A	77.6	63.3	81.0
	2B	74.6	60.4	81.2
	3A	76.5	63.7	83.3
	3B	79.0	60.8	84.9
	4A	76.3	60.7	85.3
	4B	75.9	59.7	79.9
	Avg.	77.3	61.1	82.0
COV	4%	4%	4%	
M33 - CORE 6	1A	75.0	63.3	81.9
	1B	69.2	63.6	81.5
	2A	73.5	65.1	83.3
	2B	78.2	65.9	81.6
	3A	69.8	62.6	83.6
	3B	72.6	62.5	82.9
	4A	74.2	73.1	82.4
	4B	69.1	64.8	82.4
	Avg.	72.7	65.1	82.4
COV	4%	5%	1%	

Table C.1 (contd')

Sample ID	Slice ID	Average % Embedment Depth (Peak and Valley)	Average % Coverage	Average % Embedment Depth (Each Aggregate)
M33 - CORE 7	1A	54.7	61.7	80.8
	1B	62.7	53.2	71.8
	2A	55.7	51.0	64.6
	2B	50.4	52.4	69.3
	3A	63.4	59.0	77.2
	3B	57.5	56.9	76.1
	4A	63.2	56.5	71.4
	4B	55.4	57.0	72.6
	Avg.	57.9	56.0	73.0
	COV	8%	6%	7%
M33 - CORE 8	1A	73.2	58.3	76.2
	1B	69.6	59.1	75.9
	2A	72.0	63.1	79.0
	2B	70.7	62.5	80.2
	3A	74.4	58.6	84.6
	3B	68.6	59.8	79.9
	4A	61.4	57.1	78.1
	4B	72.9	59.1	78.6
	Avg.	70.3	59.7	79.1
	COV	6%	3%	3%

APPENDIX D: Embedment Depth and Surface Coverage Area Results for Field Samples of M-86 east of Plainwell

Table D. 1 Embedment depth and surface coverage area for cross sections of field samples of M-86 east of Plainwell

Sample ID	Slice ID	Average % Embedment Depth (Peak and Valley)	Average % Coverage	Average % Embedment Depth (Each Aggregate)
M86 - CORE E	E-1	73.7	86.7	69.5
	E-2	70.5	80.6	61.9
	E-3	67.9	77.9	56.5
	E-4	54.2	79.3	63.4
	E-5	57.5	76.6	53.6
	E-6	41.4	77.0	61.5
	E-7	56.7	76.4	60.3
	E-8	66.0	77.3	57.3
	Avg.	61.0	79.0	60.5
	COV	16%	4%	8%
M86 - CORE F	F-1	56.6	78.3	63.4
	F-2	54.3	68.9	56.0
	F-3	65.3	83.6	68.6
	F-4	63.6	80.2	59.9
	F-5	66.3	79.5	59.8
	F-6	64.0	70.4	58.3
	F-7	77.5	87.9	74.8
	F-8	73.3	80.1	60.8
	Avg.	65.1	78.6	62.7
	COV	11%	8%	9%
M86 - CORE G	G-1	63.3	75.4	59.6
	G-2	60.1	78.3	64.5
	G-3	67.2	82.3	67.0
	G-4	61.8	78.5	62.2
	G-5	59.5	85.0	71.8
	G-6	62.4	74.6	58.1
	G-7	71.3	79.7	63.5
	G-8	63.8	82.9	65.9
	Avg.	63.7	79.6	64.1
	COV	6%	4%	6%

Table D.1 (contd')

Sample ID	Slice ID	Average % Embedment Depth (Peak and Valley)	Average % Coverage	Average % Embedment Depth (Each Aggregate)
M86 - CORE H	H-1	73.5	87.9	73.6
	H-2	81.5	87.6	64.8
	H-3	79.3	86.6	73.6
	H-4	67.1	84.9	59.7
	H-5	79.5	88.3	72.8
	H-6	72.9	82.9	64.9
	H-7	76.0	85.7	67.4
	Avg.	75.7	85.8	67.2
	COV	6%	2%	8%
M86 - CORE I	I-1	58.7	73.3	59.4
	I-2	60.6	76.5	62.7
	I-3	55.4	74.3	55.5
	I-4	62.0	81.3	65.0
	I-5	50.9	73.9	58.5
	I-6	59.6	74.3	58.6
	I-7	49.4	79.3	63.3
	I-8	61.7	81.7	70.1
	Avg.	57.3	76.8	61.6
COV	8%	4%	7%	
M86 - CORE J	J-1	60.8	76.8	68.0
	J-2	54.6	81.0	67.2
	J-3	54.7	72.9	57.0
	J-4	58.5	77.2	58.1
	J-5	66.1	76.5	58.9
	J-6	60.3	80.8	61.7
	J-7	72.2	85.5	66.5
	J-8	62.1	84.4	66.2
	Avg.	61.2	79.4	63.0
COV	9%	5%	7%	

Table D.1 (contd')

Sample ID	Slice ID	Average % Embedment Depth (Peak and Valley)	Average % Coverage	Average % Embedment Depth (Each Aggregate)
M86 - CORE K	K-1	70.4	83.6	68.6
	K-2	64.0	80.9	61.7
	K-3	59.8	86.3	64.8
	K-4	71.7	78.8	65.3
	K-5	64.6	80.0	62.0
	K-6	65.4	84.8	61.9
	K-7	61.3	82.3	67.9
	K-8	78.0	86.8	70.4
	Avg.	66.9	82.9	65.3
	COV	8%	3%	5%
M86 - CORE L	L-1	88.3	89.7	76.4
	L-2	85.1	91.8	76.2
	L-3	80.3	89.5	74.1
	L-4	86.2	89.5	70.6
	L-5	81.2	90.9	69.9
	L-6	84.6	90.6	67.7
	L-7	82.2	87.6	73.4
	L-8	83.9	88.1	74.7
	Avg.	84.0	89.7	72.9
	COV	3%	1%	4%

APPENDIX E: Embedment Depth and Surface Coverage Area Results for Field Samples of M-43 in Woodland

Table E. 1 Embedment depth and surface coverage area for cross sections of field samples of M-43 in Woodland

Sample ID	Slice ID	Average % Embedment Depth (Peak and Valley)	Average % Coverage	Average % Embedment Depth (Each Aggregate)
M43-CORE 1	1-1	59.6	79.5	60.8
	1-2	67.5	86.0	65.4
	1-3	64.4	86.0	70.9
	1-4	61.4	78.0	64.7
	1-5	56.5	87.4	75.4
	1-6	63.0	79.4	62.0
	1-7	65.6	78.0	60.3
	Avg.	62.6	82.1	65.6
	COV	6%	5%	8%
M43-CORE 2	2-1	86.9	93.6	88.7
	2-2	83.3	94.9	92.4
	2-3	85.8	92.5	89.2
	Avg.	85.3	93.7	90.1
	COV	2%	1%	2%
M43-CORE 3	3-1	71.8	89.6	87.0
	3-2	75.1	89.4	85.4
	3-3	81.0	96.6	91.8
	3-4	76.9	89.5	85.4
	3-5	81.5	91.9	86.9
	Avg.	77.3	91.4	87.3
	COV	5%	3%	3%
M43-CORE 4	4-1	98.7	96.3	91.6
	4-2	96.6	92.4	91.5
	4-3	98.1	94.9	90.7
	4-4	96.8	93.4	89.1
	4-5	98.1	95.9	91.0
	4-6	95.1	91.4	90.7
	Avg.	90.8	97.2	94.1
	COV	1%	1%	2%

APPENDIX F: Embedment Depth and Surface Coverage Area Results for Field Samples of US-31 in Bear Lake

Table F. 1 Embedment depth and surface coverage area for cross sections of field samples of US-31 in Bear Lake

Sample ID	Slice ID	Average % Embedment Depth (Peak and Valley)	Average % Coverage	Average % Embedment Depth (Each Aggregate)
US31 - CORE A	A-1	72.2	68.9	44.8
	A-2	57.8	70.8	38.1
	A-3	75.0	72.7	27.4
	A-4	63.3	64.0	38.7
	A-5	69.5	77.4	42.7
	A-6	76.1	73.6	48.0
	A-7	60.4	76.7	47.6
	A-8	61.0	66.4	44.0
	Avg.	66.9	71.3	41.4
	COV	10%	6%	15%
US31 - CORE B	B-1	70.9	83.5	50.1
	B-2	71.7	79.3	48.5
	B-3	75.0	77.9	49.5
	B-4	68.9	81.9	53.9
	B-5	69.0	77.7	48.4
	B-6	76.3	77.2	53.2
	B-7	81.0	74.8	40.9
	B-8	70.3	79.2	36.9
	Avg.	72.9	78.9	47.7
	COV	5%	3%	12%
US31 - CORE C	C-1	42.5	70.1	41.4
	C-2	54.6	75.3	47.4
	C-3	30.9	70.5	41.1
	C-4	44.2	69.4	42.0
	C-5	35.9	71.3	47.1
	C-6	54.9	74.3	49.6
	C-7	58.5	70.7	48.0
	C-8	62.1	77.5	45.3
	Avg.	47.9	72.4	45.2
	COV	22%	4%	7%

Table F.1 (contd')

Sample ID	Slice ID	Average % Embedment Depth (Peak and Valley)	Average % Coverage	Average % Embedment Depth (Each Aggregate)
US31 - CORE D	D-1	77.5	85.6	66.6
	D-2	65.8	77.5	57.3
	D-3	74.2	85.9	67.9
	D-4	54.5	82.3	50.6
	D-5	61.0	83.4	62.6
	D-6	68.2	77.0	48.2
	D-7	49.3	70.7	48.2
	Avg.	64.2	79.4	57.5
	COV	14%	7%	13%
US31 - CORE E	E-1	81.0	80.9	43.8
	E-2	60.6	80.0	55.1
	E-3	73.7	79.1	48.2
	E-4	81.7	81.3	55.9
	E-5	69.8	76.5	54.0
	E-6	74.7	79.4	50.7
	E-7	73.1	75.6	54.3
	E-8	76.0	82.6	55.5
	Avg.	73.8	79.4	52.2
	COV	8%	3%	8%
US31 - CORE F	F-1	76.2	78.7	59.6
	F-2	63.9	75.3	59.6
	F-3	53.6	71.9	48.1
	F-4	68.2	82.7	64.0
	F-5	69.7	84.2	64.0
	F-6	77.2	83.5	64.0
	F-7	69.4	84.9	62.9
	F-8	74.5	91.2	74.1
	Avg.	69.1	81.6	62.1
	COV	10%	7%	11%

APPENDIX G: Embedment Depth and Surface Coverage Area Results for Laboratory Samples – Group 1 & 2

Table G. 1 Embedment depth and surface coverage area for cross sections of group 1 laboratory samples

Sample ID	Side ID	Average % Embedment (Peak and Valley Method)	Average % Coverage	Sample ID	Side ID	Average % Embedment (Peak and Valley Method)	Average % Coverage
LS-1	1A	63.22	64.76	LS-5	1A	53.60	75.74
	1B	49.79	74.66		1B	66.66	72.17
	2A	47.08	53.19		2A	52.94	68.55
	2B	50.18	69.58		2B	57.34	66.27
	3A	49.05	72.47		3A	57.12	73.36
	3B	35.03	62.20		3B	53.96	57.75
	4A	46.56	60.31		4A	59.06	66.77
	4B	48.47	55.95		4B	61.50	66.51
LS-2	1A	63.16	74.47	LS-6	1A	64.73	58.34
	1B	44.52	72.13		1B	56.13	62.94
	2A	49.39	56.11		2A	70.41	70.52
	2B	60.09	72.32		2B	54.71	70.01
	3A	55.60	62.60		3A	77.06	78.21
	3B	50.96	74.58		3B	68.78	77.70
	4A	46.71	62.75		4A	64.25	79.28
	4B	62.40	51.04		4B	74.08	73.44
LS-3	1A	51.60	62.73	LS-7	1A	67.53	67.55
	1B	49.86	52.33		1B	55.02	61.53
	2A	38.74	51.13		2A	63.23	74.00
	2B	50.63	63.43		2B	64.92	67.11
	3A	28.08	57.15		3A	76.76	67.37
	3B	55.81	71.09		3B	72.73	75.13
	4A	20.94	62.27		4A	60.47	83.48
	4B	57.42	43.10		4B	65.04	72.00
LS-4	1A	42.19	72.18	LS-8	1A	59.88	70.83
	1B	50.61	46.39		1B	59.68	75.89
	2A	77.29	76.85		2A	59.29	63.38
	2B	69.02	69.11		2B	58.86	81.00
	3A	72.17	73.53		3A	75.15	72.29
	3B	61.67	76.89		3B	68.17	57.77
	4A	64.82	79.20		4A	48.95	66.99
	4B	72.00	69.79		4B	67.82	68.49

Table G. 2 Embedment depth and surface coverage area for cross sections of group 2 laboratory samples

Sample ID	Side ID	Average % Embedment (Peak and Valley Method)	Average % Coverage	Sample ID	Side ID	Average % Embedment (Peak and Valley Method)	Average % Coverage
LS-9	1A	45.07	48.59	LS-14	1A	53.27	50.24
	1B	41.67	54.58		1B	54.49	52.50
	2A	44.68	37.48		2A	50.20	40.12
	2B	48.24	57.77		2B	57.55	50.32
	3A	33.27	52.11		3A	59.63	67.68
	3B	47.47	54.72		3B	55.88	52.84
	4A	50.85	66.97		4A	60.65	62.62
	4B	57.75	62.13		4B	69.54	76.86
LS-10	1A	38.59	42.00	LS-15	1A	62.90	45.53
	1B	48.33	50.56		1B	41.00	53.44
	2A	53.36	44.84		2A	61.29	62.09
	2B	54.88	67.83		2B	61.54	72.11
	3A	62.61	61.57		3A	52.91	69.71
	3B	70.34	60.22		3B	58.72	60.25
	4A	56.74	56.01		4A	60.73	45.25
	4B	59.40	50.44		4B	51.80	64.89
LS-11	1A	49.37	54.32	LS-16	1A	47.98	74.32
	1B	59.47	63.17		1B	59.77	62.66
	2A	59.24	79.30		2A	63.19	62.93
	2B	52.36	50.00		2B	64.82	63.46
	3A	45.64	53.78		3A	62.16	62.00
	3B	62.01	68.21		3B	74.55	64.55
	4A	74.94	66.77		4A	68.09	69.56
	4B	63.07	49.18		4B	59.83	50.32
LS-12	1A	49.49	43.86	LS-17	1A	67.99	68.83
	1B	57.61	42.42		1B	61.98	64.00
	2A	48.53	58.54		2A	64.57	78.68
	2B	47.18	43.23		2B	56.21	67.84
	3A	52.82	55.74		3A	73.57	80.61
	3B	67.34	57.03		3B	66.91	68.42
	4A	54.44	42.77		4A	78.09	79.91
	4B	55.23	43.10		4B	77.43	75.98

Table G.2 (contd')

Sample ID	Side ID	Average % Embedment (Peak and Valley Method)	Average % Coverage	Sample ID	Side ID	Average % Embedment (Peak and Valley Method)	Average % Coverage
LS-18	1A	61.54	69.57	LS-22	1A	67.50	76.07
	1B	39.24	74.94		1B	62.86	79.75
	2A	55.70	75.40		2A	73.98	72.26
	2B	53.67	70.17		2B	71.91	71.74
	3A	67.09	66.10		3A	73.78	66.59
	3B	53.73	70.60		3B	64.67	74.42
	4A	59.51	73.28		4A	73.41	65.76
	4B	58.35	73.61		4B	65.66	64.10
LS-19	1A	37.47	64.29	LS-23	1A	68.53	64.06
	1B	61.29	76.18		1B	68.19	66.98
	2A	59.34	78.44		2A	73.65	81.56
	2B	60.61	66.78		2B	74.05	80.69
	3A	60.45	62.96		3A	61.33	67.12
	3B	43.49	68.52		3B	79.75	77.74
	4A	68.05	66.04		4A	65.77	76.11
	4B	69.73	65.00		4B	77.91	74.00
LS-20	1A	49.72	65.10	LS-24	1A	68.47	69.84
	1B	65.62	61.40		1B	63.03	60.54
	2A	70.13	68.45		2A	65.10	65.26
	2B	44.95	64.36		2B	71.77	79.24
	3A	62.61	77.85		3A	60.08	72.00
	3B	62.76	75.26		3B	76.96	81.09
	4A	62.18	66.54		4A	38.75	62.56
	4B	65.31	74.76		4B	61.82	84.10
LS-21	1A	63.52	61.67	LS-25	1A	72.12	80.89
	1B	62.81	56.76		1B	70.23	84.60
	2A	70.73	57.37		2A	74.10	69.53
	2B	70.06	75.91		2B	66.65	73.81
	3A	55.96	65.03		3A	74.73	75.73
	3B	51.60	56.59		3B	77.37	81.25
	4A	51.60	71.29		4A	62.40	81.16
	4B	46.99	33.89		4B	65.55	63.20

Table G.2 (contd')

Sample ID	Side ID	Average % Embedment (Peak and Valley Method)	Average % Coverage	Sample ID	Side ID	Average % Embedment (Peak and Valley Method)	Average % Coverage
LS-26	1A	52.80	47.33	LS-30	1A	65.53	75.77
	1B	39.72	46.57		1B	49.52	57.30
	2A	54.84	59.62		2A	67.36	71.59
	2B	54.09	49.09		2B	44.65	53.71
	3A	47.44	45.72		3A	46.98	55.56
	3B	39.45	44.70		3B	50.72	46.87
	4A	58.75	42.15		4A	62.97	65.49
	4B	40.65	57.86		4B	59.97	45.27
LS-27	1A	4.58	51.53	LS-31	1A	58.55	54.98
	1B	58.68	65.16		1B	46.13	61.99
	2A	61.08	50.31		2A	65.73	63.53
	2B	43.95	52.37		2B	51.47	58.65
	3A	50.69	41.62		3A	53.28	60.31
	3B	41.30	51.61		3B	57.88	51.03
	4A	51.59	50.84		4A	64.24	64.47
	4B	50.48	61.08		4B	57.12	58.76
LS-28	1A	60.61	55.04	LS-32	1A	62.58	55.27
	1B	56.18	45.84		1B	47.58	47.12
	2A	42.90	35.81		2A	62.54	55.86
	2B	58.55	60.56		2B	58.80	49.29
	3A	56.55	54.74		3A	59.67	56.22
	3B	4.45	49.22		3B	52.87	43.64
	4A	61.13	63.29		4A	58.16	54.77
	4B	63.54	54.41		4B	46.12	44.08
LS-29	1A	73.89	71.00	LS-33	1A	40.67	27.69
	1B	72.54	60.94		1B	22.78	31.17
	2A	52.32	43.10		2A	47.24	47.73
	2B	64.20	57.37		2B	49.66	62.87
	3A	55.59	48.21		3A	68.14	63.29
	3B	42.95	48.88		3B	54.19	55.23
	4A	54.54	42.30		4A	46.47	51.16
	4B	50.74	34.71		4B	57.11	62.09

Table G.2 (contd')

Sample ID	Side ID	Average % Embedment (Peak and Valley Method)	Average % Coverage	Sample ID	Side ID	Average % Embedment (Peak and Valley Method)	Average % Coverage
LS-34	1A	59.47	55.22	LS-38	1A	51.13	51.98
	1B	58.46	56.86		1B	56.59	54.45
	2A	52.10	44.63		2A	55.94	52.29
	2B	43.47	54.20		2B	35.51	42.17
	3A	56.37	43.54		3A	62.68	44.62
	3B	47.17	55.26		3B	58.16	28.51
	4A	62.40	41.17		4A	56.08	48.58
	4B	31.84	31.61		4B	60.14	53.18
LS-35	1A	58.82	49.98	LS-39	1A	60.55	49.12
	1B	41.12	52.17		1B	53.58	58.21
	2A	57.39	60.27		2A	58.71	65.18
	2B	61.30	49.97		2B	69.16	71.14
	3A	61.40	54.65		3A	64.38	65.38
	3B	53.85	47.03		3B	55.40	66.74
	4A	47.83	48.93		4A	64.50	57.86
	4B	51.70	47.97		4B	59.69	56.94
LS-36	1A	48.71	53.84	LS-40	1A	62.80	66.44
	1B	61.49	53.99		1B	58.75	59.03
	2A	62.50	54.04		2A	66.23	62.40
	2B	49.66	49.88		2B	65.06	58.73
	3A	43.35	49.03		3A	66.05	59.77
	3B	43.30	46.85		3B	61.77	60.53
	4A	56.33	52.74		4A	65.52	67.08
	4B	45.95	52.10		4B	54.87	67.14
LS-37	1A	51.28	51.90	LS-41	1A	74.76	81.92
	1B	51.74	49.87		1B	67.95	72.51
	2A	53.15	58.38		2A	59.81	56.84
	2B	57.79	54.58		2B	70.00	60.65
	3A	39.13	50.55		3A	59.81	47.77
	3B	51.48	42.07		3B	61.79	61.94
	4A	71.94	52.20		4A	59.73	58.01
	4B	58.55	54.61		4B	72.44	56.52

APPENDIX H: Percent Within Limits (PWL) results for embedment depths of field samples analyzed using image processing algorithms

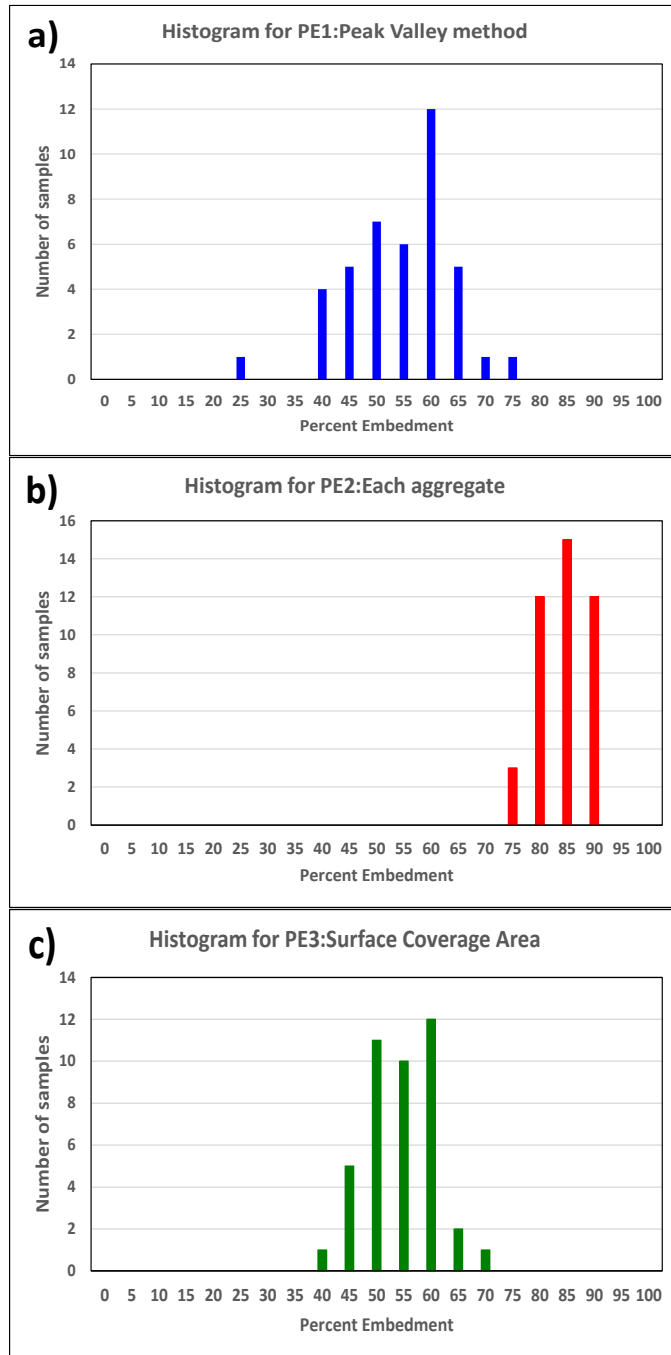


Figure H. 1 PWL result histogram for M-57 road section for a) Peak Valley Method, b) Each aggregate method and c) Surface coverage area method

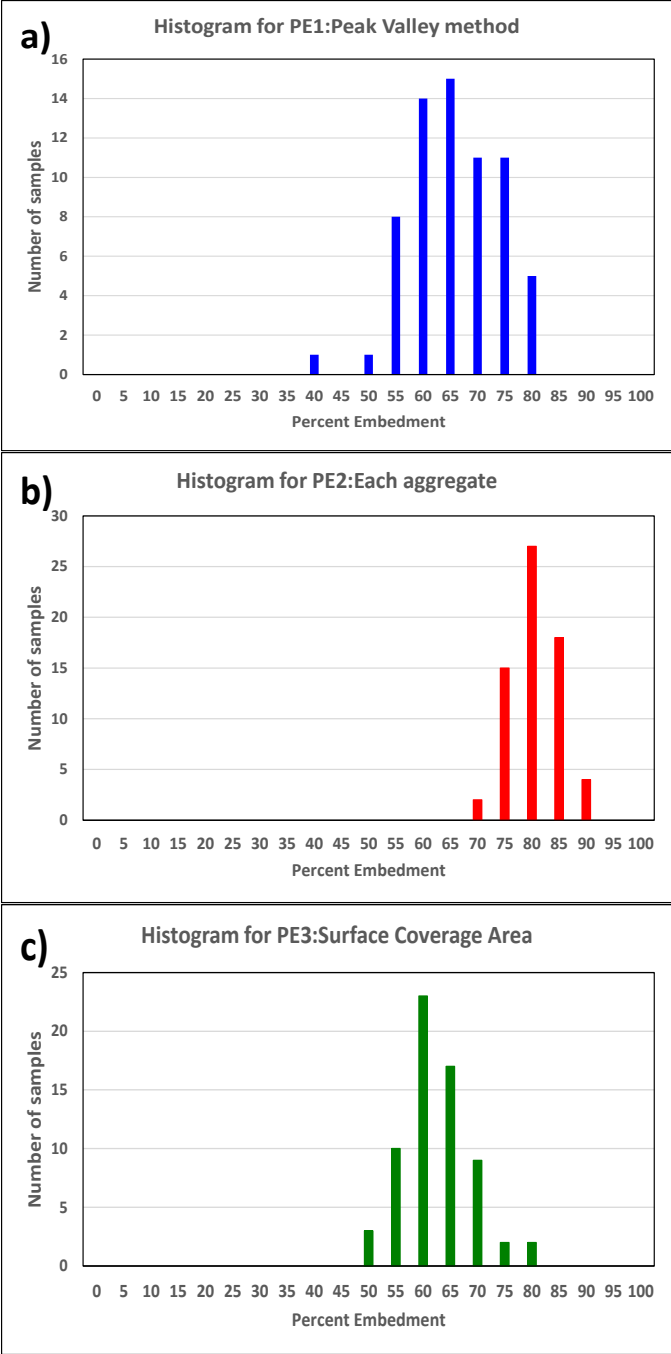


Figure H. 2 PWL result histogram for M-20 road section for a) Peak Valley Method, b) Each aggregate method and c) Surface coverage area method

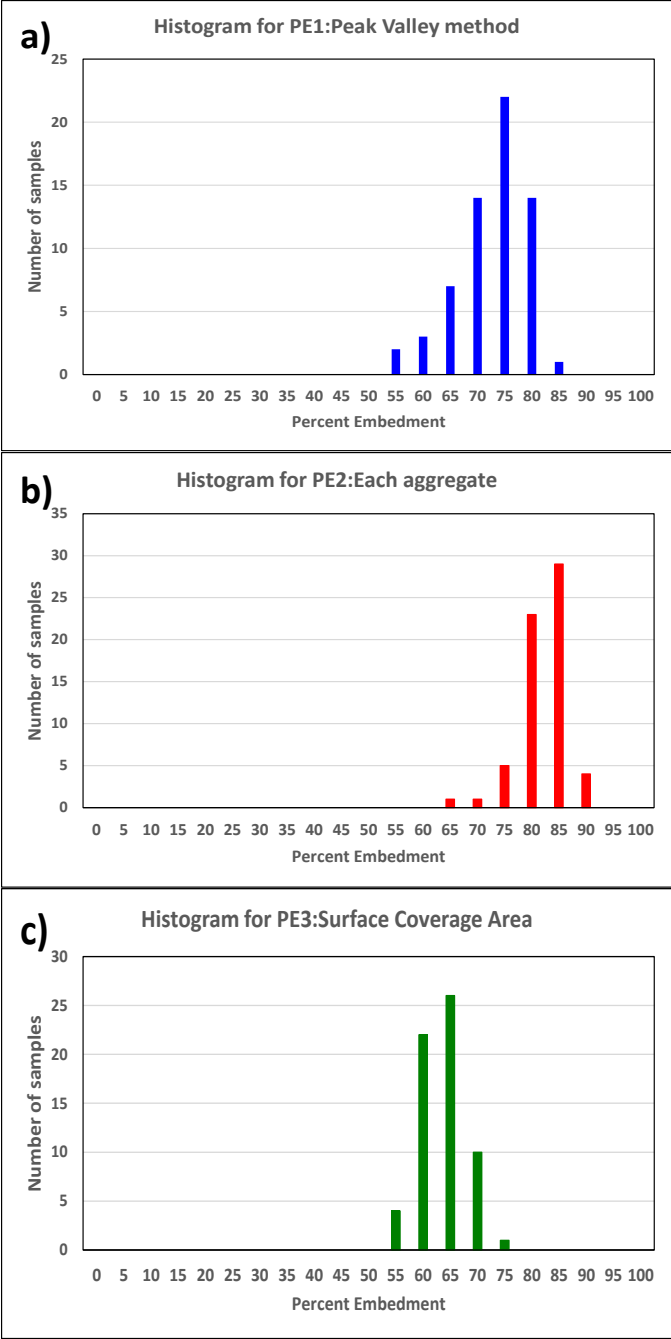


Figure H. 3 PWL result histogram for M-33 road section for a) Peak Valley Method, b) Each aggregate method and c) Surface coverage area method

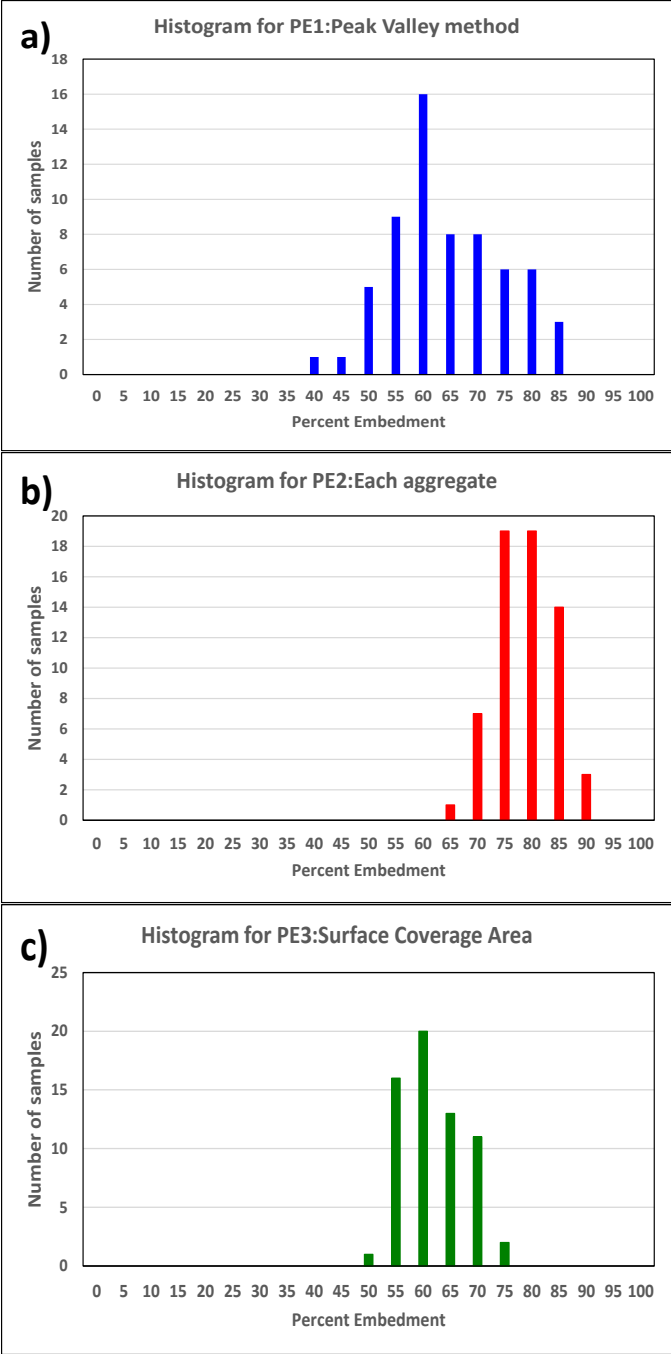


Figure H. 4 PWL result histogram for M-86 road section for a) Peak Valley Method, b) Each aggregate method and c) Surface coverage area method

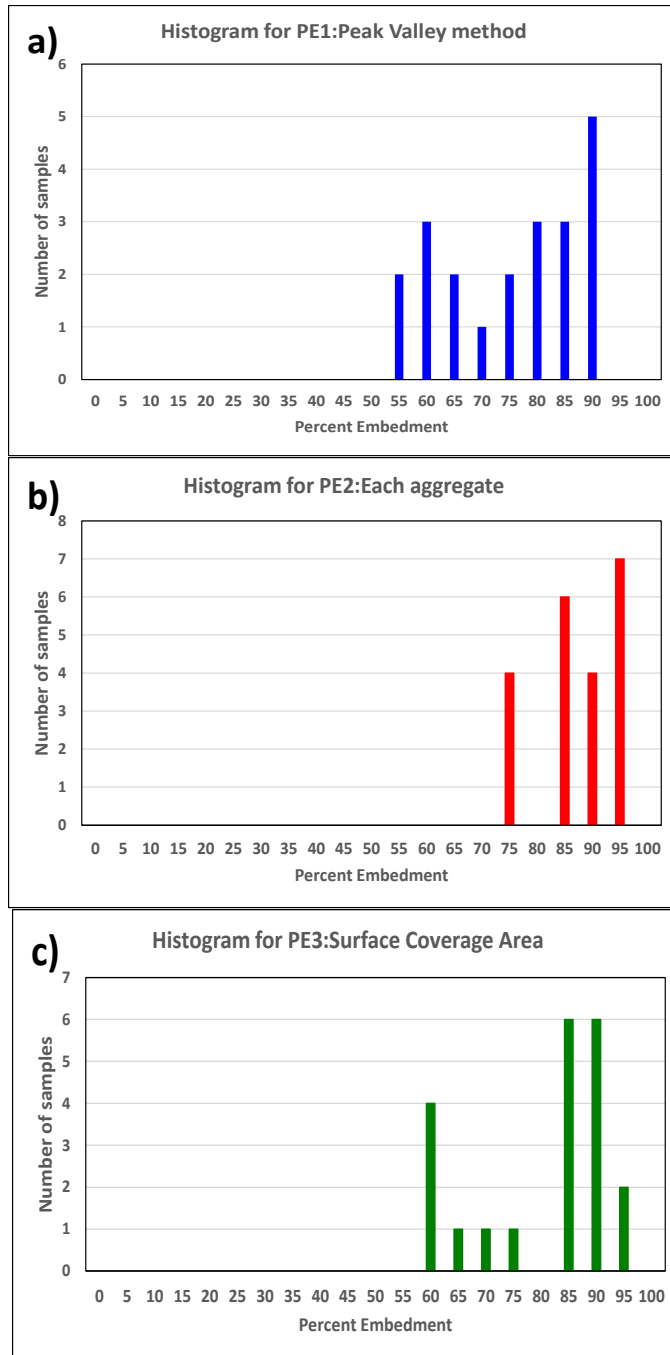


Figure H. 5 PWL result histogram for M-43 road section for a) Peak Valley Method, b) Each aggregate method and c) Surface coverage area method

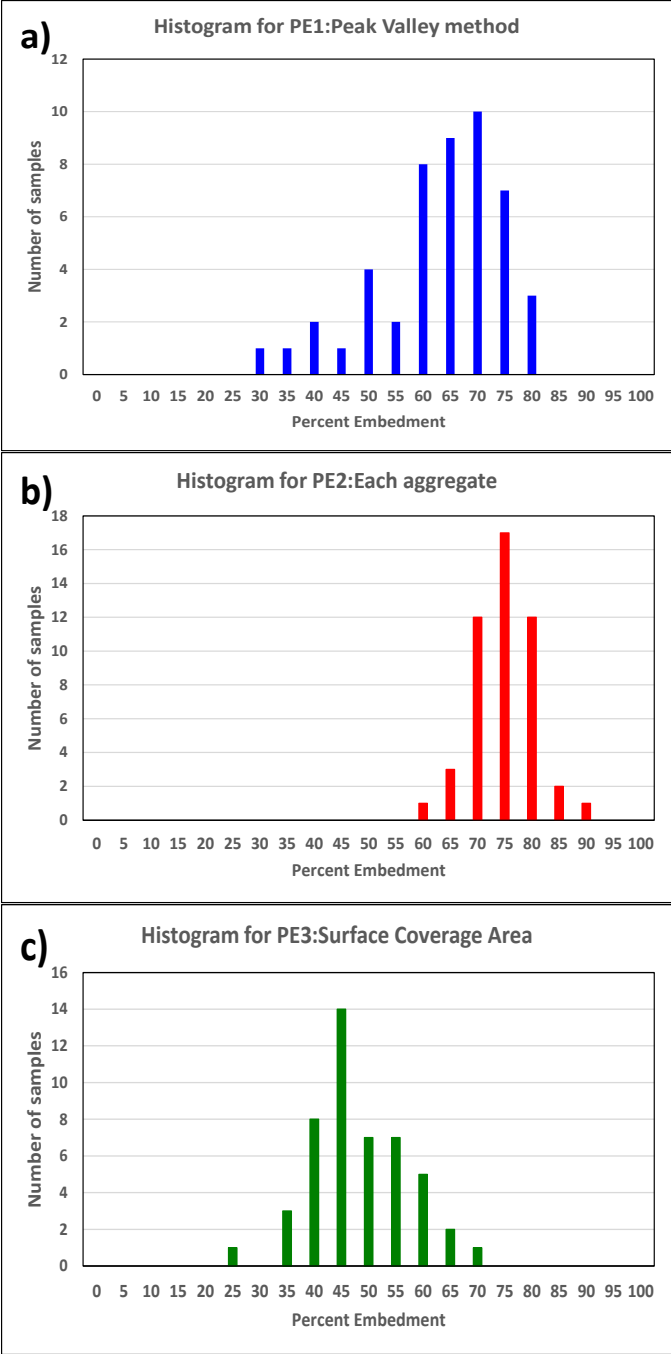


Figure H. 6 PWL result histogram for US-31 road section for a) Peak Valley Method, b) Each aggregate method and c) Surface coverage area method